

SOME APPLICATIONS OF QUANTUM ENTANGLEMENT

Thesis submitted for the degree of
Doctor of Philosophy (Sc.)

in

Physics (Theoretical)

by

Tanumoy Pramanik

Department of Physics

University of Calcutta

2013

To My Mother

Abstract

The presence of non-local correlation in quantum mechanics gives greater advantages in the information processing tasks over classical theory. This thesis is devoted to study the non-local feature of quantum mechanics and its application in different information processing tasks. In the second chapter, we propose an experimental scheme to show the presence of non-locality at the single particle level. Next, we use the correlation between different degrees of freedom of a single particle to send an unknown quantum state at a distance location, securely. We then study the winning probability of two different quantum games over all possible classical and quantum strategies. In the chapter-4, we show that the winning probability of special kind of non-local retrieval games are different when the players use classical correlation, quantum correlation and super quantum correlation. In the following chapter, we define a new quantum game that captures the reduction of uncertainty for the measurement of two non-commuting observables, optimally, with the help of non-local correlation, i.e., entanglement between the observed system and quantum memory. Next, we study the protection of information when the information transfers through a noisy amplitude damping channel. Finally, in the concluding chapter, we summarize the interesting key results of our work.

Acknowledgements

Words are not enough to express my gratitude for my supervisor Prof. Archan Subhra Majumdar. He gives me a lots of opportunities as he makes me independent in the research fields, gives me a lot of support both academic and non-academic, and allows me the flexibility to work with others. Along with the guidance of my supervisor, Prof. Guruprasad Kar, Prof. Dipankar Home, Dr. Satyabrata Adhikari, Dr. Indranil Chakrabarty help to improve my understanding in the field of quantum information and provide me fruitful discussion whenever I need.

Friends are rare to find. During my tenure, I got some good friends. I thank Priyanka Chowdhury, Abdul Wahid, Tamal Basak, Sandeep Singh, Rajiv Kumar Chouhan, Debraj Roy, Sudip Kumar Garain, Biswajit Das, Abhinav Kumar, Anshuman Dey, Subhadipa Das, Ashutosh Rai, Shiladitya Mal, MD Rajjak Gazi, Manik Banik, Sandeep Agarwal, Ambika Prasad Jena, Shahnewaz Mondal, Rajib Nath, Debmalya Mukhopadhyay, Abhijit Chakraborty, Manotosh Chakravorty. They have helped me in various occasions for both academic and non-academic needs.

I thank Professor Arup Kumar Raychaudhuri, Director, S. N. Bose National Centre for Basic Sciences, Kolkata for providing a vibrant research atmosphere. I express my gratitude to all the Deans and Registrars who held office during this period. I also thank all the academic and non-academic staff members of this centre for their assistance and active co-operation.

I have left for the end the most important, my greatest thanks for my family - my parents, my brother Monoj and my beloved Priyanka Chowdhury. Their love, care and support make me strong and give me inspiration during this journey.

I am also very thankful for the financial support from the S. N. Bose National Centre For Basic Sciences and University Grants Commission, India.

Finally, I would like to emphasize that I wish to thank everyone who have helped me though the process of the making this thesis.

List of Publications

Publications by the candidate forming part of the thesis:

- T. Pramanik and A. S. Majumdar, ‘*Improving the fidelity of teleportation through noisy channels using weak measurement*’, arXiv:1301.0281 (2013) (communicated).
- T. Pramanik, P. Chowdhury, and A. S. Majumdar, ‘*Fine-grained lower limit of quantum uncertainty in the presence of quantum memory*’, Physical Review Letters **110**, 020402 (2013).
- T. Pramanik and A. S. Majumdar, ‘*Fine-grained uncertainty relation and nonlocality of tripartite systems*’, Physical Review A **85**, 024103 (2012).
- T. Pramanik, S. Adhikari, A.S. Majumdar, and D. Home, ‘*Testing nonlocality of single photons using cavities*’, Physics Letters A **376** 344 (2012).
- T. Pramanik, S. Adhikari, A.S. Majumdar, D. Home, and A. K. Pan, ‘*Information transfer using a single particle path-spin hybrid entangled state*’, Physics Letters A **374** 1121 (2010).

Additional publications by the candidate relevant to the thesis but not forming part of it:

- T. Pramanik, S. Mal, and A. S. Majumdar; ‘*Optimal lower bound of quantum uncertainty from extractable classical information*’, arXiv:1304.4506 (2013).
- A. Dey, T. Pramanik, and A. S. Majumdar; ‘*Fine-grained uncertainty relation and biased nonlocal games in bipartite and tripartite systems*’, Physical Review A **87**, 012120 (2013).
- Sk. Sazim, S. Adhikari, S. Banerjee, and T. Pramanik; ‘*Quantification of Entanglement of teleportation in Arbitrary Dimensions*’, arXiv:1208.4200 [quant-ph] (communicated).
- S. Mal, T. Pramanik, and A. S. Majumdar; ‘*Detecting mixedness of qutrit systems using the uncertainty principle*’, Physical Review A **87**, 012105 (2013).

- I. Chakrabarty, T. Pramanik, A. K. Pati, and P. Agrawal; '*CTC assisted PR box type correlation can lead to signaling*', arXiv:1107.2908 (communicated).

Contents

Dedication	i
Abstract	ii
Acknowledgements	iii
List of Publications	iv
List of Figures	ix
List of Tables	xi
1 General Introduction	1
1.1 <i>Characterization of entanglement</i>	1
1.1.1 <i>Entanglement and separability</i>	1
1.1.2 <i>Bipartite pure entangled state</i>	2
1.1.3 <i>Bipartite mixed entangled state</i>	2
1.2 <i>Measure of mixedness</i>	3
1.2.1 <i>Linear entropy</i>	4
1.3 <i>Quantification of entanglement</i>	5
1.3.1 <i>Entanglement measure for pure states</i>	6
1.3.2 <i>Entanglement measure for bipartite mixed states</i>	6
1.4 <i>Entanglement : the non-local correlation</i>	9
1.5 <i>Applications of entanglement</i>	10
1.5.1 <i>Quantum teleportation</i>	10
1.5.2 <i>Super Dense Coding</i>	12
1.5.3 <i>Cryptography : BB84 Protocol</i>	13
1.5.4 <i>Cryptography : E91 Protocol</i>	14
1.6 <i>Uncertainty relations and their applications in quantum information theory</i>	15
1.6.1 <i>Heisenberg-Robertson uncertainty relation</i>	15
1.6.2 <i>Entropic uncertainty relation</i>	16
1.6.3 <i>Applications of Uncertainty relations</i>	17

1.7	Decoherence - the interaction between the quantum system and the environment	18
1.7.1	The bit flip channel	18
1.7.2	The phase flip channel	19
1.7.3	The bit-phase flip channel	19
1.7.4	The depolarizing channel	19
1.7.5	Amplitude damping	20
1.8	Outline of thesis	20
2	Non-locality at the single particle level	22
2.1	Non-locality of a single photon proposed by Tan, Walls and Collett	23
2.1.1	Experimental setup	23
2.1.2	Experimental result	23
2.1.3	Criticism	25
2.2	Non-locality of a single photon proposed by Hardy	25
2.2.1	Four different experiments and the contradiction	26
2.2.2	Criticism and improvements	27
2.3	Testing non-locality of single photons using cavities	28
2.3.1	Atom-cavity interaction dynamics	28
2.3.2	State preparation	30
2.3.3	The scheme	31
2.3.4	Conclusion from the experimental outcomes	36
2.3.5	Summary and outlook	36
3	Intra-particle entanglement and its application	38
3.1	Intra-particle entanglement	38
3.2	Creation of path-spin entanglement of a spin-1/2 particle	39
3.3	Path-spin entanglement as a resource	41
3.4	Summary and outlook	46
4	The fine-grained uncertainty relation and non-local games	49
4.1	Fine-grained uncertainty relation	49
4.2	Single qubit system	50
4.3	Bipartite system	51
4.3.1	CHSH game	52
4.3.2	Non-locality captured by the CHSH game	53
4.4	Tripartite system	53
4.4.1	Winning condition characterized by the Svetlichny box	55
4.4.2	Winning condition characterized by $a \oplus b \oplus c = s t + s u$	56
4.4.3	Winning condition characterized by $a \oplus b \oplus c = s t u$	57
4.5	Summary and outlook	58
5	Uncertainty relation in the presence of quantum memory	60
5.1	Quantum strategy	61

5.2	Experimental investigation of the uncertainty relation in the presence of quantum memory	61
5.3	Optimal lower bound of uncertainty	62
5.4	Application in quantum key generation	67
5.5	Summary	68
6	Improvement of teleportation fidelity with the help of weak measurement	70
6.1	Enhancement of teleportation fidelity with the help of environmental interaction	71
6.2	Weak measurement	75
6.3	Applications of Weak measurement	76
6.3.1	Entanglement protection with the help of weak measurement	77
6.3.2	Teleportation fidelity preservation with the help of weak measurement	79
6.4	Application of weak measurement without post-selection	86
6.4.1	Entanglement protection	87
6.4.2	Protection of teleportation fidelity	88
6.5	Summary	89
7	Conclusions and future directions	91
	Bibliography	95

List of Figures

2.1	Experimental setup proposed by Tan, Walls and Collett [Tan, Walls, and Collett, 1991]	25
2.2	Experimental setup for creating the state given by Eq.(2.15). A two-level atom in its upper level traverses the cavities C_1 and C_2 , before being detected in its lower level by the detector D_1 .	31
2.3	Setup for Experiment 2. Alice checks directly for a photon in cavity C_1 . Bob passes the atom a_2 , initially in the excited state, through the C_3 and C_2 , before detecting it at D_3 again in its excited state.	33
2.4	Setup for Experiment 3. Bob checks directly for a photon in cavity C_2 . Alice passes the atom a_3 , initially in the excited state, through the C_4 and C_2 , before detecting it at D_2 again in its excited state.	34
2.5	Setup for Experiment 4. Alice does the same as she did in Experiment 3, while Bob does the same as in Experiment 2.	35
3.1	A spin-1/2 particle (labelled as particle 1) with an initial spin polarized state $ 0\rangle_s^1$ falls on the beam-splitter BS1. A spin-flipper is placed along the reflected channel (labelled by $ 0\rangle_p^1$). A CNOT operation is performed by Alice involving this particle and another particle (labelled as “a”). A second CNOT operation is performed involving particle 1 and her second particle (2) which is in an unknown state $ \psi^{in}\rangle$. Alice sends the particle (1) to Bob who lets this particle fall on the beam-splitter BS2. A CNOT operation is performed by Bob involving this particle and another particle (3) possessed by him (labelled as $ 0\rangle_s^3$). Bob measures the spin of the particle (1) using the Stern-Gerlach devices SG2 and SG3. Alice then measures the spins of the particle (2) and particle (a) using the SternGerlach devices SG1 and SGA along the z-axis. According to the results of the spin measurements through SG1 and SGA (communicated classically by Alice to Bob), and through SG2 or SG3 (as performed by Bob), he applies a suitable unitary operation (U) on his particle (3) in order to recreate the original state $ \phi^{in}\rangle$ possessed by Alice.	40
5.1	The lower bound of entropic uncertainty corresponding to measurements on a two-qubit state with maximally mixed marginals in the presence of quantum memory. (i) the upper plot $\mathcal{H}(p_d^{\sigma_z}) + \mathcal{H}(p_{inf}^S)$ as predicted by using our uncertainty relation (5.9) derived here, and (ii) the lower plot $\log_2 \frac{1}{c} + \mathcal{S}(A B)$ as predicted by the analysis of Berta et al.[Berta et al., 2010] given by (5.1,5.4). The region between the two curves is inaccessible in actual measurements according to our results, since the optimal lower bound of entropic uncertainty is determined by fine-graining.	67

- 6.1 The flat plane represents the average classical fidelity $\frac{2}{3}$. The surface intersecting it represents the fidelity \bar{F}_1 corresponding to the FEF $\bar{f}_1 = \frac{1}{4} + \frac{1}{2}\sqrt{1-D_2} + \frac{1}{4}(1-D_2)$. The uppermost surface represents the fidelity F_1^O corresponding to the FEF $f_1^O = \frac{2+D_2\bar{p}_2}{2+2D_2\bar{p}_2}$ 83
- 6.2 The flat plane represents the average classical fidelity $\frac{2}{3}$. The lower surface represents the fidelity \bar{F}_2 corresponding to the FEF $\bar{f}_2 = 1 - D + \frac{D^2}{2}$. The upper surface represents the fidelity F_2^O corresponding to the FEF $f_2^O = \frac{1+\sqrt{1+D^2(1-p)^2+D^2(1-p)^2}}{2(1+D(1-p)\sqrt{1+D^2(1-p)^2+D^2(1-p)^2}}$. Here we consider $D_1 = D_2 = D$ and $p_1 = p_2 = p$ 86
- 6.3 The upper surface represents the success probability $P_{Suss}^1 = \frac{\bar{D}_2\bar{p}_2(2+D_2\bar{p}_2)}{2+2D_2\bar{p}_2}$ of *Case I*. The lower surface represents the success probability $P_{Succ}^2 = \frac{\bar{D}^2\bar{p}^2(1+D\bar{p}\sqrt{1+D^2\bar{p}^2+D^2\bar{p}^2})}{1+D^2\bar{p}^2}$ of *Case II* where we consider $D_1 = D_2 = D$ and $p_1 = p_2 = p$ 87
- 6.4 The upper surface represents the fidelity \bar{F}_1 corresponding to FEF \bar{f}_1 given by Eq.(6.10). The middle surface represents the success probability F_1^{Av} given by Eq.(6.52)of *Case I*. The lower surface represents the classical fidelity $2/3$ 89

List of Tables

3.1	States of 1st particle after Alice's measurement outcome for the measurement on her 2nd and auxiliary particle with respective probabilities	42
3.2	Bob's unitary rotation when Alice gets $ 0\rangle_s^2 0_x\rangle_s^a$	43
3.3	Bob's unitary rotation when Alice gets $ 0\rangle_s^2 1_x\rangle_s^a$	44
3.4	Bob's unitary rotation when Alice gets $ 1\rangle_s^2 0_x\rangle_s^a$	45
3.5	Bob's unitary rotation when Alice gets $ 1\rangle_s^2 1_x\rangle_s^a$	45

Chapter 1

General Introduction

1.1 *Characterization of entanglement*

1.1.1 *Entanglement and separability*

In 1935, Einstein, Podolsky, and Rosen [[Einstein, Podolsky, and Rosen, 1935](#)]; and Schrödinger [[Schrödinger, 1935](#)] used *entanglement* to bring out ill-understood features of quantum mechanics. In the EPR paper [[Einstein, Podolsky, and Rosen, 1935](#)], Einstein and co-authors argued that the presence of entanglement makes quantum physics *incomplete*. Entanglement is a signature of the super-position principle and the quantum non-factorizability. Entanglement represents a correlation among two or more quantum systems (or quantum particles). Due to the presence of the above non-classical correlation, quantum physics performs more efficiently in different information processing tasks over classical physics. In this thesis, we restrict our investigation of the application of entanglement to bipartite and the tripartite systems.

A quantum system labeled by A , in general, is considered as an n -dimensional system, i.e., it has n numbers of distinguishable states. Mathematically, a pure quantum state of the system A represents a vector in the n -dimensional Hilbert space, denoted by H_A . For the bipartite system consisting of system A and B , the combined state of the systems A and B is defined in the Hilbert space $H_A \otimes H_B$, where H_B is an n -dimensional Hilbert space associated with the system B . The

above combined state is called entangled if it can not be written as a direct product of states of the individual system.

1.1.2 *Bipartite pure entangled state*

A pure quantum state $|\psi\rangle^i$ gives the complete information about the system ‘ i ’. Mathematically, any pure state $|\psi\rangle^i$ can be written as the projector ρ^i (known as density states of the system ‘ i ’) given by

$$\rho^i = |\psi\rangle^i \langle \psi| \quad (1.1)$$

in the corresponding Hilbert space H_i . ρ^i satisfies the following constraints :

- i. *Normalization* : $Tr[\rho^i] = 1$.
- ii. *Purity* : $Tr[(\rho^i)^2] = Tr[\rho^i] = 1$.

$|\Psi\rangle^{AB}$ is said to be bipartite pure entangled state of the combined systems A and B , if and only if the state $|\Psi\rangle^{AB}$ can not be written in the following form

$$|\Psi\rangle^{AB} = |\psi\rangle^A \otimes |\phi\rangle^B, \quad (1.2)$$

where $|\psi\rangle^A$ and $|\phi\rangle^B$ are any pure states of the system A and B , respectively. More generally, a bipartite pure entangled state $|\Psi\rangle^{AB}$ can be written as

$$|\Psi\rangle^{AB} = \sum_{i=1}^n \sqrt{\lambda_i} |\psi\rangle_i^A \otimes |\phi\rangle_i^B, \quad (1.3)$$

where $|\psi\rangle_i^A$ and $|\phi\rangle_i^B$ are orthonormal pure states of the system A and B , respectively, and λ_i are known as *Schmidt co-efficients* having the properties $\lambda_i \geq 0$ and $\sum_{i=1}^n \lambda_i = 1$. For entangled state, the *Schmidt number* $n > 1$.

1.1.3 *Bipartite mixed entangled state*

Mixed state is generally defined as the statistical mixture of pure states where the mixture arises due to the effect of decoherence. A mixed state ρ^i of the system ‘ i ’

can be written as

$$\rho^i = \sum_k p_k \rho_k^i, \quad (1.4)$$

where ρ_k^i are the pure state of the system i and the mixed state ρ_i satisfies the following criteria

- i. *Normalization* : $Tr[\rho^i] = 1$.
- ii. *Mixedness* : $Tr[(\rho^i)^2] < Tr[\rho^i] = 1$.

A mixed state ρ_{AB} of the combined system A and B is called entangled, if and only if ρ_{AB} can not be written as the mixture of pure product states of the individual systems, i.e,

$$\rho_{AB} \neq \sum_i p_i \rho_i^A \otimes \chi_i^B, \quad (1.5)$$

where the co-efficients p_i are positive and satisfy $\sum_i p_i = 1$. ρ_i^A and χ_i^B are pure states of the system A and B , respectively.

1.2 *Measure of mixedness*

In the classical information theory, if a random variable X takes different value x_n with different probability p_n , then the amount of uncertainty regarding the value of X (alternatively, how much information we gain, on an average, when we learn the value of X) is specified by the *Shannon entropy* [Nielsen and Chuang, 2000]. Note that the uncertainty of the random variable X does not depend on its value, but depends on its probability distribution $\{p_n\}$. The Shannon entropy ($\mathcal{H}(X)$) associated with the probability distribution $\{p_n\}$ is defined as

$$\mathcal{H}(X) = - \sum_n p_n \log_2 p_n \quad (1.6)$$

where $\sum_n p_n = 1$. $\mathcal{H}(X)$ is maximum when all values of the random variable occur with equal probability.

Let us consider a mixed state of the form given by

$$\rho = \sum_i p_i \sigma_i, \quad (1.7)$$

where σ_i 's are pure orthogonal states, i.e.,

$$\text{Tr}[\sigma_i \cdot \sigma_j] = \delta_{ij}, \quad (1.8)$$

δ_{ij} is the Kronecker delta. For a general mixed state ρ , the amount of mixedness is quantified by the *von-Neumann entropy* [Neumann, 1955; Nielsen and Chuang, 2000] and is given by

$$\mathcal{S}(\rho) = -\text{Tr}(\rho \log_2 \rho). \quad (1.9)$$

If λ_i 's are the eigenvalues of density operator ρ , the Eq.(1.9) can be re-expressed as

$$\mathcal{S}(\rho) = -\sum_i \lambda_i \log_2 \lambda_i. \quad (1.10)$$

$\mathcal{S}(\rho)$ has maximum value for maximally mixed states (i.e., completely mixed density operator) and the maximum value for d -dimensional Hilbert space (for example, $d=2$ represents qubit system) is $\log_2 d$.

1.2.1 Linear entropy

The linear entropy is linear approximation to the Von Neumann entropy. It is obtained by approximating $\ln \rho$ with the first order term $(\rho - 1)$ in the Mercator series which is the Taylor series for the natural logarithm. Using Eqs.(1.9) and $\text{Tr}(\rho) = 1$, we get

$$S_L(\rho) = 1 - \text{Tr}(\rho^2) \quad (1.11)$$

In the d -dimensional Hilbert space, the maximum value of $S_L(\rho)$ which occurs for the maximally mixed state (e.g., $\rho = \frac{I}{d}$), is $\frac{d-1}{d}$ and the minimum value of $S_L(\rho)$ is zero for any pure state. Sometime, S_L is written with normalization as

$$S_L(\rho) = \frac{d}{d-1} (1 - \text{Tr}(\rho^2)) \quad (1.12)$$

such that, $S_L(\rho)$ lies within the range $0 \leq S_L(\rho) \leq 1$.

For the two qubit state ρ^{AB} , the linear entropy is

$$S_L(\rho^{AB}) = \frac{4}{3}(1 - \text{Tr}(\rho^{AB^2})) \quad (1.13)$$

The linear entropy and von-Neumann entropy are similar measures for the mixedness of a state, although the linear entropy is easier to calculate because it does not require the diagonalization of the density matrix.

1.3 Quantification of entanglement

Quantification of entanglement is essential for the purpose of qualifying and quantifying the success probability of different information processing tasks (e.g., quantum teleportation, quantum cryptography, super dense coding and so on) performed with the help of entanglement. Maximally entangled states give highest success probability. By calculating the amount of entanglement possessed by an entangled state, we quantify the success probability, i.e., the usefulness of the entangled state in the corresponding information processing task.

The amount of entanglement contained in an entangled state can be quantified in terms of the number of maximally entangled state needed to create the given state, or how many maximally entangled states can be prepared from the given entangled state with the help of local operations and classical communication (LOCC). LOCC can not increase the entanglement on average. Now, every good entangled measure \mathcal{E} should satisfy the following property :

- I. The amount of entanglement contained in any separable state ρ should be zero, i.e., $\mathcal{E}(\rho) = 0$.
- II. The amount of entanglement contained in any state ρ should be unaffected for any local unitary transformation of the form $U_A \otimes U_B$, i.e., $\mathcal{E}(\rho) = \mathcal{E}(U_A \otimes U_B \rho U_A^\dagger \otimes U_B^\dagger)$.
- III. The amount of entanglement can not be increased on average by applying local operation, classical communication and sub-selection, i.e., $\mathcal{E}(\rho) \geq \sum_i p_i \mathcal{E}(\rho_i)$, where p_i denotes the probability of occurring the state ρ_i .

- IV. The amount of entanglement of the two given pair of entangled particles in the state $\rho = \rho_1 \otimes \rho_2$ should have $\mathcal{E}(\rho) = \mathcal{E}(\rho_1) + \mathcal{E}(\rho_2)$, where ρ_1 and ρ_2 are the pair of entangled states of the particles.

1.3.1 Entanglement measure for pure states

1. Entropy of Entanglement : In the case of a bipartite pure entangled state $|\Psi\rangle_{AB}$ shared between the system A and B , the amount of entanglement reduces the information about the subsystem, and the state of the combined system contains the complete information. For example, for the shared maximally entangled state (whose entanglement is maximum), the subsystems are in completely mixed states. Hence, the entanglement of a bipartite pure state is quantified by the von-Neumann entropy of the subsystems given by

$$\mathcal{E}(|\Psi\rangle_{AB}) = \mathcal{S}(\rho_A) = \mathcal{S}(\rho_B), \quad (1.14)$$

where $\rho_A (= Tr_B(|\Psi\rangle_{AB}\langle\Psi|))$ and $\rho_B (= Tr_A(|\Psi\rangle_{AB}\langle\Psi|))$ are the reduced density matrices of Alice's and Bob's system obtained by taking partial trace of the combined state, ρ_{AB} over Bob's system and Alice's system, respectively.

1.3.2 Entanglement measure for bipartite mixed states

In the literature, there are many measures of entanglement for the bipartite mixed state (see the recent review [[Horodecki et al., 2009](#)]) given by

$$\rho_{AB} = \sum_{i=1}^n p_i \rho_i, \quad (1.15)$$

where $\rho_i (= |\psi\rangle_i^{AB}\langle\psi|)$ is the density matrices of the bipartite pure state $|\psi\rangle_i^{AB}$. In this thesis, we mention a few of them.

1. Entanglement of formation : It measures the minimum amount of entanglement required to prepare a quantum state. The entanglement of formation \mathcal{E}_F of a bipartite mixed state ρ_{AB} is defined by [[Chen, Albeverio, and Fei, 2005](#);

Wootters, 1998]

$$\mathcal{E}_F(\rho_{AB}) = \min_{\rho_{AB}} \sum_{i=1}^n p_i \mathcal{E}(|\psi\rangle_i^{AB} \langle \psi_i|), \quad (1.16)$$

where the minimization is taken over all possible decompositions of the density operator ρ_{AB} . Entanglement of formation gives the upper bound of all possible entanglement measures [Horodecki et al., 2000] of the state ρ_{AB} .

2. Entanglement of distillation : It measures the number of maximally entangled states, extracted with the help of LOCC from n copies of ρ_{AB} . It is defined as

$$\mathcal{E}_D(\rho_{AB}) = \lim_{m \rightarrow \infty} \frac{m}{n}, \quad (1.17)$$

where m is the number of extracted maximally entangled states. \mathcal{E}_D gives the lower bound of all possible bipartite entanglement measures [Horodecki et al., 2000] of the state ρ_{AB} .

3. Negativity : Peres [Peres, 1996] and Horodecki et al. [Horodecki et al., 1998] found a criteria to detect bipartite entanglement. This criteria for detection of entanglement is a necessary and sufficient condition for $2 \otimes 2$ and $2 \otimes 3$ dimensional Hilbert space. Before going to the details of this criteria, we recapitulate the partial transpose. The elements of density operator (say, bipartite density operator ρ_{AB}) in some product basis $\rho_{AB}^{m\mu, n\nu} = \langle m\mu | \rho_{AB} | n\nu \rangle$, the kets with Latin and Greek letters form an orthogonal basis in Hilbert space describing the first and second system respectively. Now, partial transpose of ρ is defined as $(\rho_{AB}^{m\mu, n\nu})^{T_B} = \rho_{AB}^{n\nu, m\mu}$. The theorems associated with partial transposition are given below

Theorem 1 : For a given bipartite state ρ_{AB} , if at least one eigenvalue of $\rho_{AB}^{T_B}$ is negative, then the state ρ_{AB} is entangled, and also known as NPT-state (negative partial transpose- state)

Theorem 2 : If all eigenvalue of $\rho_{AB}^{T_B}$ is positive, then the state ρ_{AB} is said to be separable, definitely, for $2 \otimes 2$ and $2 \otimes 3$ dimensional Hilbert space. Otherwise, one can not conclude about separability and entanglement of the state.

The above negative eigenvalues of the state $\rho_{AB}^{T_B}$ are useful to calculate the amount of entanglement of ρ_{AB} and this amount is given by

$$\mathcal{E}_N(\rho_{AB}) = \frac{\|\rho_{AB}^{T_B}\| - 1}{d - 1}, \quad (1.18)$$

where $\|\cdot\|$ denotes the trace norm and d is the smaller of the dimension of the bipartite system.

4. Concurrence : Concurrence is a measure of entanglement for two qubit systems, where qubit is a quantum bit which can take value either 0 or 1 or any superposition of them, whereas classical bit (cbit) is either 0 or 1. In general, the state of a qubit is given by

$$|\psi\rangle_{\text{qbit}} = \alpha|0\rangle + \beta|1\rangle, \quad (1.19)$$

where the complex coefficients satisfy $|\alpha|^2 + |\beta|^2 = 1$ and $\{|0\rangle, |1\rangle\}$ form basis states of the qubit system. The concurrence of mixed entangled state ρ_{AB} is defined by [Wootters, 1998]

$$C(\rho_{AB}) = \max(0, \sqrt{\lambda_1} - \sqrt{\lambda_2} - \sqrt{\lambda_3} - \sqrt{\lambda_4}), \quad (1.20)$$

where λ_i 's are the eigenvalues of the matrix $\rho_{AB}^{\frac{1}{2}}(\sigma_y \otimes \sigma_y)\rho_{AB}^*(\sigma_y \otimes \sigma_y)\rho_{AB}^{\frac{1}{2}}$ in the decreasing order, i.e., $\lambda_1 \geq \lambda_2 \geq \lambda_3 \geq \lambda_4$. '*' denotes the complex conjugation and σ_y denotes the Pauli operator. The concurrence is related with the entanglement of formation by the equation [Wootters, 1998]

$$\mathcal{E}_F(\rho_{AB}) = \mathcal{H}\left[\frac{1}{2}(1 + \sqrt{1 - C(\rho_{AB})})\right]. \quad (1.21)$$

5. Rényi entropy : The Rényi entropy of the order α is defined as

$$\mathcal{H}_\alpha(\rho_{AB}) = \frac{1}{1 - \alpha} \log_2 \left(\sum_i \lambda_i^\alpha \right), \quad (1.22)$$

where $\alpha \geq 0$, $\alpha \neq 1$ and λ_i 's are eigenvalues of ρ_{AB} . In particular, von-Neumann entropy is obtained in the limit of ' $\alpha \rightarrow 1$ ' from the Eq.1.22. Finally, in the limit of $\alpha \rightarrow \infty$, the Rényi entropy is of the form given by

$$\mathcal{H}_\infty(\rho_{AB}) = -\log_2 \left(\max_i \lambda_i \right). \quad (1.23)$$

$\mathcal{H}_\infty(\rho_{AB})$, known as the single-copy entanglement, measures the amount of maximally entangled state extracted from a single copy of ρ_{AB} [Eisert and Cramer, 2005].

1.4 Entanglement : the non-local correlation

The correlation of measurement outcomes for the measurement of observables on the individual components of an entangled system is not always explained with the help of classical theory [Bell, 1964; Clauser et al., 1969; Collins et al., 2002; Mermin, 1990; Svetlichny, 1987]. With the assumption of *Locality* and *Reality* principle given by [Bell, 1964; Einstein, Podolsky, and Rosen, 1935]

Locality principle : If two system are causally disconnected, the result of any measurement performed on one system can not influence the result of measurement performed on the second system. Following the theory of relativity, we say that two measurement events are disconnected if $(\Delta x)^2 > c^2(\Delta t)^2$, where (Δx) and (Δt) are the space and time separation of the two events in some inertial frame and c is the speed of light.

Reality principle : If we can predict with certainty the value of a physical quantity, then this value has physical reality, independently of our observation.

J. Bell, first introduced an inequality called Bell's inequality [Bell, 1964] under the assumption of the locality and reality principle, and showed that the presence of entanglement may violate the above inequality. Bell's inequality is given by [Bell, 1964; Clauser et al., 1969]

$$\mathcal{B}_{\text{CHSH}} = |\langle \mathcal{A}_0 \mathcal{B}_0 \rangle + \langle \mathcal{A}_0 \mathcal{B}_1 \rangle + \langle \mathcal{A}_1 \mathcal{B}_0 \rangle - \langle \mathcal{A}_1 \mathcal{B}_1 \rangle| \leq 2, \quad (1.24)$$

where Alice randomly measures either the observable \mathcal{A}_0 or the observable \mathcal{A}_1 on her system and similarly, Bob randomly measures either the observable \mathcal{B}_0 or the observable \mathcal{B}_1 on his system. It was shown that in the two qubit system, for the choice of state $|\Psi\rangle_{AB}$ given by

$$|\Psi\rangle_{AB} = \frac{|01\rangle_{AB} - |10\rangle_{AB}}{\sqrt{2}}, \quad (1.25)$$

where $|0\rangle_i$ ($|1\rangle_i$) is spin up (spin down) state of the spin-1/2 particle labeled by i ($\in \{A, B\}$) and for the choice of observables, given by

$$\begin{aligned} A_0 &= \sigma_x & B_0 &= -\frac{\sigma_z + \sigma_x}{\sqrt{2}} \\ A_1 &= \sigma_z & B_1 &= \frac{\sigma_z - \sigma_x}{\sqrt{2}}, \end{aligned} \quad (1.26)$$

$\mathcal{B}_{\text{CHSH}} = 2\sqrt{2}$ [Clauser et al., 1969]. The above violation ($2\sqrt{2}$) is maximum and occurs for a maximally entangled state given by Eq.(1.25). Such violation is captured by a number of experiments [Aspect, Dalibard, and Roger, 1982; Aspect, Grangier, and Roger, 1981, 1982; Pan et al., 2000; Tittel et al., 1998]. Hence, quantum entanglement is a non-local correlation.

1.5 Applications of entanglement

Entanglement is a useful resource for performing different informational processing tasks. It was shown that the presence of entanglement outperforms all possible classical strategies in several informational processing tasks. Such tasks are *quantum teleportation* [Bennett et al., 1993], *super dense coding* [Bennett and Wiesner, 1992], *quantum cryptography* [Bennett and Brassard, 1984; Ekert, 1991] and so on. The presence of entanglement gives higher winning probability for some *non-local games* [Oppenheim and Wehner, 2010; Pramanik and Majumdar, 2012]. In the presence of entanglement with another system known as *quantum memory*, it is possible to reduce the uncertainty for the measurement of two non-commuting observables on the observed system [Berta et al., 2010; Li et al., 2011; Pramanik, Chowdhury, and Majumdar, 2013; Prevedel et al., 2011].

1.5.1 Quantum teleportation

In quantum teleportation, Alice's task is to send quantum information which is an unknown quantum state of a spin-1/2 particle to Bob, separated at a distant location. The unknown quantum state of the spin-1/2 particle is given by

$$|\psi\rangle_1 = a|0\rangle_1 + b|1\rangle_1, \quad (1.27)$$

where the above spin-1/2 particle is labeled by subscript ‘1’ (say, 1st particle) and $|a|^2 + |b|^2 = 1$. To perform the above task Alice can use either classical strategy or quantum strategy.

Classical strategy : Here Alice randomly chooses a direction, say \hat{n} and makes a spin measurement along that direction on the given 1st particle. The observable corresponding spin measurement is $\hat{n} \cdot \vec{\sigma}$, where σ_i are the Pauli spin matrices. Alice sends the measurement outcome to Bob and from the communicated result, Bob infers about the unknown quantum state of the 1st particle.

The success of this protocol is quantified by the *average fidelity* given by

$$F_{\text{av}} = \overline{|\langle \psi_1 | \psi_{\text{final}} \rangle|^2}, \quad (1.28)$$

where the average is taken over all possible given states of the 1st particle and Alice’s measurement outcomes. $|\psi_{\text{final}}\rangle$ is the Bob’s prepared state from Alice’s communicated result. In this case, the success probability F_{av} is 2/3 [Massar and Popescu, 1995].

Quantum strategy : Here, initially Alice and Bob share a maximally entangled state $|\Psi\rangle_{AB}$ given by Eq(1.25), i.e., the system A (possessed by Alice) and B (possessed by Bob) are maximally entangled. When Alice gets the 1st particle, she makes a joint measurement on the 1st particle and the system A in the Bell basis given by

$$\begin{aligned} |\psi^\pm\rangle_{AB} &= \frac{|01\rangle_{AB} \pm |10\rangle_{AB}}{\sqrt{2}}, \\ |\phi^\pm\rangle_{AB} &= \frac{|00\rangle_{AB} \pm |11\rangle_{AB}}{\sqrt{2}}, \end{aligned} \quad (1.29)$$

and communicates the measurement outcome to Bob. To send the possible measurement outcomes to Bob, Alice needs minimum 2 cbits. Alice encodes the measurement outcomes ($|\psi^\pm\rangle_{AB}$, $|\phi^\pm\rangle_{AB}$) by two bit of strings (00, 01, 10, 11) in the following way

$$\begin{aligned} |\psi^+\rangle_{AB} &\rightarrow 00, \\ |\psi^-\rangle_{AB} &\rightarrow 01, \\ |\phi^+\rangle_{AB} &\rightarrow 10, \\ |\phi^-\rangle_{AB} &\rightarrow 11. \end{aligned} \quad (1.30)$$

After knowing the measurement outcome, Bob performs a suitable unitary rotation chosen from the set $\{I, \sigma_x, \sigma_y, \sigma_z\}$, where I is the identity matrix, on his system B to make the fidelity as large as possible. The unitary rotations corresponding to the 2 bits of classical messages are given by

$$\begin{aligned}
 00 &\rightarrow \sigma_z, \\
 01 &\rightarrow I, \\
 10 &\rightarrow i\sigma_y, \\
 11 &\rightarrow \sigma_x,
 \end{aligned} \tag{1.31}$$

where $i = \sqrt{-1}$. For the shared maximally entangled state, the average fidelity F_{av} becomes unity, i.e., the given state of the 1st particle and the final state of the system B are same. Note that, after Bell measurement at Alice's side the unknown state of the 1st particle is destroyed and by applying suitable unitary rotation (depending upon Alice's measurement outcome) on the Bob's system, the unknown state reappears. For shared non-maximally entangled states and shared mixed entangled states, $F_{\text{av}} < 1$.

Several experiments [Boschi et al., 1998; Pan et al., 1997; Ma et al., 2012] confirmed the possibility of performing teleportation in the real world and current research is going on to increase the distance between the sender and the receiver [Ma et al., 2012]. The importance of the teleportation protocol is the ability of sending an unknown quantum state to a distant location with the help of pre-shared entanglement and 2 cibt communications, whereas classically, the sender must have the power of infinite communication to send the unknown quantum state.

1.5.2 Super Dense Coding

Sending a two level system classically, the communication from the sender, Alice to the receiver, Bob is bounded by 1-cbit. But, the presence of entanglement can beat the above bound – this phenomena is know as super dense coding [Bennett and Wiesner, 1992]. Using the shared maximally entanglement system, Alice can send maximally 2-cbit classical information to Bob by sending her system.

In this protocol, Alice's system, A and Bob's system, B are in the maximally entangled state given by Eq.(1.25). Alice makes a unitary rotation chosen from the set $\{I, \sigma_x, \sigma_y, \sigma_z\}$ and sends her system to Bob. Here, Bob's task is to find

out the particular unitary rotation performed by Alice from the knowledge about the shared state. Due to the unitary rotation, the singlet state transforms to one of the Bell basis states given by Eq.(1.29). Now, after getting the particle, Bob makes a Bell basis measurement. From the measurement outcome, Bob confirms about the unitary rotation performed by Alice. In this way, Alice communicates 2-cbit given by the map (1.31) to Bob.

1.5.3 Cryptography : BB84 Protocol

To communicate a secret message to Bob over the classical channel, Alice needs to encode the message with a key. The key prevents others from knowing the message, i.e., without the key the message is not readable. Using cryptography, one can build up such a key between Alice and Bob. In classical physics, it is impossible to build up a completely secure key, i.e., only Alice and Bob know the key. This impossibility is reflected from the fact that one can know the state of a classical system without disturbing it.

Quantum physics provides the complete security since the measurement changes the state of the system, except the measurement performed in the eigenbases. First, Bennett and Brassard introduced a protocol known as BB84 to generate a secret key. This protocol is sensitive over any attack by the eavesdropper, say, Charlie [Bennett and Brassard, 1984].

In this protocol, Alice prepares a particle either in the eigenbasis of σ_z or in the eigenbasis of σ_x , randomly, and sends the particle to Bob. After getting the particle, Bob randomly makes a spin measurement either along z - or along x -direction. They repeat this procedure n times. After completing the repetition, Alice and Bob publicly discuss about the prepared direction (i.e., tells either z -direction or x -direction) and the measured direction (i.e., tells either z -direction or x -direction), respectively. They do not tell about the prepared state and the particular measurement outcome. When their direction matches, they keep the information about the state of the respective particle which gives the raw key.

For the purpose of security, they randomly choose several raw keys and check whether the prepared state (by Alice) and the collapsed state (due to Bob's measurement) of the particle are same or not. There could be some error (i.e., mismatching of the prepared state and the collapsed state) due to the presence of

noise or eavesdropper. If the error is not high, they get a string of numbers by encoding $|\uparrow_{z(x)}\rangle \longrightarrow 0$ and $|\downarrow_{z(x)}\rangle \longrightarrow 1$, and make privacy amplification from the rest of the raw key. If the error rate is too high they throw the data and restart the protocol from the beginning.

In the ‘BB84’ protocol, the security of key is guaranteed by non-commutativity of the observables σ_z and σ_x , i.e., the eigenstate of one observable has no information about the measurement outcomes of the another observable.

1.5.4 Cryptography : E91 Protocol

The E91 protocol was invented by Ekert [Ekert, 1991]. It has the same purpose as BB84. In this protocol, Alice and Bob initially share N numbers of maximally entangled states, say, singlet state given by Eq.(1.25). For each shared maximally entangled state, Alice measures the spin on her system where the spin observable is randomly chosen from the set $\{\mathcal{A}_1 = \sigma_x, \mathcal{A}_2 = \frac{\sigma_x + \sigma_y}{\sqrt{2}}, \mathcal{A}_3 = \sigma_y\}$, and similarly, Bob’s set is $\{\mathcal{B}_1 = \frac{\sigma_x + \sigma_y}{\sqrt{2}}, \mathcal{B}_2 = \sigma_y, \mathcal{B}_3 = \frac{-\sigma_x + \sigma_y}{\sqrt{2}}\}$.

After finishing N measurements on their respective systems, Alice and Bob publicly discuss about the N spin observables (only). Further, they only discuss publicly about their measurement outcomes when their chosen observables do not match. From the communicated measurement outcomes, they calculate the correlation coefficients given by

$$C(\mathcal{A}_i, \mathcal{B}_j) = p_{++}(\mathcal{A}_i, \mathcal{B}_j) + p_{--}(\mathcal{A}_i, \mathcal{B}_j) - p_{+-}(\mathcal{A}_i, \mathcal{B}_j) - p_{-+}(\mathcal{A}_i, \mathcal{B}_j), \quad (1.32)$$

where $i, j = 1, 2, 3$. $p_{\pm\pm}(\mathcal{A}_i, \mathcal{B}_j)$ is the probability that Alice’s spin measurement for the choice of observable \mathcal{A}_i gives the result ± 1 and Bob’s measurement for the choice of observable \mathcal{B}_j gives ± 1 . Using the correlation, Alice and Bob check whether

$$\begin{aligned} \mathcal{B}_{\text{CHSH}} &= C(\mathcal{A}_1, \mathcal{B}_1) - C(\mathcal{A}_1, \mathcal{B}_3) + C(\mathcal{A}_3, \mathcal{B}_1) + C(\mathcal{A}_3, \mathcal{B}_3) \\ &= -2\sqrt{2} \end{aligned} \quad (1.33)$$

is satisfied for the shared maximally entangled state. If the supplier of the singlet state wants to know the key, he provides a state which is entangled with Alice's and Bob's system. In this case $|\mathcal{B}_{\text{CHSH}}| < 2\sqrt{2}$.

When the Eq.(1.33) holds, Bob flips his measurement outcome, i.e, $0 \rightarrow 1$ and $1 \rightarrow 0$, where '+1(-1)' measurement outcome is labeled by 0(1). At the end, they are able to create a secret key string which is unknown from the rest of the world. The secret key is a result of the anti-correlation between the measurement outcomes for the measurement of the same observable on the singlet state and the fact that if two systems A , B are in the singlet state, they are not correlated with the other system even classically.

1.6 Uncertainty relations and their applications in quantum information theory

Another fundamental feature of quantum physics is the *uncertainty relation* [Deutsch, 1983; Heisenberg, 1927; Kraus, 1987; Maassen and Uffink, 1988; Robertson, 1929]. The uncertainty relation limits the precision of measurement outcomes for the measurement of two non-commuting observables on a single quantum system, i.e., when the correlations of the observed system with the other systems (called quantum memory) is not considered. The presence of quantum memory can enhance the precision of measurement outcomes [Berta et al., 2010; Li et al., 2011; Pramanik, Chowdhury, and Majumdar, 2013; Prevedel et al., 2011].

1.6.1 Heisenberg-Robertson uncertainty relation

First, Heisenberg introduced the uncertainty relation for position and momentum [Heisenberg, 1927] and later, Robertson generalized it for any two arbitrary non-commuting observables [Robertson, 1929]. The Heisenberg-Robertson uncertainty relation for the measurement of the observables \mathcal{A} and \mathcal{B} on the system A prepared in the density state ρ_A is given by

$$\Delta\mathcal{A}\Delta\mathcal{B} \geq \frac{1}{2}|\langle[\mathcal{A}, \mathcal{B}]\rangle_{\rho_A}|, \quad (1.34)$$

where the uncertainty of measurement outcomes for the measurement of the observable α ($\in \{\mathcal{A}, \mathcal{B}\}$) is measured by the standard deviation given by $\Delta\alpha = \sqrt{\text{Tr}[\alpha^2\rho_A] - \text{Tr}[\alpha\rho_A]^2}$, and the commutator $[\mathcal{A}, \mathcal{B}] = \mathcal{A}\mathcal{B} - \mathcal{B}\mathcal{A}$.

Latter, the above uncertainty relation was generalized for any two arbitrary observables which need not be complementary, and the relation is given by [Robertson, 1929; Schrödinger, 1930]

$$\Delta\mathcal{A}^2\Delta\mathcal{B}^2 \geq \left| \frac{\langle[\mathcal{A}, \mathcal{B}]\rangle_{\rho_A}}{2} \right|^2 + \left(\frac{\langle\{\mathcal{A}, \mathcal{B}\}\rangle_{\rho_A}}{2} - \langle\mathcal{A}\rangle_{\rho_A}\langle\mathcal{B}\rangle_{\rho_A} \right)^2 \quad (1.35)$$

where the expectation values are taken over the state ρ_A and the anti-commutator $\{\mathcal{A}, \mathcal{B}\} = \mathcal{A}\mathcal{B} + \mathcal{B}\mathcal{A}$.

1.6.2 Entropic uncertainty relation

There is an increasing appreciation in recent times of the limitations of the use of standard deviation as a measure of uncertainty [Bialynicki-Birula and Rudnicki, 2011]. One of the drawbacks of the uncertainty relation in terms of standard deviation is that the right-hand side of the inequality(1.34) depends on the state of the quantum system. To improve this situation as well as link uncertainty with information theoretic concepts, the uncertainty relating to the outcomes of observables has been reformulated in terms of Shannon entropy instead of standard deviation. Entropic uncertainty relation (EUR) for two observables \mathcal{A} and \mathcal{B} was first introduced by Deutsch [Deutsch, 1983], following with an improved version given by

$$\mathcal{H}(\mathcal{A}) + \mathcal{H}(\mathcal{B}) \geq \log_2 \frac{1}{c}, \quad (1.36)$$

first conjectured [Kraus, 1987], and then proved [Maassen and Uffink, 1988]. Here $\mathcal{H}(i)$ denotes the Shannon entropy of the probability distribution of the measurement outcomes of observable i ($i \in \{\mathcal{A}, \mathcal{B}\}$) and $\frac{1}{c}$ quantifies the complementarity of the observables. For non-degenerate observables, $c = \max_{i,j} |\langle a_i | b_j \rangle|^2$, where $|a_i\rangle$ and $|b_j\rangle$ are eigenvectors of \mathcal{A} and \mathcal{B} , respectively.

1.6.3 Applications of Uncertainty relations

Uncertainty relations can be used to detect the entanglement in bipartite and multiparty systems. It was shown that for an entangled system, the uncertainty relation is violated [Gillet, Bastin, and Agarwal, 2008; Nha, 2007; Song et al., 2008]. In *Chapter 5* we discuss how the presence of entanglement can reduce the lower bound of EUR, and the application of the modified lower bound in quantum cryptography [Berta et al., 2010; Li et al., 2011; Pramanik, Chowdhury, and Majumdar, 2013; Prevedel et al., 2011]. In *Chapter 4* we discuss about the fine-grained uncertainty relation [Oppenheim and Wehner, 2010; Pramanik and Majumdar, 2012] which can detect the non-local feature of a physical theory.

Entanglement detection : In $2 \otimes 2$ and $2 \otimes 3$ dimensions, any entangled state ρ_{AB} has negative partial transpose [Horodecki et al., 1998; Peres, 1996], i.e., $\rho_{AB}^{T_B}$ has at least one negative eigenvalue. Hence, $\rho_{AB}^{T_B}$ is not a valid state and it may violate the uncertainty relation.

The possibility of switching the partial transpose sign from the state ρ_{AB} to the observables R (which is in the form $\mathcal{A}_1 \otimes \mathcal{B}_1$), S (which is in the form $\mathcal{A}_2 \otimes \mathcal{B}_2$), i.e.,

$$\text{Tr}[\alpha \rho_{AB}^{T_B}] = \text{Tr}[\alpha^{T_B} \rho_{AB}], \quad (1.37)$$

where $\alpha \{R, S\}$ and α^{T_B} represents the observable when Alice chooses the observable \mathcal{A}_i and Bob chooses the observable \mathcal{B}_i^T , and the property that the partial transpose of any observable remains an observable, makes the uncertainty relation (in terms of standard deviation) capable of detecting entanglement. The new uncertainty relation which is able to detect entanglement is given by [Gillet, Bastin, and Agarwal, 2008]

$$(\Delta R^{T_B})^2 (\Delta S^{T_B})^2 \geq \left| \frac{\langle [R, S]^{T_B} \rangle_{\rho_A}}{2} \right|^2 + \left(\frac{\langle \{R, S\}^{T_B} \rangle_{\rho_A}}{2} - \langle R^{T_B} \rangle_{\rho_A} \langle S^{T_B} \rangle_{\rho_A} \right)^2. \quad (1.38)$$

The above uncertainty relation is satisfied by any separable state and violated by entangled states in the above mentioned dimensions.

1.7 Decoherence - the interaction between the quantum system and the environment

In the above description of usefulness of entanglement, the interaction of systems with the environment has not been considered. In realistic situations, the system interacts with the environment – this phenomena is known as decoherence. Due to decoherence, an initially prepared pure state becomes mixed and initially prepared entangled system after a certain time may become separable [Almeida et al., 2007]. According to the postulates of quantum mechanics, any closed quantum system evolves under a unitary transformation. Any quantum system together with the environment forms a closed quantum system. Hence, due to the interaction with the environment which is initially in the state $|e_0\rangle\langle e_0|$ (where the set $\{|e_i\rangle\}$ forms basis for the state space of environment), the system which is initially in the state ρ becomes

$$\begin{aligned}\rho' &= \text{Tr}_E[U[\rho \otimes |e_0\rangle\langle e_0|]U^\dagger] = \sum_i \langle e_i|U[\rho \otimes |e_0\rangle\langle e_0|]U^\dagger|e_i\rangle \\ &= \sum_i E_i \rho E_i^\dagger,\end{aligned}\tag{1.39}$$

where U represents the interaction of the environment with the system and E_i 's (where, $E_i = \langle e_i|U|e_0\rangle$) are the operators acting on the state space of the quantum system. For trace preserving operation, $\sum_i E_i^\dagger E_i = I$. The operator E_i 's are known as Kraus operators.

In the literature, there are various models for the environmental interaction, such as the bit flip channel, the phase flip channel, the bit-phase flip channel, the depolarizing channel, amplitude damping and so on for the qubit system. Here, we discuss about the above interactions.

1.7.1 The bit flip channel

Due to the interaction with the environment, the state of a qubit flips from $|0\rangle$ to $|1\rangle$ (and vice versa) with probability p and the state is unaffected with probability

$(1 - p)$. The Kraus operators for the bit flip operation are given by

$$\begin{aligned} E_0 &= \sqrt{1-p} I = \sqrt{1-p} \begin{pmatrix} 1 & 0 \\ 0 & 1 \end{pmatrix}, \\ E_1 &= \sqrt{p} \sigma_x = \sqrt{1-p} \begin{pmatrix} 0 & 1 \\ 1 & 0 \end{pmatrix}. \end{aligned} \quad (1.40)$$

1.7.2 The phase flip channel

The environment interacts with the system, such that with probability p , the phase of the system changes, i.e.,

$$|0\rangle \longrightarrow |0\rangle, \quad |1\rangle \longrightarrow -|1\rangle,$$

and with probability $(1 - p)$, the system is unaffected. In this case, the Kraus operators are given by

$$E_0 = \sqrt{1-p} I, \quad E_1 = \sqrt{p} \sigma_z. \quad (1.41)$$

1.7.3 The bit-phase flip channel

In this case, due to the environmental interaction, both bit and phase of the system flips with probability p , i.e.,

$$|0\rangle \longrightarrow i|1\rangle, \quad |1\rangle \longrightarrow -i|0\rangle.$$

The kraus operators are given by

$$E_0 = \sqrt{1-p} I, \quad E_1 = \sqrt{p} \sigma_y. \quad (1.42)$$

1.7.4 The depolarizing channel

In this case, the environmental interaction transforms the initial qubit state ρ to the completely mixed state, i.e., $I/2$ with probability p and with probability

$(1 - p)$, the system is left unchanged. Here, the Kraus operators are

$$\begin{aligned} E_0 &= \sqrt{1-p} I, & E_1 &= \sqrt{\frac{p}{3}} \sigma_x, \\ E_2 &= \sqrt{\frac{p}{3}} \sigma_y, & E_3 &= \sqrt{\frac{p}{3}} \sigma_z. \end{aligned} \quad (1.43)$$

The importance of the depolarizing channel is that if the singlet state (given by Eq.(1.25)) interacts with the environment via the depolarizing channel, it becomes the Werner state [Werner, 1989] which play an important role in quantum information processing.

1.7.5 Amplitude damping

This interaction captures the energy dissipation, i.e., the loss of energy of the two level quantum system by spontaneous emission. The interaction between the system and environment is given by

$$\begin{aligned} |0\rangle_S \otimes |0\rangle_E &\longrightarrow |0\rangle_S \otimes |0\rangle_E \\ |1\rangle_S \otimes |0\rangle_E &\longrightarrow \sqrt{1-D}|1\rangle_S \otimes |0\rangle_E + \sqrt{D}|0\rangle_S \otimes |1\rangle_E, \end{aligned} \quad (1.44)$$

where the subscript S and E label the system and the environment. Initially, the environment is in the zero photon state ($|0\rangle_E$). If the system is in the ground state ($|0\rangle_S$), the system does not interact with the environment, but, when the system is in the excited state ($|1\rangle_S$), with probability D , the system moves to ground state by losing a photon, and the environment moves to a one photon state by absorbing it. A feature of amplitude damping is that it could be controlled by the technique of weak measurement and its reversal [Kim et al., 2009; Lee et al., 2011].

1.8 Outline of thesis

In this thesis, the non-local correlation present in quantum mechanics and their applications are studied. The brief outline of each of the following chapters is given below.

In *Chapter-2*, we discuss different existing experimental proposals for showing the presence of non-locality at the single particle level and their criticisms. Then we

discuss the possibility of showing non-locality at the single particle level using atom-cavity interactions [Pramanik et al., 2012].

In *Chapter-3*, we use the non-local correlation present in a single particle to send the information about an unknown quantum state at a distant location, securely [Pramanik et al., 2010]. For the above purpose, we create a path-spin entangled state with the help of a beam splitter and a spin flipper. Our protocol is different from the teleportation protocol where 2-particle entanglement between the sender and the receiver is necessary.

In *Chapter-4*, we study a new uncertainty relation called fine-grained uncertainty relation where the uncertainty is measured in terms of any combination of possible measurement outcomes. When the uncertainty is measured in a coarse grained way, the corresponding uncertainty relation is unable to capture the non-local correlation present in quantum mechanics. But, the fine-grained uncertainty relation can discriminate between different physical theories according to the degree of non-locality of the corresponding physical theory for both bipartite and tripartite systems [Pramanik and Majumdar, 2012].

In *Chapter-5*, we discuss the possibility of reduction of uncertainty for the measurement of two non-commuting observables by accessing the correlation of the observed system with the quantum memory. Here, using the fine-grained uncertainty relation, we obtain the optimal reduction in quantum uncertainty in an experimental situation [Pramanik, Chowdhury, and Majumdar, 2013]. The secret key rate in quantum cryptography is lower bounded by the above reduction.

In *Chapter-6*, we study the entanglement and teleportation fidelity when the systems interact with the environment via amplitude damping decoherence. We show that using the technique of weak measurement, the enhancement of teleportation fidelity is not equivalent with the enhancement of entanglement [Pramanik and Majumdar, 2013].

In the last chapter (*Chapter-7*), we summarize the main results obtained in this thesis and discuss future directions of study.

Chapter 2

Non-locality at the single particle level

The degree of violation of Bell's inequality given by Eq.1.24 (or generalized forms of Bell's inequality for more particles) signifies the degree of non-locality of a quantum state of two [Bell, 1964; Clauser et al., 1969] or more particles [Collins et al., 2002; Mermin, 1990; Svetlichny, 1987]. For the single particle case, there is no such inequality because the measurement of the particle at one location excludes the measurement of the same particle at another location. If non-locality is to be regarded as an inherent feature of the quantum world, it is difficult to understand why this feature should be manifest only at the level of two or more particles. A quantum state should reveal its non-local property irrespective of the number of particles associated with it.

Young's interference experiment performed by Grangier, Roger, and Aspect [Grangier, Roger, and Aspect, 1986] showed the interference fringes even for the incident of a single photon on the two slits – which is not possible to explain classically. But, quantum physics explains the possibility of the interference pattern by allowing the accessibility for the photon in the both paths simultaneously. A number of works have been performed in the direction of capturing non-locality of single particle states [Dunningham and Vedral, 2007; Grangier, Roger, and Aspect, 1986; Hardy, 1993, 1994; Home and Agarwal, 1995; Tan, Walls, and Collett, 1991].

2.1 Non-locality of a single photon proposed by Tan, Walls and Collett

Tan, Walls and Collett (TWC) proposed an experimental scheme to demonstrate the non-locality of a single photon. This scheme was criticized by Hardy [Hardy, 1994] and Greenberger, Horne and Zeilinger (GHZ) [Greenberger, Horne, and Zeilinger, 1995].

2.1.1 Experimental setup

The experimental setup proposed by TWC [Tan, Walls, and Collett, 1991] is shown in the Figure 2.1. In the experimental procedure, the experimentalist, say Charlie, performs two different experiments by preparing the two different states by sending – (i) vacuum in each mode ‘ u ’ and ‘ v ’ and (ii) vacuum in the mode ‘ v ’ and single photon in the mode ‘ u ’ at the 50 – 50 beam splitter BS3. The output modes $b1$ and $b2$ are sent to Alice and Bob, respectively. Alice (Bob) uses the homodyne detector ‘HD1’ (‘HD2’) to measure the intensity from the probability of response of the detector ‘HD1’ (‘HD2’). Each homodyne detector consists of a 50 – 50 beam splitter (i.e., the homodyne detectors HD1 and HD2 have BS1 and BS2, respectively), a coherent local oscillator with amplitude $\alpha_k = \alpha \exp[i\theta_k]$ (where $k = 1$ (2) for HD1 (HD2)), and two photodetectors in the output ports of the each BS1 and BS2. In this experiment Alice and Bob both measure the probability of the response of individual photodetectors and the coincidence probabilities for the pair of photodetectors. Note that weak oscillators (i.e., α is small compared to 1) are used in the homodyne detectors and for that it is very rare to get coincidence count due to oscillators.

2.1.2 Experimental result

Case-I. Here, we consider the vacuum inputs in the two modes ‘ u ’ and ‘ v ’. The intensities at the output modes ‘ $c1$ ’, ‘ $d1$ ’ of the homodyne detector HD1 and ‘ $c2$ ’, ‘ $d2$ ’ of the homodyne detector HD2 are given by [Tan, Walls, and Collett, 1991]

$$\langle I_{c1} \rangle = \langle I_{d1} \rangle = \langle I_{c2} \rangle = \langle I_{d2} \rangle = \frac{\alpha^2}{2}, \quad (2.1)$$

where the intensity is calculated from the probability of the response of individual photodetectors. The two-photon coincidence rates which occur due to the local oscillator are given by [Tan, Walls, and Collett, 1991]

$$\langle I_{c1}I_{c2} \rangle = \langle I_{c1}I_{d2} \rangle = \langle I_{d1}I_{c2} \rangle = \langle I_{d1}I_{d2} \rangle = \frac{\alpha^4}{2} \quad (2.2)$$

Case-II. Now, we send a single photon through the mode ‘ u ’ and vacuum through the mode ‘ v ’. The state after passing through the beam splitter BS3 is given by [Tan, Walls, and Collett, 1991]

$$|\psi_P\rangle = \frac{1}{\sqrt{2}}(i|1\rangle_{b1}|0\rangle_{b2} + |0\rangle_{b1}|1\rangle_{b2}), \quad (2.3)$$

where 1st ket in each term represents the particle number on the path $b1$ and second ket represents the particle number on the path $b2$. Here, $|\psi_P\rangle$ is the maximally entangled state where the entanglement is created over the particle number found on the two paths.

In this case the intensities at each detector are given by [Tan, Walls, and Collett, 1991]

$$\langle I_{c1} \rangle = \langle I_{d1} \rangle = \langle I_{c2} \rangle = \langle I_{d2} \rangle = \frac{\alpha^2}{2} + \frac{1}{4}, \quad (2.4)$$

where the enhancement amount $\frac{1}{4}$ shows the effect of one photon entering through the input modes. The coincidence count probabilities are given by [Tan, Walls, and Collett, 1991]

$$\begin{aligned} \langle I_{c1}I_{c2} \rangle &= \langle I_{c1}I_{d2} \rangle = \frac{1}{4}[\alpha^4 + \alpha^2(1 + \sin(\theta_1 - \theta_2))] \\ \langle I_{d1}I_{c2} \rangle &= \langle I_{d1}I_{d2} \rangle = \frac{1}{4}[\alpha^4 + \alpha^2(1 - \sin(\theta_1 - \theta_2))]. \end{aligned} \quad (2.5)$$

Hence, the coincidence probabilities depends on the phase difference between the local oscillators in the homodyne detectors HD1 and HD2. The above coincidence probabilities are bounded between $[\frac{\alpha^2}{4}, (\frac{\alpha^4}{4} + \frac{\alpha^2}{2})]$.

The enhancement of the intensity at individual detectors in the case-II are easily understood from the incident of a single photon. The enhancement of the coincidence count is unable to be explained from the classical description of light, but, quantum mechanical analysis allows the presence of such correlation [Tan, Walls,

and Collett, 1991]. This captures the non-local feature of quantum mechanics at the single particle level.

2.1.3 Criticism

The above formulation was criticized by Hardy [Hardy, 1994]. According to Hardy, the proposal would fail if one were to choose to measure wave-like properties instead of particle-like ones. The measurement of wave-like properties would require a reference oscillator, thereby introducing additional particles, and putting in doubt the notion of single particle non-locality. Hardy gave a new experimental proposal to reveal the non-local feature at the single particle level.

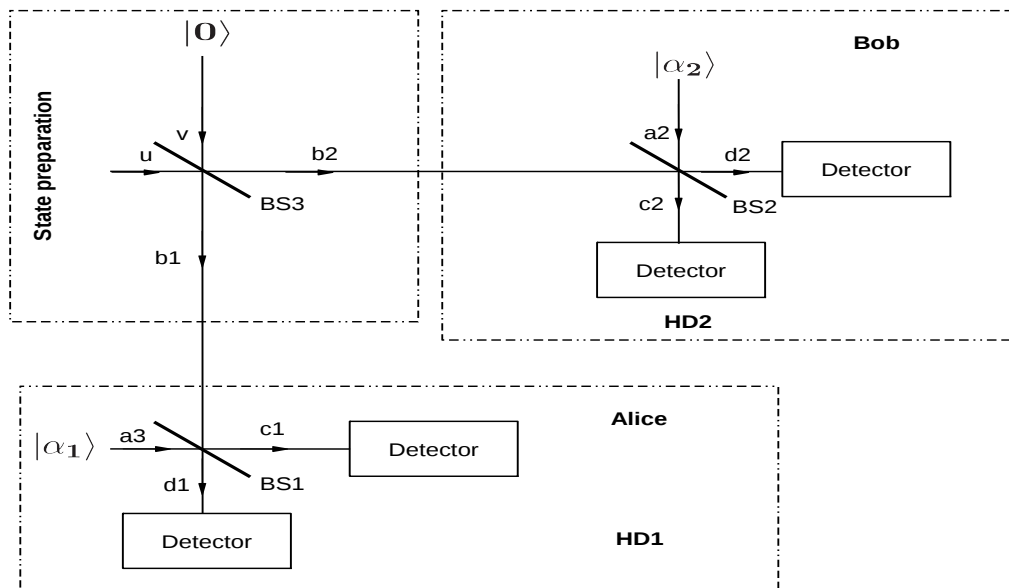


FIGURE 2.1: Experimental setup proposed by Tan, Walls and Collett [Tan, Walls, and Collett, 1991]

2.2 Non-locality of a single photon proposed by Hardy

In the work [Hardy, 1994], Hardy overcame the flaw in TWC's proposal. He considered a similar experimental configuration (given by the Figure 2.1) to the

one considered by TWC, but his analysis is completely different from TWC. In the analysis, he considered four different experiments and showed that the four experiments contradict each other under the assumption of locality.

2.2.1 Four different experiments and the contradiction

State preparation : Here, the input states of the BS3 are a vacuum state, $|0\rangle_v$ and $q|0\rangle_u + \sqrt{\frac{2}{3}}\exp(i\phi)|1\rangle_u$ (i.e., the superposition of vacuum and a particle, say photon). For simplicity, we choose $q = \frac{1}{\sqrt{3}}$ and $r = \sqrt{\frac{2}{3}}\exp(i\phi)$. The state at the output of BS3 is given by

$$|\psi\rangle_{BS3} = \frac{1}{\sqrt{3}}[|00\rangle_{b1b2} + \exp(i\phi)|01\rangle_{b1b2} + i|10\rangle_{b1b2}], \quad (2.6)$$

where the subscript $b1$ and $b2$ labels the output mode of BS3. Now, Alice and Bob either measure the photon number directly on the path $b1$ and $b2$, respectively, or with the help of homodyne detectors. Alice and Bob makes four different experiments by choosing four different measurement setups.

Experiment-1 : In this experiment, Alice and Bob directly measure the photon number by putting a detector in the paths $b1$ and $b2$, respectively. It is clear from the the state $|\psi\rangle_{BS3}$ (given in the Eq.(2.6)), Alice and Bob both cannot detect a photon as input photon number is bounded by 1. Hence, the detection of a photon by Alice prohibits the detection of another photon by Bob or vice versa.

Experiment-2 : Here, Alice measures the photon number using homodyne detection ‘HD1’ (shown in the Figure 2.1) in the path $b1$, whereas Bob directly measures the photon number in the path $b2$. In the homodyne detection Alice uses the coherent state, $|\alpha_1\rangle = |-\exp(i\phi)\rangle$. If Bob gets zero photon on the path ‘ $b2$ ’, the state on the path ‘ $b1$ ’ is

$$|\psi_{b1}\rangle = \frac{1}{\sqrt{2}}[|0\rangle_{u2} + i\exp(i\phi)]. \quad (2.7)$$

After passing through the BS1, the above state becomes

$$|\psi_{c_1d_1}\rangle = |00\rangle_{c_1d_1} + i\sqrt{2}\exp(i\phi)|10\rangle_{c_1d_1} + \dots \quad (2.8)$$

where more than one particle terms are neglected due to negligibly small coefficients. Hence, when Bob gets no photon on his path, Alice only gets a photon on the path ‘c1’ which is contributed from the second term of the RHS of Eq.(2.8). Reversing this argument, i.e., if Alice gets a photon on the path ‘d1’, Bob can not detect no photon, i.e., Bob detects a photon on the path ‘b2’.

Experiment-3 : This is similar to the ‘Experiment-2’, except here Bob measures the photon number using the setup ‘HD2’ and Alice measures the photon number directly on the path ‘b1’. Similarly, if Bob detects a photon on the path ‘d2’ and nothing at ‘c2’, Bob infers that Alice must detect a photon on the path ‘b1’.

Experiment-4 : Here, both Alice and Bob measure the photon number using the homodyne detectors. There is a nonvanishing probability that Alice gets a photon in the path ‘d2’ and no photon in the path ‘c2’, and Bob gets a photon in the path ‘d1’ and no photon in the path ‘c1’.

Contradiction : The results of ‘Experiment-2’, ‘Experiment-3’ and ‘Experiment-4’ contradict with the results of ‘Experiments-1’. The above contradiction occurs due to our assumption of locality, i.e., Bob’s (Alice’s) measurement outcomes does not depend on the choice’s of Alice’s (Bob’s) measurement settings. Hence, the violation itself shows the non-local behavior of quantum mechanics in the single particle level.

2.2.2 Criticism and improvements

In the Ref. [Greenberger, Horne, and Zeilinger, 1995], GHZ also criticized the above proposal. According to GHZ, Hardy’s proposal [Hardy, 1994] is unable to be performed in an experiment, and it shows the multiparticle non-locality. Later, Dunningham and Vedral (DV) [Dunningham and Vedral, 2007] overcame the all criticism in their proposal. But, DV’s proposal relies on using a mixture of coherent states, and is yet to be implemented experimentally. Hence we have given another experimental proposal [Pramanik et al., 2012] which relies on atom cavity interactions, and may finally be able to suggest an implementable experimental avenue regarding this conceptually appealing, but as yet not universally accepted notion of single particle non-locality.

2.3 Testing non-locality of single photons using cavities

In [Pramanik et al., 2012], we have given an experimental proposal for demonstrating non-locality of single photons inside cavities. Our proposal is based on atom-photon interactions in cavities, a well-studied arena on which controlled experiments have been performed for many years now [Raimond, Brune, and Haroche, 2001]. Here we use two-level atoms and single mode high-Q cavities which are tuned to resonant transitions between the atomic levels. For example, the use of Rydberg atoms and microwave cavities in testing several fundamental aspects of quantum mechanics have been proposed, and various interesting experiments have been performed by keeping dissipative effects under control (for details see the review [Raimond, Brune, and Haroche, 2001]). Before going to experiments, first we describe the atom-cavity interaction dynamics.

2.3.1 Atom-cavity interaction dynamics

When a two level atom passes through a cavity which is initially in the vacuum state $|0\rangle_c$, the dynamics of the atom is governed by the Jaynes-Cummings interaction Hamiltonian [Angelakis and Knight, 2002; Raimond, Brune, and Haroche, 2001; Vats and Rudolph, 2001]. The Jaynes-Cummings Hamiltonian under the dipole and rotating wave approximations is given by

$$H_{JC} = \hbar\omega_{eg}\sigma_z + \hbar\omega(a^\dagger a + \frac{1}{2}) + \hbar G(r)(a\sigma_+ + a^\dagger\sigma_-), \quad (2.9)$$

where a and a^\dagger are the photon annihilation and creation operators in the single mode cavity, and σ_z , σ_+ ($\sigma_x + \sigma_y$) and σ_- ($\sigma_x - \sigma_y$) are atomic pseudospin. ω_{eg} and ω are the transition frequency of two level atom and defect mode frequency, respectively. The atom-field coupling strength may be expressed as $G(r) = \Omega_0(\hat{\mathbf{d}}_{eg} \cdot \hat{\mathbf{e}}(r))f(r)$, where Ω_0 is the peak atomic Rabi frequency, $\hat{\mathbf{d}}_{eg}$ is the orientation of the atomic dipole moment, and $\hat{\mathbf{e}}(r)$ is the direction of electric field vector at the position of the atom. The profile $f(r)$ has an exponential envelop centered about the point in the atom's trajectory that is nearest to the center of the cavity, r_0 [Angelakis and Knight, 2002; Vats and Rudolph, 2001]. Within this envelope,

the field intensity oscillates sinusoidally, and for the fixed dipole orientation, variations in the relative orientation of the dipole and electric field gives a sinusoidal contribution, i.e.,

$$f(r) = e^{\frac{-|r-r_0|}{R_{def}}} \cos \left[\frac{\pi}{a_l}(r - r_0) \right], \quad (2.10)$$

where R_{def} defines the spatial extent of the mode which is at most a few times the lattice constant (a_l) for a strongly confined mode in a photonic band-gap [Vats and Rudolph, 2001].

Let us consider an atom which is initially in an excited state ($|e\rangle_a$) passes through the cavity which is initially in the zero photon state. Due to the interaction governed by the Hamiltonian H_{JC} , the atom-cavity state becomes

$$|\phi_e\rangle = \alpha_1|e\rangle_a|0\rangle_c + \alpha_2|g\rangle_a|1\rangle_c, \quad (2.11)$$

where $|g\rangle_a$ is the ground energy state of the atom, $|\alpha_{1(2)}|^2$ which gives the probability of finding the atom in the excited (ground) state after passing through the cavity is given by

$$\begin{aligned} \alpha_1 &= \cos \left[\int_0^t G(t') dt' \right] \\ \alpha_2 &= \sin \left[\int_0^t G(t') dt' \right], \end{aligned} \quad (2.12)$$

where t is the interaction time of the atom with the cavity. The exact form of the $\alpha_{1(2)}$ is given by

$$\alpha_{1(2)} = \cos(\sin) \left[\frac{2a_l R_{def} \Omega_0 k e^{-\frac{b}{R_{def}}} (a_l e^{\frac{b}{R_{def}}} \pi + R_{def} \sin(\frac{\pi b}{a_l}) - a_l \cos(\frac{\pi b}{a_l}))}{v(a_l^2 + \pi^2 R_{def}^2)} \right] \quad (2.13)$$

where $k = \hat{\mathbf{d}}_{eg} \cdot \hat{\mathbf{e}}(r)$ and $(r - r_0)$ is replaced by $(vt - b)$ with v being the velocity of the atom in the cavity, $2b$ is the effective length of interaction in the cavity and the interaction time $t = \frac{2b}{v}$. Following [Angelakis and Knight, 2002], we henceforth set $a_l = 624 \text{ nm} = R_{def}$, $b = 10R_{def}$, and $\Omega_0 = 1.1 \times 10^{10} \text{ rad/s}$ in our calculations.

2.3.2 State preparation

Let us consider two spatially separated observers Alice and Bob possess two cavity C_1 and C_2 , respectively. With the help of an atom a_1 and a detector D_1 , they prepare the cavities C_1 and C_2 in a particular state to accomplish further experiments to show the presence of non-locality at the single particle level.

In the state preparation procedure (shown in the Figure 2.2), Alice and Bob prepare cavity C_1 and C_2 in the zero photon state, i.e., in the state $|0\rangle_{C_1}$ and $|0\rangle_{C_2}$, respectively. Now, an atom a_1 prepared in the excited state $|e\rangle_{a_1}$ traverses through the cavity C_1 with flight time t_{11} and then subsequently through the cavity C_2 with flight time t_{12} . The cavities are tuned to the resonant frequency, i.e., $\omega_{eg} = \omega$. Before detecting the atom a_1 , a $\frac{\pi}{2}$ R_1 Ramsey pulse which causes the transitions given by

$$\begin{aligned} |e\rangle &\rightarrow \frac{|e\rangle - |g\rangle}{\sqrt{2}} \\ |g\rangle &\rightarrow \frac{|e\rangle + |g\rangle}{\sqrt{2}}, \end{aligned} \quad (2.14)$$

is applied at the exit point of the C_2 . Let us consider the case when the atom a_1 is detected in the state $|g\rangle_{a_1}$ at the detector D_1 used in the state preparation process. Since the atom is initially prepared in its excited state and the two cavities are prepared in the zero photon state, the atom can make a transition to its lower state only by release of a single photon in either of the two cavities. After detection of the atom a_1 in the state $|g\rangle_{a_1}$, two cavities C_1 and C_2 are in the one photon state given by [Pramanik et al., 2012]

$$\begin{aligned} |\psi\rangle = & -\alpha_1(t_{11})\alpha_1(t_{12})|0\rangle_{C_1}|0\rangle_{C_2} + \alpha_2(t_{11})|1\rangle_{C_1}|0\rangle_{C_2} \\ & +\alpha_1(t_{11})\alpha_2(t_{12})|0\rangle_{C_1}|1\rangle_{C_2} \end{aligned} \quad (2.15)$$

where the second (third) term on the r.h.s. represents the single photon in the cavity C_1 (C_2) and no photon in cavity C_2 (C_1). The first term arises as a result of $\frac{\pi}{2}$ R_1 pulse introduced as part of the detection mechanism. Note that though the state given in the Eq.(2.15) is similar to the single photon state used by Hardy [Hardy, 1994] and Dunningham and Vedral [Dunningham and Vedral, 2007] in

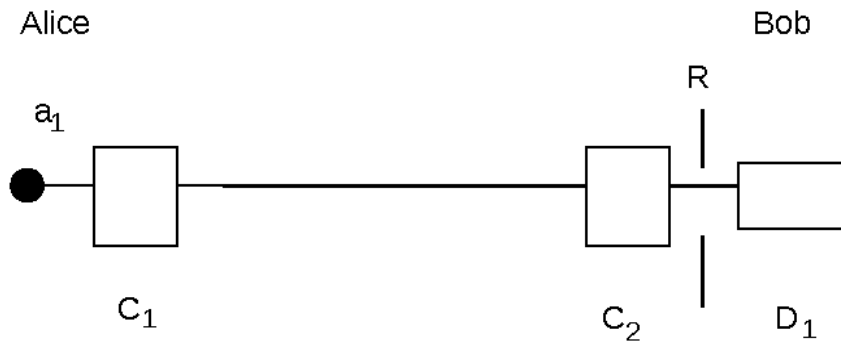


FIGURE 2.2: Experimental setup for creating the state given by Eq.(2.15). A two-level atom in its upper level traverses the cavities C_1 and C_2 , before being detected in its lower level by the detector D_1 .

their arguments on single photon non-locality, the physical constituents are quite different.

2.3.3 The scheme

After preparing the state, both Alice and Bob either measure directly the photon number of their respective cavities or make a local operation on their cavities and then measure the cavity photon state. Thus, there are four different experiments. In the local operation, another cavity in zero photon state and an excited atom are taken. We consider the case when the auxiliary atom is detected in the excited state. Hence, the additional particle will not cause additional non-locality to be introduced in the state given by Eq.(2.15).

Operationally, to measure the cavity photon state Alice (Bob) has to take an auxiliary atom in a ground state and pass it through her (his) cavity with a chosen parameter $v = 161$ m/s and $k = 1$ (making $\alpha_1 = 0$ and $\alpha_2 = 1$ in the Eq.(2.11)). If Alice detects the atom in the excited state, the cavity loses one photon to the atom which goes to the excited state. On the other hand, when the cavity is in zero photon state the auxiliary atom is detected in ground energy state.

Experiment-1 : In this case, both Alice and Bob measure the cavity photon state inside their respective cavities, i.e., in C_1 and C_2 , respectively. As an initially prepared excited atom a_1 is detected in ground state, it releases one photon either inside C_1 or C_2 . Hence, the term $|1\rangle_{C_1}|1\rangle_{C_2}$ is absent in the Eq.(2.15) and it makes

impossible to get one photon by each of them inside their respective cavities, i.e., detecting one photon by Alice and one photon by Bob never happens together.

Experiment-2 : In this case, after preparing the state given by Eq.(2.15), Alice directly measures the photon state inside her cavity C_1 , as Experiment-1. Before measuring the cavity photon state of C_2 , Bob applies a local operation on it (see the Figure 2.3). In the local operation, Bob takes an auxiliary cavity C_3 in zero photon state, i.e., $|0\rangle_{C_3}$ and passes an auxiliary atom a_2 which is initially in the excited state, i.e., $|e\rangle_{a_2}$ through C_3 and C_2 with flight times t_{23} and t_{22} , respectively. Before detecting the atom a_2 at the detector D_3 , Bob applies a $\frac{\pi}{2}$ R_1 pulse on it.

Bob applies the local operation (as stated above) when Alice detect no photon inside her cavity C_1 . The probability of getting zero photon inside the cavity C_1 is given by $\alpha_1^2(t_{11})$. Bob will consider the case when the initially excited atom a_2 is detected in the state $|e\rangle_{a_2}$ at D_3 . Hence, effectively, the atom a_2 does not lose any energy during its flight. By choosing the velocity of a_2 (corresponding to the flight time t_{22}) through the cavity C_2 to be $v_{a_2} = 161$ m/s and $k(a_2; C_2) = 1$, the combined state of C_2 and C_3 is given by

$$\begin{aligned} |\psi\rangle_B = & N_1((- \alpha_1(t_{12})\alpha_1(t_{23}) + \alpha_2(t_{12})\alpha_1(t_{23}))|1\rangle_{C_2}|0\rangle_{C_3} \\ & - (\alpha_1(t_{12})\alpha_2(t_{23}) + \alpha_2(t_{12})\alpha_2(t_{23}))|0\rangle_{C_2}|1\rangle_{C_3}), \end{aligned} \quad (2.16)$$

where, $N_1 = 1/\sqrt{1 - 2\alpha_2(t_{12})\alpha_1(t_{12})(\alpha_1^2(t_{23}) - \alpha_2^2(t_{23}))}$. Note here that the above choice of v_{a_2} and $k(a_2 : C_2)$ rules out the occurrence of two photon state, i.e., $|1\rangle_{C_1}|1\rangle_{C_3}$ (since $\alpha_1(t_{22}) = 0$ and $\alpha_2(t_{22}) = 1$). Further, it is clear from the Eq.(2.16) that the choice of the velocity $v_{a_1} = 179$ m/s and $k(a_1 : C_2) = 1$ (i.e., $\alpha_1(t_{12}) = \alpha_2(t_{12}) = 1/\sqrt{2}$) (the coefficient of $|1\rangle_{C_2}|0\rangle_{C_3}$ vanishes) force Bob to get the photon in the cavity C_3 only, and not in the cavity C_2 . In other words, with the above parameters, when Alice detects no photon in her cavity C_1 , if Bob detects a single photon, it must be in the cavity C_3 , and not in the cavity C_2 . Now, reversing this argument, if Bob detects a photon in cavity C_2 , and nothing in C_3 (it follows from Eqs.(2.15) and (2.16) that such an outcome occurs with a finite probability given by $(1 - \alpha_1^2(t_{11})\alpha_2^2(t_{23}))$), then Alice cannot detect no photons inside her cavity C_1 , i.e., she must detect a single photon there, since this is the only other possible outcome [Pramanik et al., 2012].

Note here that in the above argument we have considered that Bob's auxiliary atom a_2 (which was initially in excited state) is detected in the excited state

$|e\rangle_{a_2}$. However, it is also possible to make a similar argument when the atom is detected in the ground state $|g\rangle_{a_2}$, but the only difference between the two cases are the values of the experimental parameters required for the scheme to work out. For example, in this case, the combined state of the cavities C_2 and C_3 is $N_1[-\alpha_1(t_{23})(\alpha_1(t_{12}) + \alpha_2(t_{12}))|1\rangle_{C_2}|0\rangle_{C_3} + \alpha_2(t_{23})(\alpha_2(t_{12}) - \alpha_1(t_{12}))|0\rangle_{C_2}|1\rangle_{C_3}]$, where $N_1^2 = 1/(1 + 2\alpha_1(t_{12})\alpha_2(t_{12})(\alpha_1^2(t_{23}) - \alpha_2^2(t_{23})))$, with the probability of detection of a_2 in ground state being $1/(2N_1^2)$. In this case, Bob has to choose $v_{a_1} = 146$ m/s (instead of 179 m/s as required in the former case) in order to get a photon in the cavity C_3 and not in C_2 .

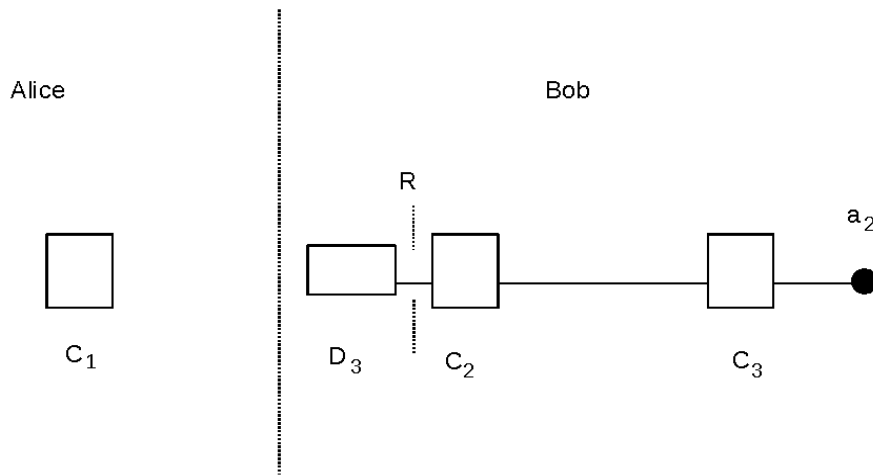


FIGURE 2.3: Setup for Experiment 2. Alice checks directly for a photon in cavity C_1 . Bob passes the atom a_2 , initially in the excited state, through the C_3 and C_2 , before detecting it at D_3 again in its excited state.

Experiment-3 : This experiment is similar to the Experiment-2, but, the role of Alice and Bob are reversed. Bob checks directly the cavity photon state of his cavity C_2 and Alice checks the photon state of her cavity C_1 after making local operations on it (see the Figure 2.4). Here Alice takes an auxiliary atom a_3 in the state $|e\rangle_{a_3}$ and sends it through the auxiliary cavity C_4 chosen in zero photon state $|0\rangle_{C_4}$, and subsequently the cavity C_1 which is prepared in the state given by Eq.(2.15) with flight time t_{34} and t_{31} , respectively. Before detecting the atom a_3 at the detector D_3 , Alice applies a $\frac{\pi}{2}$ R_1 pulse on it.

Now consider the case, when Bob's measurement reveals zero photon state of his cavity C_2 and a_3 is detected in $|e\rangle_{a_3}$. Then by choosing the values $v_{a_3} = 161$ m/s

and $k(a_3; C_1) = 1$ to discard the occurrence of the two photon state, the combined state of C_4 and C_1 are given by

$$|\psi\rangle_A = N_3(\alpha_{t_{34}}(-\alpha_1(t_{11})\alpha_1(t_{12}) + \alpha_2(t_{11}))|0\rangle_{C_4}|1\rangle_{C_1} - \alpha_2(t_{34})(\alpha_1(t_{11})\alpha_1(t_{12}) + \alpha_2(t_{11}))|1\rangle_{C_4}|0\rangle_{C_1}) \quad (2.17)$$

with $N_3 = 1/(\frac{\alpha_1^2(t_{11})}{2} + \alpha_2^2(t_{11}) - \sqrt{2}\alpha_1(t_{11})\alpha_2(t_{11})(\alpha_1^2(t_{34}) - \alpha_2^2(t_{34})))^{1/2}$. To rule out the possibility of detecting the photon in the cavity C_1 , Alice chooses $\alpha_1(t_{12}) = \frac{1}{\sqrt{2}}$ and sets the velocity of a_1 , v_{a_1} to be 179 m/s and $k(a_1; C_1) = 0.979$ (i.e., $\alpha_1(t_{11}) = \sqrt{2}\alpha_2(t_{11})$). Hence, Alice only gets the photon in the cavity C_4 , but not in C_1 . In the event, when Bob detects no photon in his cavity C_2 and if Alice detects a single photon, it must be in the cavity C_4 and not in the cavity C_1 . Now, reversing that argument, if Alice detects a photon in the cavity C_1 and nothing in the cavity C_4 (which follows from Eqs.(2.15) and (2.17)), Bob can not detect no photon in his cavity C_2 , i.e., he must detect a single photon in C_2 (since, this is the only possibility) and this possibility occurs with a probability $1 - \alpha_2^2(t_{34})\alpha_1^2(t_{11})$ [Pramanik et al., 2012].

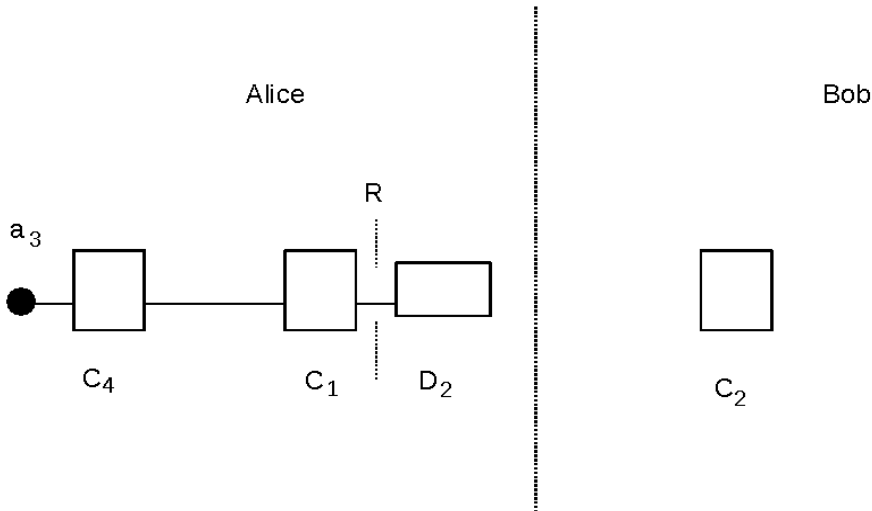


FIGURE 2.4: Setup for Experiment 3. Bob checks directly for a photon in cavity C_2 . Alice passes the atom a_3 , initially in the excited state, through the C_4 and C_2 , before detecting it at D_2 again in its excited state.

Experiment-4 : In this case, both Alice and Bob decide to measure the cavity photon state of their respective cavities after applying the local operations (shown

in Figure 2.5). Alice sends her auxiliary atom a_3 through C_4 and C_1 , and Bob sends his auxiliary atom a_2 through C_3 and C_2 , consecutively. Before detecting the auxiliary atom, Alice and Bob both apply $\frac{\pi}{2} R_1$ pulse on it. They both consider the case when auxiliary atoms are detected in $|e\rangle_{a_3}$ and $|e\rangle_{a_2}$. Over all possible measurement outcomes for both Alice and Bob, there is a non-vanishing probability of getting a single photon in cavity C_1 and nothing in C_4 , while Bob detects a single photon in cavity C_2 and nothing in C_3 which is reflected from the following term

$$\begin{aligned}
 |\psi\rangle_{AB} = & [-\alpha_1(t_{11})\alpha_1(t_{12})\alpha_1(t_{23})\alpha_1(t_{34})\alpha_2(t_{31})\alpha_2(t_{22}) \\
 & +\alpha_1(t_{11})\alpha_1(t_{12})\alpha_1(t_{23})\alpha_1(t_{34})\alpha_2(t_{31}) \\
 & +\alpha_2(t_{11})\alpha_1(t_{23})\alpha_1(t_{34})\alpha_2(t_{22})] |1\rangle_{C_1} |1\rangle_{C_2} |0\rangle_{C_3} |0\rangle_{C_4} \\
 & + \dots
 \end{aligned} \tag{2.18}$$

in their joint state $|\psi\rangle_{AB}$. Such an outcome occurs with a probability $0.0847\alpha_1^2(t_{23})\alpha_1^2(t_{34})$. Note here that one can choose values for the parameters $k(a_2; C_3)$ and $k(a_3; C_4)$ such that the probability is non vanishing. The maximum probability 0.0847 occurs for $k(a_2; C_3) = k(a_3; C_4) = 0.8$ (i.e, $\alpha_1(t_{23}) = \alpha_1(t_{34}) = 1$) [Pramanik et al., 2012].

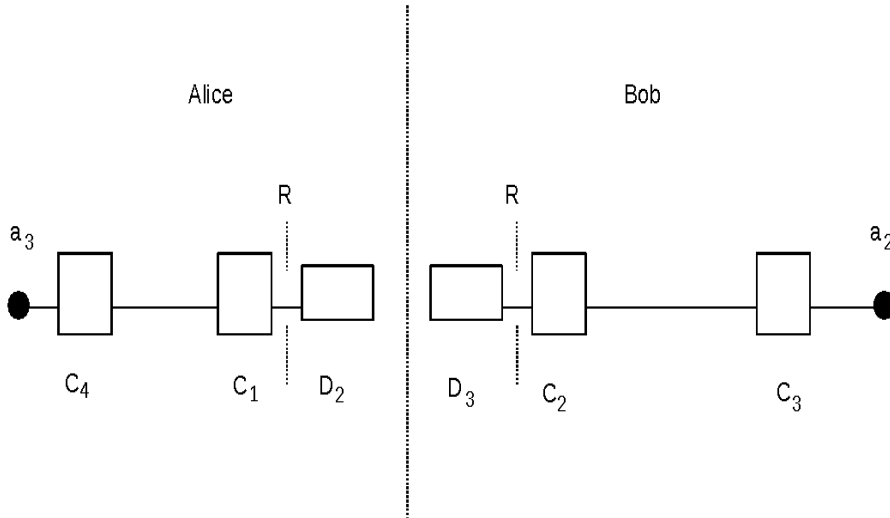


FIGURE 2.5: Setup for Experiment 4. Alice does the same as she did in Experiment 3, while Bob does the same as in Experiment 2.

2.3.4 Conclusion from the experimental outcomes

Here, we discuss the results of four different experiments. Experiment-4 shows contradiction when combined with other three experiments. According to the logic of Experiment-3, if Alice finds a photon in cavity C_1 , she concludes that Bob must detect a photon if he directly checks the photon state of his cavity C_2 without using auxiliary resource of C_3 and a_2 . Similarly, using the logic of Experiment-2, when Bob finds a photon in the cavity C_2 , he infers that Alice's would get a photon in the cavity C_1 when she measures the cavity photon state of C_1 without using any auxiliary resource such as C_4 and a_3 . However, Experiment-1 prohibits both them to detect a photon each by directly checking for it in their respective cavities C_1 and C_2 without using their auxiliary resources. The contradiction arises from the fact that the above inferences of Alice and Bob are based on the criterion of locality [Hardy, 1994]. According to the locality criterion, the probability of Bob obtaining an outcome is independent on whether Alice performs local operation or not, and vice versa. Without assuming locality, there is no contradiction. Hence, we conclude the presence of single particle (photon) non-locality.

2.3.5 Summary and outlook

We compare our scheme to show the the presence of non-locality at single particle level with the earlier works performed by Hardy [Hardy, 1994] and Dunningham and vedral [Dunningham and Vedral, 2007]. Apart from the analogous nature of the argument leading to the above mentioned contradiction with the locality assumption, the algebra of the relevant states bears formal resemblance to those used in the earlier works [Dunningham and Vedral, 2007; Grangier, Roger, and Aspect, 1986; Hardy, 1994]. In the present scheme, we have used a two level atom passing through two initially empty cavities to generate the entangled state (shared between Alice and Bob) at the single particle level, instead of using beam splitters and incident vacuum modes. Also, there are some differences in the detection mechanism used in Experiments-2,3 and 4. Here we have used auxiliary cavities and additional two level atoms, instead of the homodyne detection scheme. In our scheme, the two-photon terms vanish by choosing the interaction parameters, whereas, in the scheme [Dunningham and Vedral, 2007], the two-photon terms are avoided by state truncation method. Note that the

choice of the velocities of the atoms that we have proposed in the various experiments ($v_{a_1} = 179$ m/s, and $v_{a_2} = v_{a_3} = 161$ m/s) fall within the thermally accessible range of velocities [Angelakis and Knight, 2002; Vats and Rudolph, 2001]. The values for the other interaction parameter ($k \equiv \hat{\mathbf{d}}_{eg} \cdot \hat{\mathbf{e}}(\mathbf{r})$) that we have chosen ($k(a_1; C_1) = 0.979$, $k(a_1; C_2) = k(a_2; C_2) = k(a_3; C_1) = 1$, and $k(a_2; C_3) < 1$, $k(a_3; C_4) < 1$), should also be attainable [Pramanik et al., 2012]. Further, resonant interactions between atoms and cavities enables us to avoid using coherent [Hardy, 1994] or mixed states [Dunningham and Vedral, 2007] that may be difficult to create experimentally. Hence, our proposal [Pramanik et al., 2012] is based on generating atom-cavity entanglement that has already been practically operational for many years now [Raimond, Brune, and Haroche, 2001]. Thus, our scheme should facilitate testing the non-locality of single photons in an actual experiment free of conceptual loopholes. In the next chapter we will focus on a slightly different manifestation of single particle non-locality, viz., intra-particle entanglement and its application to information processing.

Chapter 3

Intra-particle entanglement and its application

3.1 Intra-particle entanglement

Intra-particle entanglement is the entanglement between different degrees of freedom of the same particle. Recent experiments have explored the possibility of generating entanglement between polarization and linear momentum [Boschi et al., 1998; Michler, Weinfurter, and Zukowski, 2000], and polarization and angular momentum [Barreiro, Wei, and Kwiat, 2008] of a single particle. In order to demonstrate contextuality of quantum mechanics, the path-spin entanglement of a single spin-1/2 particle was proposed [Basu et al., 2001]. Experiments [Hasegawa et al., 2003] confirmed the existence of such path-spin intra-particle entanglement for single neutron. It is possible to swap intra-particle entanglement onto the standard inter-particle entanglement of two qubits [Adhikari et al., 2010]. In [Pramanik et al., 2010], we have shown the procedure of generating the entanglement between the path and spin degrees of freedom of a spin-1/2 particle, with the help of a beam splitter and spin flipper. Using this path-spin entanglement as a resource, we have formulated a protocol for transferring of the state of an unknown qubit to a distant location.

3.2 Creation of path-spin entanglement of a spin-1/2 particle

Let Alice prepares a spin-1/2 particle (say, 1st particle) which is polarized along ‘+ \hat{z} ’-axis, i.e., the particle initially is in the state $|0\rangle_s \left(= \begin{pmatrix} 1 \\ 0 \end{pmatrix} \right)$. By considering the path (or position) variable, the joint path-spin state of the 1st particle is given by

$$|\mathbf{S}\rangle_{ps}^1 = |\psi_0\rangle_p^1 \otimes |0\rangle_s^1 \quad (3.1)$$

where the subscripts ‘p’ and ‘s’ label the path and spin variables, respectively, and the subscript ‘1’ labels the 1st particle. Then, the particle is passed through a beam-splitter (BS1). Since, the beam splitter affects only the path state without disturbing the spin state of the particles, the input and output relation is described by the unitary rotation

$$\begin{pmatrix} |\psi_0\rangle_p \\ |\psi_0^\perp\rangle_p \end{pmatrix} = \begin{pmatrix} \alpha & i\beta \\ -\beta & i\alpha \end{pmatrix} \begin{pmatrix} |1\rangle_p \\ |0\rangle_p \end{pmatrix} \quad (3.2)$$

where α and β are real and satisfy the relation $\alpha^2 + \beta^2 = 1$. α^2 and β^2 give the transmission and reflection probabilities, respectively. The reflected and transmitted paths are labeled by $|0\rangle_p \left(\equiv \begin{pmatrix} 1 \\ 0 \end{pmatrix} \right)$ and $|1\rangle_p \left(\equiv \begin{pmatrix} 0 \\ 1 \end{pmatrix} \right)$, respectively, and they are orthogonal to each other. For the purpose of finding the particle in the reflected path, the projector $P(|0\rangle_p) (= |0\rangle_p\langle 0|$ which gives the value ‘+1’ when particle is found in the reflected path) is measured and for the transmitted path, the projector $P(|1\rangle_p) (= |1\rangle_p\langle 1|$ which gives the value ‘-1’ when the particle is found in the transmitted path) is measured.

The state of the 1st particle emergent from BS1 is given by

$$|\mathbf{S}_1\rangle_{ps}^1 = (\alpha|1\rangle_p^1 + i\beta|0\rangle_p^1) \otimes |0\rangle_s^1. \quad (3.3)$$

Next, we place a spin flipper (SF) in the reflected path which flips the spin states, i.e., $|0\rangle_s^1 \rightarrow |1\rangle_s^1$ or vice-versa. In the experimental situation, the spin flipper is realized by a uniform magnetic field directed along $+\hat{x}$ -axis. Due to the effect of

SF, The state of the 1st particle becomes

$$|\mathbf{S}_2\rangle_{ps}^1 = \alpha|0\rangle_s|1\rangle_p + i\beta|1\rangle_s|0\rangle_p. \quad (3.4)$$

The state $|\mathbf{S}_2\rangle_{ps}^1$ is entangled between path and spin degrees of freedom of the 1st particle, i.e., the intra-particle entanglement is created. The state preparation is shown in the Figure 3.1. After preparing the path-spin state, Alice uses it to perform different information processing tasks, such as, sending an unknown quantum state to Bob separated at a distant location.

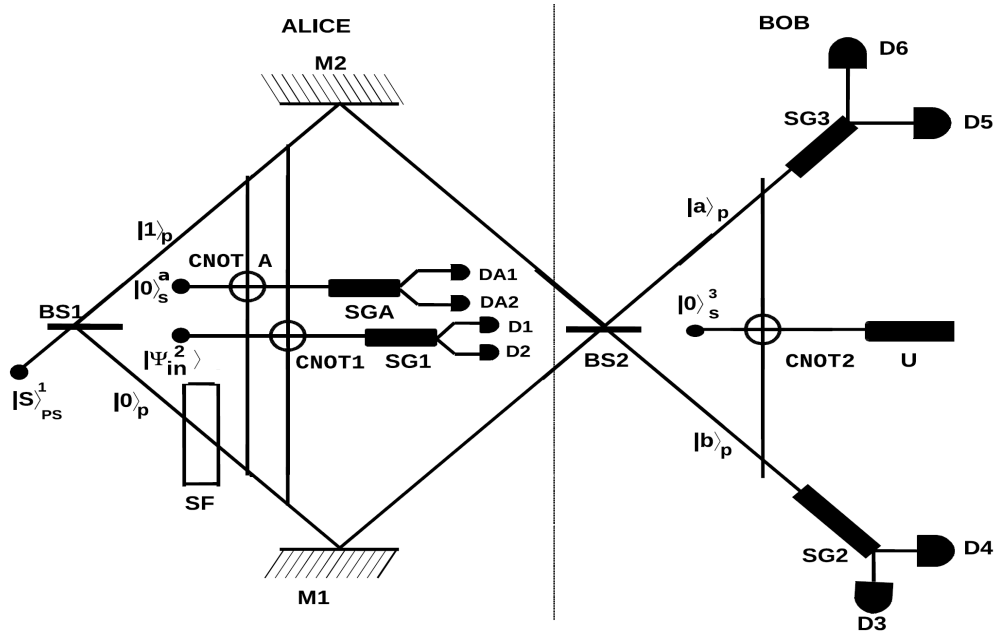


FIGURE 3.1: A spin-1/2 particle (labelled as particle 1) with an initial spin polarized state $|0\rangle_s^1$ falls on the beam-splitter BS1. A spin-flipper is placed along the reflected channel (labelled by $|0\rangle_p^1$). A CNOT operation is performed by Alice involving this particle and another particle (labelled as “a”). A second CNOT operation is performed involving particle 1 and her second particle (2) which is in an unknown state $|\psi^{in}\rangle$. Alice sends the particle (1) to Bob who lets this particle fall on the beam-splitter BS2. A CNOT operation is performed by Bob involving this particle and another particle (3) possessed by him (labelled as $|0\rangle_s^3$). Bob measures the spin of the particle (1) using the Stern-Gerlach devices SG2 and SG3. Alice then measures the spins of the particle (2) and particle (a) using the SternGerlach devices SG1 and SGA along the z-axis. According to the results of the spin measurements through SG1 and SGA (communicated classically by Alice to Bob), and through SG2 or SG3 (as performed by Bob), he applies a suitable unitary operation (U) on his particle (3) in order to recreate the original state $|\phi^{in}\rangle$ possessed by Alice.

3.3 Path-spin entanglement as a resource

For the purpose of sending an unknown quantum state of a particle labeled by ‘2’ given by

$$|\psi\rangle_2 = a|0\rangle_2 + b|1\rangle_2, \quad (3.5)$$

where $|a|^2 + |b|^2 = 1$, at a distant location, we have given an information transferring protocol. According to this protocol, Alice prepares a path-spin hybrid entangled state, and a particle (i.e., 2nd particle) in an unknown quantum state is given to Alice whose task is to send that unknown state to Bob located at a distant place. To protect the information about the unknown quantum state (which will be discuss later), Alice prepares an auxiliary particle (labeled by ‘a’) in the state $|0\rangle_s^a$. In the beginning of our protocol, Alice makes a CNOT operation where the 1st particle’s spin state acts as a control qubit and auxiliary particle’s spin state acts as a target qubit. After the CNOT operation the combined state of the 1st and the auxiliary particle is given by

$$|S_3\rangle_{pss}^{1a} = (\alpha|1\rangle_p^1|0\rangle_s^1|0\rangle_s^a + i\beta|0\rangle_p^1|1\rangle_s^1|1\rangle_s^a). \quad (3.6)$$

In the next step, Alice makes another CNOT operation where the 1st particle’s spin state acts as a control qubit and the second particle’s spin state (given by Eq.(3.5)) acts as a target qubit. The resultant combined state of the three particles is given by

$$\begin{aligned} |\psi\rangle^{12a} = & \alpha a|1\rangle_p^1|0\rangle_s^1|0\rangle_s^2|0\rangle_s^a + i\beta a|0\rangle_p^1|1\rangle_s^1|1\rangle_s^2|1\rangle_s^a \\ & + \alpha b|1\rangle_p^1|0\rangle_s^1|1\rangle_s^2|0\rangle_s^a + i\beta b|0\rangle_p^1|1\rangle_s^1|0\rangle_s^2|1\rangle_s^a \end{aligned} \quad (3.7)$$

Note here that the CNOT operations performed by Alice do not depend on the paths (i.e., reflected and transmitted paths) of the 1st particle after emerging from the beam splitter. The CNOT operations have to be done after making path-spin entanglement without which the protocol has no advantage as in this step, Alice encodes the information about the unknown state with the path-spin entangled particle and the auxiliary particle.

After completing the encoding, Alice sends the path-spin entangled particle, i.e., the first particle to Bob over the classical channel. When Bob confirms that he

has received the particle, Alice makes a spin measurement along the ‘ z ’-axis on her 2nd particle and another spin measurement along the ‘ x ’-axis on her auxiliary particle (labeled by ‘ a ’) with the help of Stern-Gerlach devices (SG1 in Fig.3.1). The observables corresponding to the spin measurements along z - and x - axis are given by σ_z and σ_x , respectively. Eq.(3.7) can be rewritten as

$$\begin{aligned}
|\psi\rangle^{12a} = & \frac{1}{\sqrt{2}}[(a\alpha|1\rangle_p^1|0\rangle_s^1 + ib\beta|0\rangle_p^1|1\rangle_s^1)|0\rangle_s^2|0_x\rangle_s^a \\
& + (a\alpha|1\rangle_p^1|0\rangle_s^1 - ib\beta|0\rangle_p^1|1\rangle_s^1)|0\rangle_s^2|1_x\rangle_s^a \\
& + (ia\beta|0\rangle_p^1|1\rangle_s^1 + b\alpha|1\rangle_p^1|0\rangle_s^1)|1\rangle_s^2|0_x\rangle_s^a \\
& + (-ia\beta|0\rangle_p^1|1\rangle_s^1 + b\alpha|1\rangle_p^1|0\rangle_s^1)|1\rangle_s^2|1_x\rangle_s^a], \quad (3.8)
\end{aligned}$$

where $|0_x\rangle_s^1 \equiv \frac{|0\rangle_s^1 + |1\rangle_s^1}{\sqrt{2}}$ ($|1_x\rangle_s^1 \equiv \frac{|0\rangle_s^1 - |1\rangle_s^1}{\sqrt{2}}$) is the spin up (spin down) state along the x -direction. Using the Eq.(3.8), one can construct the Table 3.1 which gives the states of the 1st particle possessed by Bob corresponding to the possible measurement outcomes for the spin measurements on Alice’s second particle and the auxiliary particle with respective probabilities.

TABLE 3.1: States of 1st particle after Alice’s measurement outcome for the measurement on her 2nd and auxiliary particle with respective probabilities

Spin measurement of 2nd and auxiliary particle	State of 1st particle after spin measurement	Probability of spin measurement
$ 0\rangle_s^2 0_x\rangle_s^a$	$a\alpha 1\rangle_p^1 0\rangle_s^1 + ib\beta 0\rangle_p^1 1\rangle_s^1$	$\frac{a^2\gamma^2 + b^2\beta^2}{2}$
$ 0\rangle_s^2 1_x\rangle_s^a$	$a\alpha 1\rangle_p^1 0\rangle_s^1 - ib\beta 0\rangle_p^1 1\rangle_s^1$	$\frac{a^2\gamma^2 + b^2\beta^2}{2}$
$ 1\rangle_s^2 0_x\rangle_s^a$	$a\beta 0\rangle_p^1 1\rangle_s^1 - ib\alpha 1\rangle_p^1 0\rangle_s^1$	$\frac{a^2\beta^2 + b^2\alpha^2}{2}$
$ 1\rangle_s^2 1_x\rangle_s^a$	$a\beta 0\rangle_p^1 1\rangle_s^1 + ib\alpha 1\rangle_p^1 0\rangle_s^1$	$\frac{a^2\beta^2 + b^2\alpha^2}{2}$

Subsequently, Alice communicates 2-cbits to Bob to inform about her spin measurement outcomes on the 2nd particle and the auxiliary particle. To recreate the unknown state at his location, Bob takes another particle, say 3rd particle in the spin up state, i.e, $|0\rangle_s^3$ together with the 1st particle which Alice sends to him and performs following operations depending upon Alice’s measurement outcomes :

Case I. Here we consider the case when Alice gets spin up ($|0\rangle_s^2$) state for the measurement of σ_z on her 2nd particle and spin up ($|0_x\rangle_s^2$) state for the measurement of σ_x on her auxiliary particle. This event occurs with the probability

$$P(0_Z 0_x) = \frac{a^2 \gamma^2 + b^2 \beta^2}{2}.$$

In this case, after getting the particle, Bob sends it through the 50 – 50 beam splitter (BS2 in Figure 3.1). The actions of the beam splitter on the states $|0\rangle_p^1$ and $|1\rangle_p^1$ are given by

$$\begin{aligned} |0\rangle_p^1 &\longrightarrow \frac{1}{\sqrt{2}}[|a\rangle_p^1 + i|b\rangle_p^1] \\ |1\rangle_p^1 &\longrightarrow \frac{1}{\sqrt{2}}[|b\rangle_p^1 + i|a\rangle_p^1], \end{aligned} \quad (3.9)$$

where $|a\rangle_p^1$ and $|b\rangle_p^1$ are the new paths of the 1st particle after emerging from the beam splitter BS2. Now, Bob makes a CNOT operation where the spin states of the 1st particle act as a control qubit, and spin states of the 3rd particle act as a target qubit. The combined state of the two particles after the CNOT operation is given by

$$\begin{aligned} |\psi\rangle^{13} = & \frac{1}{\sqrt{2(a^2\alpha^2 + b^2\beta^2)}} [a\alpha|b\rangle_p^1|0\rangle_s^1|0\rangle_s^3 - b\beta|b\rangle_p^1|1\rangle_s^1|1\rangle_s^3 \\ & + i a\alpha|a\rangle_p^1|0\rangle_s^1|0\rangle_s^3 + i b\beta|a\rangle_p^1|1\rangle_s^1|1\rangle_s^3] \end{aligned} \quad (3.10)$$

Next, Bob measures the spin of the 1st particle using two sets of Stern-Gerlach apparatus SG3 (placed at path $|a\rangle_p$) and SG2 (placed at path $|b\rangle_p$) where the inhomogeneous magnetic field is directed along the x -axis. Bob gets one of the four possible outcomes, i.e., $|a\rangle_p^1 \otimes |0_x\rangle_s^1$, $|a\rangle_p^1 \otimes |1_x\rangle_s^1$, $|b\rangle_p^1 \otimes |0_x\rangle_s^1$, $|b\rangle_p^1 \otimes |1_x\rangle_s^1$ with equal probability $\frac{1}{4}$. Depending upon the exact measurement outcome, Bob performs a suitable unitary operation, given in the Table 3.2, to recreate the state as close as possible to the state, given by Eq.(3.5), for his 3rd particle.

TABLE 3.2: Bob's unitary rotation when Alice gets $|0\rangle_s^2|0_x\rangle_s^a$

Path and spin measurement	unitary rotation	final state of Bob's 3rd particle, $ \psi^{out}\rangle$
$ a\rangle_p^1 \otimes 0_x\rangle_s^1$	I	$\frac{a\alpha 0\rangle_s^3 + b\beta 1\rangle_s^3}{\sqrt{a^2\alpha^2 + b^2\beta^2}}$
$ a\rangle_p^1 \otimes 1_x\rangle_s^1$	σ_z	$\frac{a\alpha 0\rangle_s^3 + b\beta 1\rangle_s^3}{\sqrt{a^2\alpha^2 + b^2\beta^2}}$
$ b\rangle_p^1 \otimes 0_x\rangle_s^1$	σ_z	$\frac{a\alpha 0\rangle_s^3 + b\beta 1\rangle_s^3}{\sqrt{a^2\alpha^2 + b^2\beta^2}}$
$ b\rangle_p^1 \otimes 1_x\rangle_s^1$	I	$\frac{a\alpha 0\rangle_s^3 + b\beta 1\rangle_s^3}{\sqrt{a^2\alpha^2 + b^2\beta^2}}$

In this case, the average fidelity (where average is taken over all Bob's outcomes) of the state transfer process is given by

$$F_{av}^1 = \overline{|\langle \psi^{in} | \psi^{out} \rangle|^2} = \frac{(a^2\alpha + b^2\beta)^2}{a^2\alpha^2 + b^2\beta^2}. \quad (3.11)$$

Case II. In this case we consider that Alice's spin measurement on her 2nd particle reveals a spin up state ($|0\rangle_s^2$), and the measurement on the auxiliary particle reveals a spin down state ($|1\rangle_s^a$). This event occurs with probability $P(0_Z1_x) = \frac{a^2\gamma^2 + b^2\beta^2}{2}$.

Bob follows the same procedures as in the Case I, i.e., he sends the 1st particle (sent by Alice) through the 50–50 beam splitter, subsequently makes a CNOT operation with it and the 3rd particle, and then measures the spin of the 1st particle using his Stern-Gerlach apparatus. Finally, depending on his measurement outcomes, he makes a suitable unitary rotation as shown in the Table 3.3. The average fidelity of the state transfer is same as F_{av}^1 given by Eq.(3.11).

TABLE 3.3: Bob's unitary rotation when Alice gets $|0\rangle_s^2|1\rangle_s^a$

Path and spin measurement	unitary rotation	final state of Bob's 3rd particle, $ \psi^{out}\rangle$
$ a\rangle_p^1 \otimes 0\rangle_s^1$	σ_z	$\frac{a\alpha 0\rangle_s^3 + b\beta 1\rangle_s^3}{\sqrt{a^2\alpha^2 + b^2\beta^2}}$
$ a\rangle_p^1 \otimes 1\rangle_s^1$	I	$\frac{a\alpha 0\rangle_s^3 + b\beta 1\rangle_s^3}{\sqrt{a^2\alpha^2 + b^2\beta^2}}$
$ b\rangle_p^1 \otimes 0\rangle_s^1$	I	$\frac{a\alpha 0\rangle_s^3 + b\beta 1\rangle_s^3}{\sqrt{a^2\alpha^2 + b^2\beta^2}}$
$ b\rangle_p^1 \otimes 1\rangle_s^1$	σ_z	$\frac{a\alpha 0\rangle_s^3 + b\beta 1\rangle_s^3}{\sqrt{a^2\alpha^2 + b^2\beta^2}}$

Case III. Here we consider that Alice's spin measurement on her 2nd particle reveals a spin down state ($|1\rangle_s^2$) and, the measurement on the auxiliary particle reveals a spin up state ($|0\rangle_s^a$). This event occurs with probability $P(1_Z0_x) = \frac{a^2\beta^2 + b^2\alpha^2}{2}$.

Bob again follows a similar procedure as in Cases I and II. The possible unitary operations that he has to perform are listed in the Table 3.4. In this case, the average fidelity of state transfer is given by

$$F_{av}^2 = \overline{|\langle \psi^{in} | \psi^{out} \rangle|^2} = \frac{(a^2\beta + b^2\alpha)^2}{a^2\beta^2 + b^2\alpha^2}. \quad (3.12)$$

TABLE 3.4: Bob's unitary rotation when Alice gets $|1\rangle_s^2|0_x\rangle_s^a$

Path and spin measurement	unitary rotation	final state of Bob's 3rd particle, $ \psi^{out}\rangle$
$ a\rangle_p^1 \otimes 0_x\rangle_s^1$	σ_x	$\frac{a\beta 0\rangle_s^3 + b\alpha 1\rangle_s^3}{\sqrt{a^2\beta^2 + b^2\alpha^2}}$
$ a\rangle_p^1 \otimes 1_x\rangle_s^1$	$i\sigma_y$	$\frac{a\beta 0\rangle_s^3 + b\alpha 1\rangle_s^3}{\sqrt{a^2\beta^2 + b^2\alpha^2}}$
$ b\rangle_p^1 \otimes 0_x\rangle_s^1$	$i\sigma_y$	$\frac{a\beta 0\rangle_s^3 + b\alpha 1\rangle_s^3}{\sqrt{a^2\beta^2 + b^2\alpha^2}}$
$ b\rangle_p^1 \otimes 1_x\rangle_s^1$	σ_x	$\frac{a\beta 0\rangle_s^3 + b\alpha 1\rangle_s^3}{\sqrt{a^2\beta^2 + b^2\alpha^2}}$

Case IV. Here we consider that Alice's spin measurement on her 2nd particle reveals a spin down state ($|1\rangle_s^2$) and, the measurement on the auxiliary particle reveals a spin up state ($|1_x\rangle_s^a$). This event occurs with probability $P(1_Z 1_x) = \frac{a^2\beta^2 + b^2\alpha^2}{2}$.

Bob again follows a similar procedure as in Cases I, II and III. The possible unitary operations that he has to perform are listed in Table 3.5. In this case, the average fidelity of state transfer is same as F_{av}^2 , given by Eq.(3.12).

TABLE 3.5: Bob's unitary rotation when Alice gets $|1\rangle_s^2|1_x\rangle_s^a$

Path and spin measurement	unitary rotation	final state of Bob's 3rd particle, $ \psi^{out}\rangle$
$ a\rangle_p^1 \otimes 0_x\rangle_s^1$	$i\sigma_y$	$\frac{a\beta 0\rangle_s^3 + b\alpha 1\rangle_s^3}{\sqrt{a^2\beta^2 + b^2\alpha^2}}$
$ a\rangle_p^1 \otimes 1_x\rangle_s^1$	σ_x	$\frac{a\beta 0\rangle_s^3 + b\alpha 1\rangle_s^3}{\sqrt{a^2\beta^2 + b^2\alpha^2}}$
$ b\rangle_p^1 \otimes 0_x\rangle_s^1$	σ_x	$\frac{a\beta 0\rangle_s^3 + b\alpha 1\rangle_s^3}{\sqrt{a^2\beta^2 + b^2\alpha^2}}$
$ b\rangle_p^1 \otimes 1_x\rangle_s^1$	$i\sigma_y$	$\frac{a\beta 0\rangle_s^3 + b\alpha 1\rangle_s^3}{\sqrt{a^2\beta^2 + b^2\alpha^2}}$

Considering all the four cases together, it follows from Eqs. (3.11) and (3.12), and the fact that Alice gets four different outcomes with probability shown in the Table 3.1, that the average fidelity (where the average is taken over all possible

outcomes at Alice's side and Bob's side) of state transfer is given by

$$\begin{aligned} F_{av} &= (P(0_z0_x) + P(0_z1_x))F_{av}^1 + (P(1_z0_x) + P(1_z1_x))F_{av}^2 \\ &= a^4 + b^4 + 4\alpha\beta a^2b^2. \end{aligned} \quad (3.13)$$

If the path-spin entangled state of Alice's 1st particles is maximally entangled, i.e., $\alpha = \beta = \frac{1}{\sqrt{2}}$ (which is experimentally realized when Alice uses a 50 – 50 beam splitter), the average fidelity is equal to 1. In this case, Alice perfectly teleports the unknown state, i.e., at the end of the protocol, Bob's 3rd particle state is same as Alice's initial unknown state of the 2nd particle.

3.4 Summary and outlook

To summarize, in this work we have shown that using the entanglement between different degrees of freedom of the same particle, one can transfer the state of unknown qubit at a distant location. To accomplish this protocol, we have used beam splitters, a spin flipper, CNOT gates, Stern-Gerlach devices for the spin measurement and unitary transformations. Our protocol may be viewed as a variant of the standard teleportation scheme for a single qubit. The difference here is that since the resource of intra-particle entanglement cannot be initially shared between the two distant parties, the resource particle itself has to be transferred from Alice to Bob at some stage. Note however, that Alice keeps the particle whose state is teleported at his location, and Alice's measurement destroys the initial unknown state of the 2nd particle, thus avoiding any conflict with the no-cloning theorem. It may be noted here that the act of physically sending one or more particles across distances is an unavoidable component of information theoretic protocols involved with setting-up entanglement over distances. Whereas, in the standard teleportation scheme, this process has to be initiated at the beginning in order to set-up a shared entangled state between two parties, in the present scheme involving path-spin entanglement of a single particle, the particle is sent from Alice to Bob in the middle of the protocol.

As Alice sends the path-spin entangled particle to Bob over the channel, it is natural to ask the question – is the information about the unknown state of the 2nd particle lost when the 1st particle is lost in transit? Here we show that even if the particle is intercepted by say, a different receiver Eve (instead of Bob) it is

impossible for Eve to extract the information encoded in the 2nd particle. The Eq.(3.7) can be rewritten as

$$|\psi\rangle^{12a} = \alpha|1\rangle_p^1|0\rangle_s^1(a|0\rangle_s^2 + b|1\rangle_s^2)|0\rangle_s^a + i\beta|0\rangle_p^1|1\rangle_s^1(a|1\rangle_s^2 + b|0\rangle_s^2)|1\rangle_s^a. \quad (3.14)$$

Now, consider the scenario that the path-spin entangled particle is held by Eve (instead of Bob), and the auxiliary particle ‘a’ and the 2nd particle are held by Alice. From the Eq.(3.14), it is clear that whatever local operations are performed by Eve on the 1st particle, Eve is unable to get any information about the state of 2nd particle given by Eq.(3.5). Eve would be successful in her task only if Alice were to make the measurement on the 2nd particle before sending the 1st particle. Further, it is also possible for Alice to restore the unknown quantum state in the 2nd particle. When Bob confirms to Alice that he didn’t get the particle, Alice makes a spin measurement on her auxiliary particle in the z -direction. According to the measurement outcome, she performs a suitable unitary transformation on her 2nd particle – either Alice does nothing when she gets $|0\rangle_s^a$ or applies the unitary operation σ_x when she gets $|1\rangle_s^a$, to restore the unknown state to be teleported corresponding to the 2nd particle. Note that the auxiliary particle is used to protect the the information about the unknown state to be teleported when the path-spin entangled particle is lost in the transit.

In conclusion, it may be considerably easier to create the intra-particle path-spin entanglement using beam-splitters, and spin flipper, as we have shown, than generating inter-particle entanglement through the controlled interaction of two particles. Since one does not have to preserve the entanglement between two distant parties, our scheme should be less susceptible to decoherence effects, and thus provides an advantage over the standard scheme using two entangled qubits. The path (or linear momentum) degrees of freedom for physical particles are always present in any experimental set-up. Here we have exploited these path variables to first generate path-spin entanglement at the level of a single particle, and then use it as physical resource for performing teleportation. This opens up the possibility of exploiting path-spin intra-particle entanglement for performing further information theoretic tasks. It may be also noted that though our protocol is demonstrated here for spin-1/2 particles such as neutrons, it could be easily implemented for other types of quanta such as photons using suitable optical devices. Finally, our analysis generally reemphasizes the notion that entanglement is a fundamental

concept independent of either any particular physical realization of Hilbert space [Ma et al., 2009; Zukowski and Zeilinger, 1991], or delocalisability of the involved modes, and specifically highlights that hybrid entanglement at the level of a single particle [Basu et al., 2001; Hasegawa et al., 2003] could be regarded as a real physical resource.

Chapter 4

The fine-grained uncertainty relation and non-local games

A lot of research has been done to improve the uncertainty relation first proposed by Heisenberg [Heisenberg, 1927]. The uncertainty captured by the standard deviation has been upgraded by the entropic uncertainty relation (EUR) [Deutsch, 1983; Kraus, 1987; Maassen and Uffink, 1988]. The state dependency of the lower bound in the Heisenberg uncertainty relation is also improved in the entropic form. But, the EUR [Maassen and Uffink, 1988] is unable to capture the non-local feature of quantum physics which is revealed by the violation of Bell's inequality. In a recent work, Oppenheim and Wehner [Oppenheim and Wehner, 2010] have introduced a new kind of uncertainty relation, called *fine-grained* uncertainty relation (FUR) which is capable of distinguishing the plurality of simultaneous possible outcomes of a set of measurements.

4.1 Fine-grained uncertainty relation

In the fine-grained uncertainty relation, the uncertainty of a particular measurement outcome (say, the k -th outcome) for the measurement of an observable \mathcal{A} is determined by the corresponding probability p_k . To describe the fine-grained uncertainty relation, we consider an observable t chosen from the set of n observables \mathcal{T} with probability $p(t)$ ($\in \mathcal{D}$, the probability distribution $\{p(t)\}$ of choosing different measurements). Here, the uncertainty of a particular measurement outcome $x^{(t)}$ for the measurement of an observable t is measured by the probability of

obtaining that outcome, i.e., $p(x^{(t)}|t)$, and the average uncertainty where the average is taken over all possible measurements on the state of the observed physical system σ is bounded by [Oppenheim and Wehner, 2010]

$$P(\sigma, \mathbf{x}) := \sum_{t=0}^{n-1} p(t)p(x^{(t)}|t)_\sigma \leq \zeta_{\mathbf{x}}(\mathcal{T}, \mathcal{D}), \quad (4.1)$$

where $P(\sigma, \mathbf{x})$ is the total probability of possible outcomes $\{x^{(1)}, \dots, x^{(n)}\} \in \mathbf{x}$. $\zeta_{\mathbf{x}}(\mathcal{T}, \mathcal{D})$ which gives the maximum probability, is given by

$$\zeta_{\mathbf{x}}(\mathcal{T}, \mathcal{D}) = \max_{\chi} \sum_{t=0}^{n-1} p(t)p(x^{(t)}|t)_\sigma, \quad (4.2)$$

where the maximization is taken over all possible strategies, χ which consists the choice of state σ and the choice of measurements.

The connection of FUR with uncertainty is as follows – when the probability $p(x^{(t)}|t)_\sigma$ is less than unity for any measurement t , there is uncertainty associated with the measurement t , and hence, $\zeta < 1$. We discuss below the applications of FUR to single qubit, bipartite, and tripartite systems. The fine-grained form of the uncertainty relation is able to capture the non-local feature of bipartite [Oppenheim and Wehner, 2010] and tripartite systems [Pramanik and Majumdar, 2012].

4.2 Single qubit system

To describe the fine-grained uncertainty for the single qubit system, we consider the following game. Let us consider that a player, say Alice, initially possesses a qubit in the state ρ_A . She receives a binary question ‘ s ’ $\in \{0, 1\}$ with the probability $p(s)$. For simplicity, here we consider $p(s) = \frac{1}{2}$, i.e., Alice receives questions $s = 0$ and $s = 1$ with equal probability. According to the given question, Alice measures either the observable $\mathcal{A}_0 = \sigma_z$ (i.e., she measures spin along z -direction) when she receives $s = 0$ or the observable $\mathcal{A}_1 = \sigma_x$ (i.e., she measures spin along x -direction) when she receive $s = 1$, on her qubit.

Winning condition : Alice wins the game, if she gets a specific outcome ‘ a ’ (which can take either $a = 0$ for spin up outcome and $a = 1$ for spin down outcome) for the measurement of both σ_x and σ_z on her qubit.

Winning probability : The maximum winning probability for the winning conditions $a = 0$ and $a = 1$ are the same and given by

$$\zeta = \max_{\rho_A} \frac{1}{2} \sum_{s=0}^1 Tr[\mathcal{A}_s^a \rho_A] = \frac{1}{2} + \frac{1}{2\sqrt{2}}, \quad (4.3)$$

where \mathcal{A}_s^a is the projector for the measurement outcome ‘ a ’ of the observable ‘ s ’, i.e.

$$\mathcal{A}_s^a = |a_s\rangle\langle a_s|, \quad (4.4)$$

where $|a_s\rangle$ form basis of the observable A .

Maximally certain state : The state which gives the maximum winning probability, i.e., $\frac{1}{2} + \frac{1}{2\sqrt{2}}$ is called the maximally certain state for that winning condition. For the winning condition $a = 0$ and the set of measurements $\{\sigma_z, \sigma_x\}$, the maximally certain states are $\rho_A^M = \frac{1}{2}(I \pm \frac{\sigma_x + \sigma_z}{2})$, and for the winning condition $a = 1$ and for the same choice of observables, the maximally certain states are $\rho_A^M = \frac{1}{2}(I \pm \frac{\sigma_x - \sigma_z}{2})$.

4.3 Bipartite system

To describe the FUR in the bipartite system, Oppenheim and Wehner [Oppenheim and Wehner, 2010] have considered specific examples of non-local retrieval games (for which there exists only one winning answer for one of the two parties). To capture the non-locality in the bipartite system they gave an example of a non-local retrieval game known as the CHSH game [Clauser et al., 1969]. According to the CHSH game, Alice and Bob are given the questions ‘ s ’ (chosen from the set $\in \mathcal{S}$) and ‘ t ’ (chosen from the set $\in \mathcal{T}$), respectively, with some probability $p(s, t)$ (which is considered as $p(s)p(t)$, for simplicity); and Alice’s answer ‘ a ’ or Bob’s answer ‘ b ’ will be the winning answer if ‘ a ’ given ‘ b ’ satisfies certain rules, i.e., for every settings ‘ s ’ and the corresponding outcome ‘ a ’ of Alice, there is a

string $\mathbf{x}_{s,a} = (x_{s,a}^{(1)}, \dots, x_{s,a}^t, \dots, x_{s,a}^{(n)})$ of length $n = |\mathcal{T}|$ that determines the correct answer $b = x_{s,a}^t$ for the question ‘ t ’ for Bob.

4.3.1 CHSH game

In the prescribed non-local CHSH game, Alice and Bob receive binary questions $s, t \in \{0, 1\}$ (representing two different measurement settings on each side), respectively and they win the game if their binary outcomes $a, b \in \{0, 1\}$ satisfy the condition $a \oplus b = s t$. Before playing the game, Alice and Bob discuss about the choice of strategies – *i.* the choice of shared state, *ii.* the choice of measurement settings, and once the game starts, they do not communicate with each other. The winning probability of the game for a physical theory described by the bipartite state (σ_{AB}) is bounded by

$$\begin{aligned} P^{\text{game}}(\mathcal{S}, \mathcal{T}, \sigma_{AB}) &= \sum_{s,t} p(s, t) \sum_a p(a, b = x_{s,a}^t | s, t)_{\sigma_{AB}} \\ &\leq P_{\text{max}}^{\text{game}} = \max_{\mathcal{S}, \mathcal{T}, \sigma_{AB}} P^{\text{game}}, \end{aligned} \quad (4.5)$$

where $p(a, b = x_{s,a}^t | s, t)_{\sigma_{AB}}$ is the winning probability when Alice gets outcome ‘ a ’ for her choice of observable ‘ s ’ and Bob’s choice ‘ t ’, and it is given by

$$p(a, b = x_{s,a}^t | s, t)_{\sigma_{AB}} = \sum_b V(a, b | s, t) \langle (\mathcal{A}_s^a \otimes \mathcal{B}_t^b) \rangle_{\sigma_{AB}}, \quad (4.6)$$

where $\mathcal{A}_s^a (= \frac{I + (-1)^a \mathcal{A}_s}{2})$ is a measurement of the observable \mathcal{A}_s performed by Alice corresponding to setting ‘ s ’ giving outcome ‘ a ’; $\mathcal{B}_t^b (= \frac{I + (-1)^b \mathcal{B}_t}{2})$ is a measurement of the observable \mathcal{B}_s performed by Bob corresponding to setting ‘ t ’ giving outcome ‘ b ’. $V(a, b | s, t)$ is the winning condition given by

$$\begin{aligned} V(a, b | s, t) &= 1 && \text{iff } a \oplus b = s t \\ &= 0 && \text{otherwise.} \end{aligned} \quad (4.7)$$

$P_{\text{max}}^{\text{game}}$ is the maximum winning probability, where maximization is taken over all possible strategies, i.e., σ_{AB} , \mathcal{S} and \mathcal{T} . Using Eqs.(4.5), (4.6) and (4.7) and by considering $p(s, t) = p(s)p(t) = \frac{1}{4}$, one can calculate the expression of $P^{\text{game}}(\mathcal{S}, \mathcal{T}, \sigma_{AB})$

for the bipartite state, σ_{AB} given by

$$P^{\text{game}}(\mathcal{S}, \mathcal{T}, \sigma_{AB}) = \frac{1}{2} \left(1 + \frac{\langle \mathcal{B}_{\text{CHSH}} \rangle_{\sigma_{AB}}}{4} \right), \quad (4.8)$$

where $\mathcal{B}_{\text{CHSH}} = \mathcal{A}_0 \otimes \mathcal{B}_0 + \mathcal{A}_0 \otimes \mathcal{B}_1 + \mathcal{A}_1 \otimes \mathcal{B}_0 - \mathcal{A}_1 \otimes \mathcal{B}_1$, known as the Bell-CHSH operator [Bell, 1964; Clauser et al., 1969].

4.3.2 Non-locality captured by the CHSH game

The importance of FUR in the bipartite system is that FUR gives the different maximum winning probabilities under different physical theories, depending upon the strength of non-locality (captured by the Bell-CHSH inequality) of the corresponding physical theory in the bipartite system for the CHSH game. The maximum winning probability $P_{\text{max}}^{\text{game}}$ of the CHSH game in classical physics is $\frac{3}{4}$ (as classically, the Bell-CHSH inequality is bounded by 2), in quantum physics is $(\frac{1}{2} + \frac{1}{2\sqrt{2}})$ (due to the maximum violation of Bell inequality, $\mathcal{B}_{\text{CHSH}} = 2\sqrt{2}$), and by no-signaling theory with maximum Bell violation ($\mathcal{B}_{\text{CHSH}} = 4$, that occurs for the Popescu-Rohrlich box [Popescu and Rohrlich, 1994]) is 1.

4.4 Tripartite system

In [Pramanik and Majumdar, 2012], we have generalized the fine-grained uncertainty relation for the case of tripartite systems. To discriminate between different no-signaling theories on the basis of their degree of non-locality, we consider three different non-local retrieval games similar to the CHSH game for bipartite systems. Here, Alice, Bob and Charlie receive binary questions ‘ s ’, ‘ t ’, and ‘ u ’ $\in \{0, 1\}$. According to the given question, each player measures an observable chosen from the set of two observables. If their answer ‘ a ’, ‘ b ’, and ‘ c ’ $\in \{0, 1\}$ (which corresponds to their respective measurement outcomes) satisfy certain rules, they win the game.

Winning condition : We restrict our analysis to the three kinds of no-signaling boxes, known as full correlation boxes, for which one or two-party correlations in the system vanishes [Barrett et al., 2005; Pironio, Bancal, and Scarani, 2011]. The players Alice, Bob, and Charlie win the game, if Alice’s answer ‘ a ’, Bob’s

answer ‘ b ’, and Charlie’s answer ‘ c ’ (where the binary answers correspond to the measurement outcome of their respective system) satisfy the set of rules given by

$$\text{either} \quad a \oplus b \oplus c = s t + t u + u s \quad (4.9)$$

$$\text{or} \quad a \oplus b \oplus c = s t + s u \quad (4.10)$$

$$\text{or else} \quad a \oplus b \oplus c = s t u \quad (4.11)$$

The Mermin inequality is violated by all three boxes [Mermin, 1990], whereas the box (known as the Svetlichny box) given by Eq.(4.9) only violates the Svetlichny inequality [Svetlichny, 1987].

Winning probability : Under the physical theory described by a shared tripartite state σ_{ABC} , Alice, Bob, and Charlie win the game (ruled by the winning condition given by either of Eqs. (4.9), (4.10) and (4.11)) with a probability bounded by

$$\begin{aligned} P^{\text{game}}(\mathcal{S}, \mathcal{T}, \mathcal{U}, \sigma_{ABC}) &= \sum_{s,t,u} p(s, t, u) \sum_{a,b} p(a, b, c = x_{s,t,a,b}^{(u)} | s, t, u)_{\sigma_{ABC}} \\ &\leq P_{\max}^{\text{game}}, \end{aligned} \quad (4.12)$$

where $p(s, t, u)$ is the probability that Alice receives question ‘ s ’, Bob ‘ t ’, and Charlie ‘ u ’, and $p(a, b, c = x_{s,t,a,b}^{(u)} | s, t, u)_{\sigma_{ABC}}$ is the winning probability when Alice gets the measurement outcome ‘ a ’ for the measurement setting ‘ s ’, Bob gets the measurement outcome ‘ b ’ for the measurement setting ‘ t ’, and Charlie gets the measurement outcome ‘ c ’ for the measurement setting ‘ u ’, given by

$$p(a, b, c = x_{s,t,a,b}^{(u)} | s, t, u)_{\sigma_{ABC}} = \sum_c V(a, b, c | s, t, u) \langle \mathcal{A}_s^a \otimes \mathcal{B}_t^b \otimes \mathcal{C}_u^c \rangle_{\sigma_{ABC}}, \quad (4.13)$$

where \mathcal{A}_s^a , \mathcal{B}_t^b , and \mathcal{C}_u^c are the measurement corresponding to setting ‘ s ’ and outcome ‘ a ’ at Alice’s side, setting ‘ t ’ and outcome ‘ b ’ at Bob’s side, setting ‘ u ’ and outcome ‘ c ’ at Charlie’s side, respectively. $V(a, b, c | s, t, u)$ inserts the winning condition given by either of Eqs.(4.10), (4.10) and (4.11) in the probability $p(a, b, c = x_{s,t,a,b}^{(u)} | s, t, u)_{\sigma_{ABC}}$ and makes it winning probability. The maximum winning probability is given by

$$P_{\max}^{\text{game}} = \max_{\mathcal{S}, \mathcal{T}, \mathcal{U}, \sigma_{ABC}} P^{\text{game}}(\mathcal{S}, \mathcal{T}, \mathcal{U}, \sigma_{ABC}), \quad (4.14)$$

where the maximization is taken over all possible measurement settings at respective sides, and the shared tripartite state. The maximum winning probability gives the signature of the allowed probability distribution under that theory. In [Pramanik and Majumdar, 2012] we have studied the cases of classical, quantum, and no-signaling theories with superquantum correlations for the above different full-correlation boxes (rules of the non-local game) separately.

4.4.1 Winning condition characterized by the Svetlichny box

Let us consider a non-local game where the players Alice, Bob, and Charlie win the game if their outcomes are correlated with their input by the Eq.(4.9). Also, for simplicity, we assume that the probability with which the players received the questions is independent of each other, i.e, $p(s, t, u) = p(s)p(t)p(u) = \frac{1}{8}$. With consideration of the above conditions, the expression of $P^{\text{game}}(\mathcal{S}, \mathcal{T}, \mathcal{U}, \sigma_{ABC})$ for the shared state $\sigma_{A,B,C}$ (among Alice, Bob, and Charlie) is given by

$$P^{\text{game}}(\mathcal{S}, \mathcal{T}, \mathcal{U}, \sigma_{ABC}) = \frac{1}{2} \left[1 + \frac{\langle \mathbf{S}_1 \rangle_{\sigma_{ABC}}}{8} \right], \quad (4.15)$$

where

$$\begin{aligned} \mathbf{S}_1 = & \mathcal{A}_0 \otimes \mathcal{B}_0 \otimes \mathcal{C}_0 + \mathcal{A}_0 \otimes \mathcal{B}_0 \otimes \mathcal{C}_1 + \mathcal{A}_0 \otimes \mathcal{B}_1 \otimes \mathcal{C}_0 \\ & + \mathcal{A}_1 \otimes \mathcal{B}_0 \otimes \mathcal{C}_0 - \mathcal{A}_0 \otimes \mathcal{B}_1 \otimes \mathcal{C}_1 - \mathcal{A}_1 \otimes \mathcal{B}_0 \otimes \mathcal{C}_1 \\ & - \mathcal{A}_1 \otimes \mathcal{B}_1 \otimes \mathcal{C}_0 - \mathcal{A}_1 \otimes \mathcal{B}_1 \otimes \mathcal{C}_1. \end{aligned} \quad (4.16)$$

Now, with the help of the Svetlichny inequality [Svetlichny, 1987] given by

$$\langle \mathbf{S}_1 \rangle_{\sigma_{ABC}} \leq 4, \quad (4.17)$$

one can easily find out that the maximum winning probability for any theory supported by local-hidden variables, i.e., classical physics, is $\frac{3}{4}$.

For quantum physics where the inequality (4.17) is violated, we consider two classes of pure entangled states for tripartite systems, i.e., the *GHZ* state, given by

$$|GHZ\rangle_{ABC} = \frac{|000\rangle_{ABC} + |111\rangle_{ABC}}{\sqrt{2}}, \quad (4.18)$$

and the W state, given by

$$|W\rangle_{ABC} = \frac{|001\rangle_{ABC} + |010\rangle_{ABC} + |100\rangle_{ABC}}{\sqrt{3}}. \quad (4.19)$$

The maximum violation of the Svetlichny inequality occurs for the GHZ state, and is given by the amount $4\sqrt{2}$ [Ajoy and Rungta, 2010; Collins et al., 2002; Mitchell, Popescu, and Roberts, 2004; Seevinck and Svetlichny, 2002], whereas the W state violates the Svetlichney inequality by an amount 4.354 [Cereceda, 2002]. Hence, the value of P_{\max}^{game} allowed in quantum physics is $\frac{1}{2} + \frac{1}{2\sqrt{2}}$. For the case of no-signaling theory, the algebraic maximum of the Svetlichny inequality is 8 [Barrett et al., 2005; Pironio, Bancal, and Scarani, 2011], and the value of P_{\max}^{game} in this case is 1, corresponding to a correlation with maximum non-locality [Pramanik and Majumdar, 2012].

4.4.2 Winning condition characterized by $a \oplus b \oplus c = s t + s u$

In this case, Alice, Bob and Charlie win the game if their input (i.e., measurement settings) and output (i.e., measurement outcomes) are correlated by the Eq.(4.10). The winning probability $P^{\text{game}}(\mathcal{S}, \mathcal{T}, \mathcal{U}, \sigma_{ABC})$ is given by

$$P^{\text{game}}(\mathcal{S}, \mathcal{T}, \mathcal{U}, \sigma_{ABC}) = \frac{1}{2} \left[1 + \frac{\langle \mathbf{S}_2 \rangle_{\sigma_{ABC}}}{8} \right], \quad (4.20)$$

where

$$\begin{aligned} \mathbf{S}_2 = & \mathcal{A}_0 \otimes \mathcal{B}_0 \otimes \mathcal{C}_0 + \mathcal{A}_0 \otimes \mathcal{B}_0 \otimes \mathcal{C}_1 + \mathcal{A}_0 \otimes \mathcal{B}_1 \otimes \mathcal{C}_0 \\ & + \mathcal{A}_1 \otimes \mathcal{B}_0 \otimes \mathcal{C}_0 + \mathcal{A}_0 \otimes \mathcal{B}_1 \otimes \mathcal{C}_1 - \mathcal{A}_1 \otimes \mathcal{B}_0 \otimes \mathcal{C}_1 \\ & - \mathcal{A}_1 \otimes \mathcal{B}_1 \otimes \mathcal{C}_0 + \mathcal{A}_1 \otimes \mathcal{B}_1 \otimes \mathcal{C}_1. \end{aligned} \quad (4.21)$$

It can be seen that the maximum value of $\langle \mathbf{S}_2 \rangle_{\sigma_{ABC}}$ is 4, when all the variables $\mathcal{A}_i, \mathcal{B}_i, \mathcal{C}_i$ take value either '+1' or '-1'. Hence, the value of P_{\max}^{game} for classical physics is $\frac{3}{4}$. To find out the maximum value of $\langle \mathbf{S}_2 \rangle_{\sigma_{ABC}}$ in quantum physics, we maximize $\langle \mathbf{S}_2 \rangle_{\sigma_{ABC}} = \text{Tr}[\mathbf{S}_2 \sigma_{ABC}]$ over spin-up and spin-down measurements along all possible unit Bloch vectors on both the GHZ and the W state. The projector for the spin measurements along the unit Bloch vector \vec{n}^{X_α} is given by

$$\Pi_{X_\alpha}^\pm = \frac{1}{2}(I \pm \vec{n}^{X_\alpha} \cdot \vec{\sigma}), \quad (4.22)$$

where $\vec{n}^{X_\alpha} (\equiv \{\sin(\theta_{X_\alpha}) \cos(\phi_{X_\alpha}), \sin(\theta_{X_\alpha}) \sin(\phi_{X_\alpha}), \cos(\theta_{X_\alpha})\})$; $\vec{\sigma} \equiv \{\sigma_x, \sigma_y, \sigma_z\}$ are the Pauli matrices with with $X = A$ (for Alice), B (for Bob), and C (for Charlie); $\alpha = 0, 1$ represents the spin measurement along two different directions. Using MATHEMATICA, it is found numerically that the maximum value of $\langle \mathbf{S}_2 \rangle_{\sigma_{ABC}}$ for both the GHZ state and W state is 4, i.e.,

$$\max[\langle \mathbf{S}_2 \rangle_{GHZ (W)}] = 4. \quad (4.23)$$

For example, $\max[\langle \mathbf{S}_2 \rangle_{GHZ (W)}] = 4$ occurs for the choice $\theta_{A_1} = \theta_{B_0} = \frac{\pi}{2}$, $\theta_{B_1} = \theta_{C_0} = \theta_{C_1} = \frac{3\pi}{2}$, $\theta_{A_0} = \phi_{A_0} = \phi_{A_1} = \phi_{B_0} = \phi_{B_1} = \phi_{C_1} = 0$ and $\phi_{C_0} = \pi$ [Pramanik and Majumdar, 2012]. The value of maximum winning probability, P_{\max}^{game} for the non-local game characterized by the winning condition given by Eq.(4.10) is $\frac{3}{4}$ for both the shared GHZ and W states. Hence, the degree of non-locality captured by this particular full correlation Mermin box [Mermin, 1990] is unable to distinguish classical theory from quantum theory. Nonetheless, similar to the case of the Svetlichny box [Svetlichny, 1987] given by Eq.(4.9), the value of P_{\max}^{game} in no-signaling theory with maximum non-locality is 1, here too.

4.4.3 Winning condition characterized by $a \oplus b \oplus c = s t u$

When the winning condition is chosen by the condition given by Eq.(4.11), the winning probability $P^{\text{game}}(\mathcal{S}, \mathcal{T}, \mathcal{U}, \sigma_{ABC})$ is given by

$$P^{\text{game}}(\mathcal{S}, \mathcal{T}, \mathcal{U}, \sigma_{ABC}) = \frac{1}{2} \left[1 + \frac{\langle \mathbf{S}_3 \rangle_{\sigma_{ABC}}}{8} \right], \quad (4.24)$$

where

$$\begin{aligned} \mathbf{S}_3 = & \mathcal{A}_0 \otimes \mathcal{B}_0 \otimes \mathcal{C}_0 + \mathcal{A}_0 \otimes \mathcal{B}_0 \otimes \mathcal{C}_1 + \mathcal{A}_0 \otimes \mathcal{B}_1 \otimes \mathcal{C}_0 \\ & + \mathcal{A}_1 \otimes \mathcal{B}_0 \otimes \mathcal{C}_0 + \mathcal{A}_0 \otimes \mathcal{B}_1 \otimes \mathcal{C}_1 + \mathcal{A}_1 \otimes \mathcal{B}_0 \otimes \mathcal{C}_1 \\ & + \mathcal{A}_1 \otimes \mathcal{B}_1 \otimes \mathcal{C}_0 - \mathcal{A}_1 \otimes \mathcal{B}_1 \otimes \mathcal{C}_1. \end{aligned} \quad (4.25)$$

In this case, the maximum value of $\langle \mathbf{S}_3 \rangle_{\sigma_{ABC}}$ is 6 for classical theory and the value of maximum winning probability, P_{\max}^{game} is $\frac{7}{8}$. In quantum mechanics, the maximum value of $\langle \mathbf{S}_3 \rangle_{\sigma_{ABC}}$ is obtained by maximizing spin measurements along unit Bloch vectors numerically, as discussed above. For both GHZ state and W

state, the maximum value of $\langle \mathbf{S}_3 \rangle_{\sigma_{ABC}}$ is given by

$$\max[\langle \mathbf{S}_3 \rangle_{GHZ (W)}] = 6, \quad (4.26)$$

which occurs for $\theta_{A_0} = \theta_{A_1} = \theta_{B_1} = \theta_{C_0} = \theta_{C_1} = \frac{3\pi}{2}$, $\theta_{B_0} = \frac{\pi}{2}$, $\phi_{A_0} = \phi_{A_1} = \phi_{B_0} = \phi_{C_0} = \phi_{C_1} = 0$, and $\phi_{B_1} = \pi$. Hence, the value of P_{\max}^{game} in the quantum mechanics is $\frac{7}{8}$ [Pramanik and Majumdar, 2012]. Thus, the full-correlation Mermin box (where the input and output is correlated by Eq.(4.11)) also fails to distinguish between classical and quantum physics using the fine-grained uncertainty relation. However, in the no-signaling theory with maximum non-locality, the maximum value of $\langle \mathbf{S}_3 \rangle_{\sigma_{ABC}}$ is 8, and the corresponding maximum winning probability P_{\max}^{game} is 1 [Pramanik and Majumdar, 2012].

4.5 Summary and outlook

In this chapter, we have generalized the connection of fine grained uncertainty relation, as expressed in terms of the maximum winning probability of prescribed retrieval non-local games, and the degree of non-locality of the underlying physical theory [Oppenheim and Wehner, 2010] to the case of tripartite systems. We have shown that FUR determines the degree of non-locality as manifested by the Svetlichny inequality for tripartite systems corresponding to the winning condition given by Eq.(4.9), in the same way as FUR determines non-locality of bipartite system manifested by Bell- CHSH inequality. Thus, with the help of FUR one is able to differentiate the various classes of theories (i.e., classical physics, quantum physics, and non-signaling theories with maximum non-locality or superquantum correlations) by the value of P_{\max}^{game} for tripartite systems. Furthermore, within quantum theory, it is clear from the upper bound of P_{\max}^{game} that the *GHZ* state is more non-local than the *W* state [Ajoy and Rungta, 2010; Cereceda, 2002; Collins et al., 2002; Mitchell, Popescu, and Roberts, 2004; Seevinck and Svetlichny, 2002]. Finally, it may be noted that by considering the winning conditions of the tripartite games given by the other two full correlation boxes [i.e., Eqs. (4.10) and (4.11)], which violate the Mermin inequality but not the Svetlichny inequality, the fine-grained uncertainty relation is unable to discriminate quantum physics from classical physics in terms of the degree of non-locality. In the next chapter, we show that with the help of FUR, one can optimally reduce the uncertainty of

measurement outcomes for the measurement of two non-commuting observables in the presence of quantum memory.

Chapter 5

Uncertainty relation in the presence of quantum memory

Uncertainty relations in the form of both standard deviation (given by Eqs.(1.34) and (1.35)) and entropy (given by Eq.(1.36)) bound the precision of measurement outcomes for the measurement of two non-commuting observables. In the derivation of above uncertainty relations (given by Eqs. (1.34), (1.35), and (1.36)), the correlation of the observed system (labeled by ‘ A ’) with the other system known as quantum memory (labeled by ‘ B ’) is not considered. To answer the question – is it possible to reduce the uncertainty further from the given bound by Eq.(1.36) with the help of the correlation with the other systems, Berta et al. derived a new form of the uncertainty relation in the presence of quantum memory [Berta et al., 2010] where they have shown the possibility of lowering the uncertainty for the measurement of two non-commuting observables. For a shared maximum entanglement between the observed system and quantum memory, the above uncertainty can be made to be zero, i.e., there is no uncertainty for the measurement of two non-commuting observables by accessing the quantum memory.

To derive the uncertainty relation in the presence of quantum memory, a memory game is considered [Berta et al., 2010]. According to the proposed game, Bob prepares a quantum system (labeled by ‘ A ’) in a state ρ_A and sends it to Alice who measures an observable chosen from the set $\{R, S\}$ (which was known to Bob) on it and communicates the choice of the observable to Bob. Bob’s task is to minimize his uncertainty about Alice’s measurement outcome. To win the above game, Bob applies a quantum strategy as described below.

5.1 Quantum strategy

To improve the situation, Bob correlates his system ‘ B ’ with the system ‘ A ’ which he sends to Alice. With the help of the above correlation, Bob tries to infer Alice’s measurement outcome. Theoretically, it has been shown [Berta et al., 2010] that Bob can enhance his knowledge about Alice’s outcomes by preparing ρ_{AB} in an entangled state. The uncertainty relation in the presence of quantum memory is given by [Berta et al., 2010]

$$\mathcal{S}(R|B) + \mathcal{S}(S|B) \geq \log_2 \frac{1}{c} + \mathcal{S}(A|B), \quad (5.1)$$

where $\mathcal{S}(R|B)$ [$\mathcal{S}(S|B)$] is the conditional von-Neumann entropy of the state given by

$$\rho_{R(S)B} = \sum_j (|\psi_j\rangle\langle\psi_j| \otimes I) \rho_{AB} (|\psi_j\rangle\langle\psi_j| \otimes I), \quad (5.2)$$

where $|\psi_j\rangle$ are the eigenstates of the observable R (S). $\mathcal{S}(R|B)$ [$\mathcal{S}(S|B)$] quantifies the uncertainty corresponding to the measurement R (S) on the system ‘ A ’ given information stored in the system ‘ B ’ (i.e., quantum memory) and $\mathcal{S}(A|B)$ quantifies the amount of entanglement between the quantum system possessed by Alice and the quantum memory possessed by Bob. For the measurement of two non-commuting observables R and S for which the lower bound of Bob’s uncertainty (given by Eq.(5.1)) is maximum with respect to the measurement settings, i.e., $\log_2 \frac{1}{c} = 1$, and for a shared maximally entangled state, i.e., $\mathcal{S}(A|B) = -1$, Bob’s uncertainty (given by Eq.(5.1)) becomes zero, i.e., Bob knows Alice’s measurement outcome for her declared observable with certainty.

5.2 Experimental investigation of the uncertainty relation in the presence of quantum memory

Two recent experiments, using respectively, a pure entangled state [Prevedel et al., 2011] and a mixed entangled state [Li et al., 2011] show the effectiveness of quantum memory in reducing quantum uncertainty. In the experimental situation, Alice and Bob measure the same observables on their respective system, i.e., when Alice communicates, Bob measures the same observable as Alice. Alice and Bob

calculate the quantity $\mathcal{H}(p_d^R) + \mathcal{H}(p_d^S)$, where p_d^R (p_d^S) is the probability of getting different outcomes when both Alice and Bob measure the same observable R (S). Using Fano's inequality [Fano, 1961] given by

$$\mathcal{H}(p_d^R) + \mathcal{H}(p_d^S) \geq \mathcal{S}(R|B) + \mathcal{S}(S|B), \quad (5.3)$$

one can rewrite the inequality (5.1) in the form given by

$$\mathcal{H}(p_d^R) + \mathcal{H}(p_d^S) \geq \log_2 \frac{1}{c} + \mathcal{S}(A|B). \quad (5.4)$$

The right hand side is a function of the measurement settings and the bipartite state ρ_{AB} . It was experimentally observed by Li et al. [Li et al., 2011] that the left hand side exceeds the right hand side for the case of a Bell-diagonal state.

5.3 Optimal lower bound of uncertainty

In [Pramanik, Chowdhury, and Majumdar, 2013], we have given the optimal lower bound for the sum of Bob's uncertainty given by the L.H.S. of the inequality (5.4). We have shown that the bound $\log_2 \frac{1}{c} + \mathcal{S}(A|B)$ given in the inequality (5.4) is not optimal for the quantity $\mathcal{H}(p_d^R) + \mathcal{H}(p_d^S)$. We have found the optimal lower bound (in the experimental situation [Li et al., 2011]) from the maximum (or minimum) winning probability (which minimize Bob's uncertainty) of the quantum memory game. Bob prepares two system 'A' and 'B' in a two-qubit state ρ_{AB} and sends the system 'A' to Alice who measures an observable chosen from the set of two non-commuting observables $\{R, S\}$ and communicates the chosen observable to Bob. Bob measures the same observable on his possessed system 'B'. Alice and Bob win the game if there binary outcomes ' a ' $\in \{0, 1\}$ (for Alice) and ' b ' $\in \{0, 1\}$ (for Bob) satisfy $a \oplus b = 1$ (they get opposite outcomes), i.e., when Alice gets spin up, Bob will get spin down or vice versa [Li et al., 2011]. We find the winning probability using the fine-grained uncertainty relation [Oppenheim and Wehner, 2010; Pramanik and Majumdar, 2012].

In the above game, Bob's uncertainty about Alice's measurement outcome (i.e., the winning probability of getting different outcomes for the measurements R and S) is given by $\mathcal{H}(p_d^R) + \mathcal{H}(p_d^S)$ which is the left-hand side of the entropic uncertainty relation given by the inequality (5.4). We minimize the quantity $\mathcal{H}(p_d^R) + \mathcal{H}(p_d^S)$

with respect to all incompatible measurement settings such that $R \neq S$, i.e.,

$$\mathcal{H}(p_d^R) + \mathcal{H}(p_d^S) \geq \min_{R, S \neq R} [\mathcal{H}(p_d^R) + \mathcal{H}(p_d^S)]. \quad (5.5)$$

Without loss of generality, the choice of one variable, e.g., R , may be fixed, say, $R = \sigma_z$ (i.e., spin measurement along the z -direction) to find the minimum value in the above inequality. The Eq.(5.5) can be rewritten in the form

$$\mathcal{H}(p_d^R) + \mathcal{H}(p_d^S) \geq \mathcal{H}(p_d^{\sigma_z}) + \min_{S \neq \sigma_z} [\mathcal{H}(p_d^S)]. \quad (5.6)$$

The uncertainty captured by the entropy $\mathcal{H}(p_d^S)$ is minimum when the certainty [Oppenheim and Wehner, 2010] measured by p_d^S of the required outcome (restricted by $a \oplus b = 1$) is infimum, i.e., $\min_{S \neq \sigma_z} [\mathcal{H}(p_d^S)] = \mathcal{H}(p_{inf}^S)$.

With the help of the fine-grained uncertainty relation [Oppenheim and Wehner, 2010], we calculate the infimum value of p_d^S for the prescribed game [Pramanik, Chowdhury, and Majumdar, 2013]. In the context of this particular game considered here [$s = t$ in Eq.(4.5)], the fine-grained uncertainty relation is given by

$$P^{\text{game}} = \sum_{a,b} V(a,b) \text{Tr}[(A_s^a \otimes B_t^b) \rho_{AB}] \leq p_{\text{inf}}^S = \inf_{S(\neq \sigma_z)} [P^{\text{game}}], \quad (5.7)$$

where the winning condition of the prescribed game is given by

$$\begin{aligned} V(a,b) &= 1 && \text{iff } a \oplus b = 1 \\ &= 0 && \text{otherwise.} \end{aligned} \quad (5.8)$$

Here, A_S^a is the projector for observable S with outcome ‘ a ’ given by $S^\alpha = \frac{I + (-1)^\alpha \vec{n}_S \cdot \vec{\sigma}}{2}$ (and similarly for B_S^b), where $\vec{n}_S \equiv \{\sin(\theta_S) \cos(\phi_S), \sin(\theta_S) \sin(\phi_S), \cos(\theta_S)\}$; $\vec{\sigma} \equiv \{\sigma_x, \sigma_y, \sigma_z\}$ are the Pauli matrices; α takes value either 0 (for spin up projector) or 1 (for spin down projector). Note that our prescribed winning condition given by Eq.(5.8) is different from the winning condition used in the Ref. [Oppenheim and Wehner, 2010] for the purpose of capturing the non-locality of bipartite system. Here, we have adapted the fine-grained uncertainty relation making it directly applicable to the experimental situation of quantum memory, by introducing a new winning condition modeling the experiments [Li et al., 2011].

After obtaining the quantity p_{inf}^S , the inequality (5.6) becomes

$$\mathcal{H}(p_d^R) + \mathcal{H}(p_d^S) \geq \mathcal{H}(p_d^{\sigma_z}) + \mathcal{H}(p_{inf}^S), \quad (5.9)$$

where the R.H.S. gives the optimal lower bound of entropic uncertainty in the presence of quantum memory. The value of $\mathcal{H}(p_{inf}^S)$ is calculated for the given quantum state ρ_{AB} using the expression (5.7). As a result, the lower bound of the entropic uncertainty in the presence of quantum correlations is now determined by the minimum entropy corresponding to the infimum winning probability of the above game, replacing the earlier lower bound given by the right-hand side of inequality (5.1) [Berta et al., 2010; Li et al., 2011]. Note that the inequality (5.9) can be derived for any choice of R other than σ_z as well. Our proposed uncertainty relation is independent of measurement settings as it optimizes the reduction of uncertainty quantified by the conditional Shannon entropy over all possible observables. Given a bipartite state possessing quantum correlations, inequality (5.9) provides the fundamental limit to which uncertainty in the measurement outcomes of any two incompatible variables can be reduced.

Next, we find out the optimal lower bound of entropic uncertainty in the presence of quantum memory for various two qubit state, e.g., pure entangled state, Werner state, Bell diagonal state, with the help of Eq.(5.9) where, p_{inf}^S is calculated with the help of Eq.(5.7) (the optimization over all spin projectors is performed using MATHEMATICA).

Pure Entangled state : Let us consider, Bob prepares the two system A and B in the two qubit pure entangled state $|\psi\rangle_{AB}^{PE}$ (labeled by superscript PE) given by

$$|\psi\rangle_{AB}^{PE} = \sqrt{\alpha}|01\rangle_{AB} - \sqrt{1-\alpha}|10\rangle_{AB} \quad (5.10)$$

where α lies between 0 and 1, i.e., $0 \leq \alpha \leq 1$. The state ρ_{AB}^{PE} ($= |\psi\rangle_{AB}^{PE}\langle\psi|$) becomes maximally entangled when $\alpha = \frac{1}{2}$. Bob sends the system A to Alice. For the shared state ρ_{AB}^{PE} , the lower bound of the inequality (5.9) (i.e., R.H.S of the inequality (5.9)) is given by

$$\mathcal{L}_1(\rho_{AB}^{PE}) = \mathcal{H}(p_d^{\sigma_z}) + \mathcal{H}(p_{inf}^S) = \mathcal{H}\left(\frac{1}{2} + \sqrt{\alpha(1-\alpha)}\right) \quad (5.11)$$

where $p_d^{\sigma_z} = 1$ and $p_{\text{inf}}^S = \frac{1}{2} + \sqrt{\alpha(1-\alpha)}$ which is achieved for the choice $S = \sigma_x$. The lower bound given by the inequality (5.4) (i.e., R.H.S. of the inequality (5.4)) is

$$\begin{aligned}\mathcal{L}_2(\rho_{AB}^{PE}) &= \log_2 \frac{1}{c} + \mathcal{S}(A|B) \\ &= \log_2 \left[\frac{1}{\max[\cos(\frac{\theta_S}{2})^2, \sin(\frac{\theta_S}{2})^2]} \right] - \mathcal{H}(\alpha),\end{aligned}\quad (5.12)$$

which varies from $\mathcal{H}(\alpha)$ to $1 - \mathcal{H}(\alpha)$ depending upon the measurement settings $\{\theta_S, \phi_S\}$. From Eqs.(5.11) and (5.12), one can see that $\mathcal{L}_1(\rho_{AB}^{PE}) \geq \mathcal{L}_2(\rho_{AB}^{PE})$, where the equality sign holds for $\alpha = \frac{1}{2}$, i.e., $\mathcal{L}_1(\rho_{AB}^{PE}) = \mathcal{L}_2(\rho_{AB}^{PE}) = 0$. Hence, the bound $\mathcal{L}_2(\rho_{AB}^{PE})$ is not achievable except for the shared maximally entangled state, i.e., $\alpha = \frac{1}{2}$.

For the shared maximally entangled state, Alice's and Bob's outputs are strongly correlated when both Alice and Bob measure the same observable on their respective systems. When Alice communicates about her measurement setting, Bob knows certainly about Alice's outcome by measuring the same observable on his system. The lower bound of entropic uncertainty relation should thus be reduced to zero, as observed experimentally [Prevedel et al., 2011].

Bell diagonal state : The bell diagonal state used in the Ref. [Li et al., 2011] is give by

$$\rho_{AB}^{BD} = p |\phi^+\rangle_{AB} \langle \phi^+| + (1-p) |\psi^-\rangle_{AB} \langle \psi^-| \quad (5.13)$$

where $|\phi^+\rangle_{AB} = \frac{1}{\sqrt{2}}(|00\rangle_{AB} + |11\rangle_{AB})$, $|\psi^-\rangle_{AB} = \frac{1}{\sqrt{2}}(|01\rangle_{AB} - |10\rangle_{AB})$, and the mixing parameter, p lies between 0 and 1. The lower bound of entropic uncertainty in the presence of quantum memory (given by inequality (5.4)) for the state ρ_{AB}^{BD} is given by $\mathcal{H}(p)$ ($\mathcal{H}(1-p)$) which is also the optimal lower bound given by the inequality (5.9), where $p_d^{\sigma_z} = (1-p)$ and $p_{\text{inf}}^S = 1$. Note that the choice $R = \sigma_z$, $S = \sigma_x$ (taken by Li et al. [Li et al., 2011]) is unable to minimize the left-hand side of inequality(5.4).

Werner state : Here we consider that Alice and Bob share the Werner state given by [Werner, 1989]

$$\rho_{AB}^W = \alpha |\psi^-\rangle_{AB} \langle \psi^-| + \frac{1-\alpha}{4} I \otimes I, \quad (5.14)$$

where I is the $2 \otimes 2$ unit matrix and α is the mixedness parameter lying between 0 and 1. The optimal lower bound (given by inequality (5.9)),

$$\mathcal{L}_1(\rho_{AB}^W) = 2\mathcal{H}\left(\frac{1-p}{2}\right) \quad (5.15)$$

which is realized for the choice $R = \sigma_z$ and $S = \sigma_x$ always exceeds the lower bound

$$\mathcal{L}_2(\rho_{AB}^W) = -3\frac{1-p}{4}\log_2\frac{1-p}{4} - \frac{1+3p}{4}\log_2\frac{1+3p}{4}, \quad (5.16)$$

given by inequality (5.4), except for $\alpha = 0$ (maximally mixed state leading to maximum and equal uncertainty using both the approaches), and for $p = 1$ (maximally entangled state leading to vanishing uncertainty in both approaches). Hence, the lower bound $\mathcal{L}_2(\rho_{AB}^W)$ is not optimal and it is not possible to be experimentally [Li et al., 2011] realized.

Two qubit mixed state with maximally mixed marginals : Finally, consider the general class of two qubit mixed state with maximally mixed marginals, given by

$$\rho_{AB}^{MM} = \frac{1}{4}(I \otimes I + \sum_{i=1}^3 c_i \sigma_i \otimes \sigma_i), \quad (5.17)$$

where the c_i are real constants satisfying the constraints

$$\begin{aligned} 0 &\leq \frac{1 - c_1 - c_2 - c_3}{4} \leq 1, \\ 0 &\leq \frac{1 + c_1 - c_2 - c_3}{4} \leq 1, \\ 0 &\leq \frac{1 - c_1 + c_2 - c_3}{4} \leq 1, \\ 0 &\leq \frac{1 - c_1 - c_2 + c_3}{4} \leq 1, \end{aligned} \quad (5.18)$$

such that the state ρ_{AB}^{MM} is physical. In [Pramanik, Chowdhury, and Majumdar, 2013], the lower bound of the inequality (5.9) with respect to the observable S is calculated and then compared with the lower bound of inequality (5.4). For wide range of choices of the state parameter c_i , we have found that the fundamental limit set by the inequality (5.9) as obtained through fine graining exceeds the lower bound applying the right-hand side of Eq.(5.4). A typical example, using the values $c_1 = 0.5$, $c_2 = -0.2$, $c_3 = -0.3$, in the Figure 5.1, $\mathcal{H}(p_d^R) + \mathcal{H}(p_d^S)$ is compared with $\log_2 \frac{1}{c} + \mathcal{S}(A|B)$ [Pramanik, Chowdhury, and Majumdar, 2013].

From the Figure 5.1, it is clear that optimal lower bound $\mathcal{H}(p_d^{\sigma_z}) + \mathcal{H}(p_{inf}^S) \approx 1.754$ is attained for $S = \sigma_x$, while for the same observable, one obtains the right hand side of Eq.(5.4) as $\log_2 \frac{1}{c} + \mathcal{S}(A|B) \approx 1.558$.

It is clear from the Figure 5.1, that when the specific state is used as quantum memory, the lower bound as predicted by the analysis of Berta et al. [Berta et al., 2010] is never achieved in an actual experiment using any choice of measurement settings $\{\theta_S, \phi_S\}$.

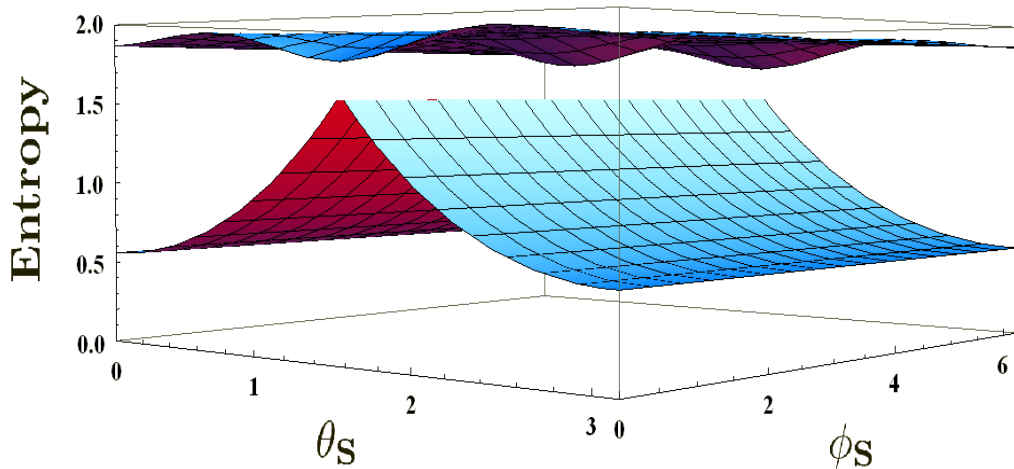


FIGURE 5.1: The lower bound of entropic uncertainty corresponding to measurements on a two-qubit state with maximally mixed marginals in the presence of quantum memory. (i) the upper plot $\mathcal{H}(p_d^{\sigma_z}) + \mathcal{H}(p_{inf}^S)$ as predicted by using our uncertainty relation (5.9) derived here, and (ii) the lower plot $\log_2 \frac{1}{c} + \mathcal{S}(A|B)$ as predicted by the analysis of Berta et al.[Berta et al., 2010] given by (5.1,5.4). The region between the two curves is inaccessible in actual measurements according to our results, since the optimal lower bound of entropic uncertainty is determined by fine-graining.

5.4 Application in quantum key generation

The entropic uncertainty relation in the presence of quantum memory could be used in quantum key distribution protocols. The amount of key K extracted per state is bounded by

$$K \geq \mathcal{S}(R|E) - \mathcal{S}(R|B), \quad (5.19)$$

where the quantum state ρ_{ABE} is shared between Alice, Bob and the eavesdropper, Eve (labeled by E) [Ekert, 1991]. Using the relation $\mathcal{S}(RB) = \mathcal{S}(RE)$ and $\mathcal{S}(AB) = \mathcal{S}(E)$ (which hold for the shared pure state ρ_{ABC}), the inequality (5.1) becomes

$$\mathcal{S}(R|E) + \mathcal{S}(S|B) \geq \log_2 \frac{1}{c}, \quad (5.20)$$

as conjectured by Boileau and Renes [Renes and Boileau, 2009]. Combining the inequalities (5.19) and (5.20), the lower bound of the key extraction rate is given by

$$K \geq \log_2 \frac{1}{c} - \mathcal{S}(R|B) - \mathcal{S}(S|B). \quad (5.21)$$

As the lower bound $\log_2 \frac{1}{c} + \mathcal{S}(A|B)$ (given by Eq.(5.4)) is not always reachable in the experimental situation, hence, using inequalities (5.3) and (5.9) we have given the optimal lower bound of key extraction rate [Pramanik, Chowdhury, and Majumdar, 2013] given by

$$K_{\text{Optimal}} \geq \log_2 \frac{1}{c} - \mathcal{H}(p_d^{\sigma_z}) - \mathcal{H}(p_{\text{inf}}^S), \quad (5.22)$$

where $K_{\text{Optimal}} \leq K$, i.e., the bound derived here is upper bounded by the result of Berta et al. [Berta et al., 2010]. The implication is that the saturation of the bound derived earlier [Berta et al., 2010] is not possible for all states, and the bound derived here represents the optimal lower limit of key extraction valid for any shared correlation, and for all measurement settings used by Alice and Bob.

5.5 Summary

In conclusion, the presence of entanglement of the observed system with the quantum memory can help to reduce the uncertainty for the measurement of two non-commuting observables. The lower bound of the uncertainty relation in the presence of quantum memory gives also the lower bound of the amount of secret key extracted per state [Berta et al., 2010]. Two recent experiments (using pure [Prevedel et al., 2011] and mixed [Li et al., 2011] entangled state) capture the effectiveness of reducing the uncertainty in the presence of quantum memory. The lower bound of the uncertainty relation given in [Berta et al., 2010; Li et al.,

2011; Prevedel et al., 2011] is dependent on measurement settings. In [Pramanik, Chowdhury, and Majumdar, 2013], we have given the optimal lower bound of the uncertainty relation in the experimental situation [Li et al., 2011] with the help of the fine-grained uncertainty relation [Oppenheim and Wehner, 2010]. The optimal lower bound is captured by the maximum winning probability (which gives minimum uncertainty) obtained with the help of the fine-grained uncertainty relation [Oppenheim and Wehner, 2010]. Our bound is independent of measurement settings. In various examples, e.g., pure entangled state, Werner state, mixed entangled state with maximally mixed marginals, we have shown that the lower bound given in [Berta et al., 2010; Li et al., 2011; Prevedel et al., 2011] is unreachable, whereas the lower bound given in [Berta et al., 2010] for maximally entangled and Bell diagonal state (used in the experiment [Li et al., 2011]) can be experimentally realized [Pramanik, Chowdhury, and Majumdar, 2013]. The lower bound of the secret key rate is modified by K_{Optimal} given by Eq.(5.22).

Chapter 6

Improvement of teleportation fidelity with the help of weak measurement

In the earlier chapters, we have seen how an unknown qubit state is sent to a distant location with the help of inter-particle entanglement. i.e., the entanglement between, say, spin degrees of freedom of two spatially separated particles (known as teleportation), and with the help of intra-particle entanglement, i.e., the entanglement between, say, the path and spin degrees of freedom of a single spin-1/2 particle. In the above protocols, we did not consider mixed states (which occur due to the decoherence, i.e., the interaction of the system with the environment) . But, in any experiment, systems interact with the environment continuously.

Due to the presence of decoherence, the quantum correlation present in an entangled state decays and in certain situation the entanglement vanishes completely, which is known as entanglement sudden death [[Almeida et al., 2007](#)]. As a result, the teleportation fidelity decreases. It has been noted that under certain specially chosen conditions, decoherence can have its reverse effect, i.e., entanglement between two systems could be created or increased by their collective interactions with the common environment [[Bose et al., 1999](#); [Braun, 2002](#); [Duan and Kimble, 2003](#); [Plenio and Huelga, 2002](#)]. Several experimental proposals have been suggested to capture such effects in entanglement generation using trapped ions and cavity fields [[Ghosh, Majumdar, and Nayak, 2006](#); [Kim et al., 2002](#); [Kraus and Cirac, 2004](#)]. However, for the specific case of teleportation it has been

observed that the effect of amplitude damping on one of the qubits of a shared bipartite state could lead to the enhancement of fidelity above the classical limit for a class of states whose fidelity just below the quantum region [Badziag et al., 2000]. Such an improvement is possible for low values of the damping parameter, and occurs only for restricted class of states [Bandyopadhyay, 2002]. Recently, it has been shown that quantum entanglement can be protected with the help of weak measurement and its reversal, when the system interacts with environment via amplitude damping channel [Kim et al., 2009, 2012; Koashi and Ueda, 1999; Korotkov and Jordan, 2006; Lee et al., 2011; Man, Xia, and An, 2012].

6.1 Enhancement of teleportation fidelity with the help of environmental interaction

For the purpose of teleportation, Alice prepares two qubits labeled by ‘1’ and ‘2’ in one of the four maximally entangled states, given by

$$|\psi\rangle_{\pm}^M = \frac{|00\rangle_{12} \pm |11\rangle_{12}}{\sqrt{2}} \quad (6.1)$$

$$|\phi\rangle_{\pm}^M = \frac{|01\rangle_{12} \pm |10\rangle_{12}}{\sqrt{2}} \quad (6.2)$$

and then she sends the 2nd qubit labeled by ‘2’ to Bob over the noisy channel, where the 1st qubit labeled by ‘1’ is kept with herself. At the time of transit over the environmental, the 2nd qubit interacts with the environment, and as an effect, the entanglement between the qubits decreases, and the maximally entangled state becomes a mixed state σ_{12} . The success of teleportation using the state σ_{12} is quantified by the fidelity (defined in the Eq.(3.11)). The teleportation fidelity $F(\sigma_{12})$ of the state σ_{12} is given by [Horodecki et al., 1999]

$$F(\sigma_{12}) = \frac{2f(\sigma_{12}) + 1}{3}, \quad (6.3)$$

where the fully entangled fraction (FEF), $f(\sigma_{12})$ is defined by

$$f(\sigma_{12}) = \max_{|\phi\rangle} \langle \phi | \sigma_{12} | \phi \rangle, \quad (6.4)$$

where maximizing is taken over all two qubit maximally entangled states $|\phi\rangle$. For the shared maximally entangled state σ_{12}^M , $f(\sigma_{12}^M) = 1$ and $F(\sigma_{12}^M) = 1$. In the

absence of entanglement, i.e., by using shared randomness, one can achieve the average teleportation fidelity of $2/3$ [Massar and Popescu, 1995]. Hence, if the FEF $f(\sigma_{12}) \leq 1/2$, the state σ_{12} is useless for teleportation, as the corresponding teleportation fidelity $F(\sigma_{12})$ lies in the classical region (i.e., $F(\sigma_{12}) \leq 2/3$).

In the Ref. [Badziag et al., 2000], the authors investigated the possibility of getting quantum advantage, i.e., the fidelity to lie between $2/3$ and 1 from the shared entangled state σ_{12} with $f(\sigma_{12}) \leq \frac{1}{2}$ with the help of LOCC (local operations and classical communications). They proved that any bistochastic map (Λ) which preserves both the trace and identity (I), i.e., ($\Lambda(I) = I$) fails to improve the FEF from classical region ($0 \leq f \leq 1/2$) to quantum region ($f > 1/2$) and they also showed that for a class of states ρ_{12} given by [Badziag et al., 2000]

$$\rho_{12} = \begin{pmatrix} \lambda_{11} & 0 & 0 & \lambda_{14} \\ 0 & \lambda_{22} & -\gamma_{23} & 0 \\ 0 & -\gamma_{23} & \lambda_{33} & 0 \\ \lambda_{14} & 0 & 0 & \lambda_{44} \end{pmatrix}, \quad (6.5)$$

where $\gamma_{23} \geq 0$ and λ_{14} are real; and $\lambda_{22} + \lambda_{33} \geq \frac{1}{2}$, $\gamma_{23} \geq (1 - \lambda_{22} - \lambda_{33})/2$, the fidelity ($F(\rho_{12}) = (1 + \lambda_{22} + \lambda_{33} + 2\gamma_{23})/3 \geq 2/3$) can be enhanced by applying a non-bistochastic map $\bar{\Lambda}$ (which preserves the trace but not the identity). For the choice of parameters $\lambda_{11} = \lambda_{14} = 0$, $\lambda_{22} = 3 - 2\sqrt{2}$, $\lambda_{33} = 1$, $\lambda_{44} = 2\sqrt{2} - 2$ and $\gamma_{23} = \sqrt{2} - 1$, the fidelity of the above state which initially belongs to the classical region (i.e., $F(\rho_{12}) = 2/3$) can be enhanced upto $\frac{2.06}{3}$ (which lies in the quantum region) by applying $\bar{\Lambda}_\alpha$ on any qubits (say, α -th qubit, where $\alpha \in \{1, 2\}$) [Badziag et al., 2000]. The map $\bar{\Lambda}_\alpha$ which is responsible for the enhancement of fidelity in the above example, represents the dissipative interaction of any one qubit with the environment via amplitude damping channel (ADC). The map $\bar{\Lambda}_\alpha$ is given by

$$\bar{\Lambda}_\alpha(\rho_\alpha) = W_{\alpha,0}\rho_\alpha W_{\alpha,0}^\dagger + W_{\alpha,1}\rho_\alpha W_{\alpha,1}^\dagger, \quad (6.6)$$

where $\alpha \in \{1, 2\}$, $\rho_{1(2)} = Tr_{2(1)}[\rho_{12}]$, and the operators $W_{\alpha,i}$ are given by

$$W_{\alpha,0} = \begin{pmatrix} 1 & 0 \\ 0 & \sqrt{D_\alpha} \end{pmatrix}, \quad W_{\alpha,1} = \begin{pmatrix} 0 & \sqrt{D_\alpha} \\ 0 & 0 \end{pmatrix}, \quad (6.7)$$

where $\bar{D}_\alpha = 1 - D_\alpha$. Here D_1 and D_2 are the strength of interactions of the 1st qubit (belonging to Alice) and 2nd qubit (belonging to Bob) with the environment,

respectively, and $\sum_i W_{\alpha,i}^\dagger W_{\alpha,i} = I$. The above map describes the interaction of the environment (which is initially in the state $|0\rangle_E$) with the qubit by the following transitions

$$\begin{aligned} |0\rangle_i |0\rangle_E &\longrightarrow |0\rangle_i |0\rangle_E, \\ |1\rangle_i |0\rangle_E &\longrightarrow \sqrt{D_\alpha} |1\rangle_i |0\rangle_E + \sqrt{1-D_\alpha} |0\rangle_i |1\rangle_E \end{aligned} \quad (6.8)$$

where $i \in \{1, 2\}$ and $\alpha = 1(2)$ for $i = 1(2)$.

Later, in the Ref. [Bandyopadhyay, 2002] the author showed that the above interesting class of states ρ_{AB} , used in the Ref. [Badziag et al., 2000] are obtained when Alice prepares the two qubit maximally entangled state only in the class given by Eq.(6.1) and sends one qubit (say, second qubit labeled by ‘2’) to Bob over ADC. Now, for the purpose of enhancing the fidelity, Alice allows her qubit (i.e., the 1st qubit labeled by ‘1’) also to interact with the environment via ADC. Here, two possible cases are considered. In the *Case-I*, the environmental interaction with single qubit is considered and in the *Case-II*, the environmental interaction with both qubits is considered.

Case I : According to the protocol demonstrated in the Ref. [Bandyopadhyay, 2002], after preparing qubit ‘1’ and ‘2’ either in the state given by Eq.(6.1) or in the state given by Eq.(6.2), when Alice sends the 2nd qubit to Bob over a noisy channel, the shared state after environmental interaction is given by

$$\begin{aligned} \rho'_{|\psi\rangle_{\pm}^M(|\phi\rangle_{\pm}^M)} &= (I \otimes W_{2,0}) \rho_{|\psi\rangle_{\pm}^M(|\phi\rangle_{\pm}^M) (I \otimes W_{2,0}^\dagger) \\ &+ (I \otimes W_{2,1}) \rho_{|\psi\rangle_{\pm}^M(|\phi\rangle_{\pm}^M) (I \otimes W_{2,1}^\dagger), \end{aligned} \quad (6.9)$$

where $\rho_{|\psi\rangle_{\pm}^M(|\phi\rangle_{\pm}^M)}$ is the density state of $|\psi\rangle_{\pm}^M$ ($|\phi\rangle_{\pm}^M$). The FEF of the state $\rho'_{|\psi\rangle_{\pm}^M(|\phi\rangle_{\pm}^M)}$ is same and is given by [Bandyopadhyay, 2002]

$$\bar{f}_1(\rho') = \frac{1}{4} + \frac{1}{2} \sqrt{1-D_2} + \frac{1}{4}(1-D_2). \quad (6.10)$$

and the corresponding fidelity turns out to be $\bar{F}_1(\rho') = \frac{4+2\sqrt{1-D_2}-D_2}{6}$, obtained with the help of Eq.(6.3). In the range $(2\sqrt{2}-2) \leq D_2 \leq 1$, the teleportation fidelity $\bar{F}_1(\rho')$ lies in the classical region, and for others values, i.e., $0 \leq D_2 < 2\sqrt{2}-2$, $\bar{F}_1(\rho')$ lies in the quantum region.

Case II : Here, environment affects both the qubits. After environmental interaction, the two qubit state $|\psi\rangle_{\pm}^M (|\phi\rangle_{\pm}^M)$ becomes

$$\begin{aligned} \rho''_{|\psi\rangle_{\pm}^M (|\phi\rangle_{\pm}^M)} = & (W_{1,0} \otimes I) \rho'_{|\psi\rangle_{\pm}^M (|\phi\rangle_{\pm}^M)} (W_{1,0}^\dagger \otimes I) \\ & + (W_{1,1} \otimes I) \rho'_{|\psi\rangle_{\pm}^M (|\phi\rangle_{\pm}^M)} (W_{1,1}^\dagger \otimes I), \end{aligned} \quad (6.11)$$

where $\rho'_{|\psi\rangle_{\pm}^M (|\phi\rangle_{\pm}^M)}$ is given by Eq.(6.9). The FEF of the state, $\rho''_{|\phi\rangle_{\pm}^M}$ is given by [Bandyopadhyay, 2002]

$$\begin{aligned} \bar{f}_{21}(\rho''_{|\phi\rangle_{\pm}^M}) &= 1 - D \quad \forall D \leq \frac{2}{3} \\ &= \frac{D}{2} \quad \forall D \geq \frac{2}{3}, \end{aligned} \quad (6.12)$$

where $D_1 = D_2 = D$, i.e., both qubits interact with the same environment. It is easily seen from the Eq.(6.12) that the FEF, $\bar{f}_{21}(\rho''_{|\phi\rangle_{\pm}^M})$ (and hence the corresponding teleportation fidelity $\bar{F}_{21}(\rho''_{|\phi\rangle_{\pm}^M})$) always belongs to classical region for all values of D chosen from the region $0 \leq D \leq 1$.

For the other state, $\rho''_{|\psi\rangle_{\pm}^M}$, the FEF is given by [Bandyopadhyay, 2002]

$$\bar{f}_{22}(\rho''_{|\psi\rangle_{\pm}^M}) = 1 - D + \frac{1}{2}D^2. \quad (6.13)$$

The fidelity $\bar{F}_{22}(\rho''_{|\psi\rangle_{\pm}^M})$ corresponding to the FEF $\bar{f}_{22}(\rho''_{|\psi\rangle_{\pm}^M})$ lies in the quantum region, i.e., $\bar{F}_{22}(\rho''_{|\psi\rangle_{\pm}^M}) > \frac{2}{3}$ for $0 \leq D < 1$.

Now, we compare the teleportation fidelity achieved in the *Case-I* with the *Case-II*. For the prepared state $|\psi\rangle_{\pm}^M$, the teleportation fidelity $\bar{F}_1(\rho'_{|\psi\rangle_{\pm}^M})$ (for the case where decoherence affects a single qubit) lies in the classical region (i.e., $\bar{F}_1(\rho'_{|\psi\rangle_{\pm}^M}) \leq \frac{2}{3}$) for $(2\sqrt{2} - 2) \leq D_2 = D \leq 1$, and in the quantum region for $0 \leq D_2 = D < (2\sqrt{2} - 2)$, whereas, $\bar{F}_{22}(\rho''_{|\psi\rangle_{\pm}^M})$ lies in the quantum region (i.e., $\bar{F}_{22}(\rho''_{|\psi\rangle_{\pm}^M}) > \frac{2}{3}$) for $0 \leq D < 1$. Hence, due to the effect of decoherence on the 1st qubit, those states $\rho'_{|\psi\rangle_{\pm}^M}$ which were unable to give non-classical teleportation fidelity now show non-classical fidelity, except for the state $\rho'_{|\psi\rangle_{\pm}^M}$ with $D = 1$. For the other class of prepared state, $|\phi\rangle_{\pm}^M$, there is no such improvement. According to Bandyopadhyay [Bandyopadhyay, 2002], the improvement of fidelity from the classical region to the quantum region is due to the enhancement of classical correlation by the application of ADC on the 1st qubit, as LOCC by itself is unable to increase the entanglement.

6.2 Weak measurement

Projective measurement, associated with an observable, β (which represents a Hermitian operator) is given by

$$\beta = \sum_b \beta_b P_b, \quad (6.14)$$

where $P_b (= |b\rangle\langle b|)$ is the projector on the eigenbasis $|b\rangle$ (i.e., $P_i P_j = \delta_{ij}$) of the observable β , β_b is the corresponding measurement outcome and $\sum_i P_i = I$. Due to a projective measurement on an observed system which was initially in the state ρ , it collapses to one of the eigenbasis $\{|b\rangle\}$ of the observable with probability $Tr[P_b \rho]$. Projective measurement is irreversible as it has no inverse. For example, in the qubit system for the measurement of σ_z , the projectors are given by

$$P_0 = |0\rangle\langle 0| = \begin{pmatrix} 1 & 0 \\ 0 & 0 \end{pmatrix}, \quad P_1 = |1\rangle\langle 1| = \begin{pmatrix} 0 & 0 \\ 0 & 1 \end{pmatrix}, \quad (6.15)$$

where the projector P_0 collapses the state of the system to the spin up state ($|0\rangle$, with the corresponding measurement outcome $\beta_0 = +1$) and the projector P_1 collapses the state of the system to the spin down state ($|1\rangle$, with the corresponding measurement outcome $\beta_1 = -1$), along the z -direction. Here, P_0 and P_1 are singular matrices, and hence, they have no inverse. However, the most general measurement is positive operator valued measurement (POVM). In the case of POVM, the restriction of forming basis for P_a , i.e., $P_i P_j = \delta_{ij}$ is withdrawn. But, the POVM is achieved as projective measurement in higher dimension, i.e., by performing the joint measurement on the combined observed and auxiliary system.

Weak measurement is achieved by reducing the sensitivity of the detector, i.e., the detector clicks with probability p_k if the input qubit (labeled by k) is in the state $|1\rangle_k$ and never clicks if the input state is in the state $|0\rangle_k$ [Kim et al., 2009; Lee et al., 2011]. In the technique of weak measurement we use post-selected states (corresponding to the non-clicking of the detector) for further tasks. The measurement corresponding to the detection of the particle is given by

$$M_{k,1} = \begin{pmatrix} 0 & 0 \\ 0 & \sqrt{p_k} \end{pmatrix}, \quad (6.16)$$

which does not have any inverse, and hence, $M_{k,1}$ is irreversible, i.e., when the detector clicks, it is unable to get back to the input state in a reversible way. The measurement operator when the detector does not click is given by

$$M_{k,0} = \begin{pmatrix} 1 & 0 \\ 0 & \sqrt{\bar{p}_k} \end{pmatrix}, \quad (6.17)$$

where $\bar{p} = 1 - p$ and $M_{k,0}^\dagger M_{k,0} + M_{k,1}^\dagger M_{k,1} = 1$. When the detector does not click, the input state $|1\rangle_k$ partially collapses towards $|0\rangle_k$ and the input state $|0\rangle_k$ is unaffected. From Eq.(6.17), it is clear that $M_{k,0}$ is reversible having mathematical inverse, i.e.,

$$M_{k,0}^{-1} = \begin{pmatrix} 1 & 0 \\ 0 & q_k \end{pmatrix} \quad (6.18)$$

where $q_k = \frac{1}{\sqrt{\bar{p}_k}}$.

6.3 Applications of Weak measurement

Weak measurement plays an important role to protect the quantum coherence of a single qubit against the interaction with the environment via amplitude damping decoherence [Korotkov and Keane, 2010; Lee et al., 2011]. The amplitude damping decoherence (given by Eq.(1.45)) leaves the system unchanged when the system is in the ground state ($|0\rangle$). However, when the system is in the excited state ($|1\rangle$), it jumps to ground state by emitting one photon to the environment with probability D . The weak measurement $M_{k,0}$ (given by Eq.(6.17)) can be reversed when the system is in the excited state, since its inverse exists. Hence, weak measurement can protect the quantum coherence against the amplitude damping decoherence. Extending this for two qubits, Kim et al. [Kim et al., 2012] have shown experimentally that the entanglement can be protected with the help of weak measurement in the presence of amplitude damping decoherence. In [Pramanik and Majumdar, 2013], we have optimally protected the teleportation fidelity with the help of the technique of weak measurement and its reversal when the systems interacts with the environment via amplitude damping channel. Here, we have also shown that the protection of entanglement is not equivalent with the protection of teleportation fidelity.

6.3.1 Entanglement protection with the help of weak measurement

The procedure begins by preparing maximally entangled state either in the class given by Eq.(6.1) or in the class given by Eq.(6.2), and then uses the technique of weak measurement and reverse weak measurement to protect the entanglement when one or both qubits are affected by environment modeled by amplitude damping channel. Here, we study entanglement protection when either one qubit is affected by the environment, or both qubits are affected by the environment.

Alice prepares two qubits either in the class given by Eq.(6.1) or in the class given Eq.(6.2) and sends the 2nd qubit to Bob over the environment. Due to the interaction of the 2nd qubit with the environment, the shared state becomes $\rho'_{|\psi\rangle_{\pm}^M(|\phi\rangle_{\pm}^M)}$ given by Eq.(6.9). The entanglement (measured by concurrence [Wootters, 1998]) of the above state is given by

$$C1_D = C(\rho'_{|\psi\rangle_{\pm}^M(|\phi\rangle_{\pm}^M}) = \sqrt{1 - D}, \quad (6.19)$$

where $D_2 = D$.

Now, to protect the entanglement from the environmental interaction, Alice makes a weak measurement with strength $p_2 = p$ on the 2nd qubit. Due to the weak measurement the shared state $\rho_{|\psi\rangle_{\pm}^M(|\phi\rangle_{\pm}^M)}$ becomes

$$\rho_{|\psi\rangle_{\pm}^M(|\phi\rangle_{\pm}^M}^W = (I \otimes M_{1,0})\rho_{|\psi\rangle_{\pm}^M(|\phi\rangle_{\pm}^M}(I \otimes M_{1,0})^\dagger. \quad (6.20)$$

Note that, here Alice uses the post-selected state, i.e., when detector clicks she discards the prepared state, and when detector does not click, she keeps the two qubits state for further processing.

Next, Alice sends the 2nd qubit over the environment. Due to the interaction with the environment, the shared state becomes $\rho_{|\psi\rangle_{\pm}^M(|\phi\rangle_{\pm}^M}^D = I \otimes \bar{\Lambda}_2(\rho_{|\psi\rangle_{\pm}^M(|\phi\rangle_{\pm}^M}^W)$, where the action of $\bar{\Lambda}_2$ on the second qubit is defined in the Eq.(6.6). After getting the 2nd particle, Bob makes a reverse weak measurement given by [Kim et al., 2012]

$$N_2 = \begin{pmatrix} \sqrt{q_2} & 0 \\ 0 & 1 \end{pmatrix}, \quad (6.21)$$

where $\bar{q}_2 = 1 - q_2$ and q_2 is the strength of measurement by Bob. After weak measurement, the shared state becomes

$$\rho_{|\psi\rangle_{\pm}^M(|\phi\rangle_{\pm}^M)}^R = (I \otimes N_2)\rho_{|\psi\rangle_{\pm}^M(|\phi\rangle_{\pm}^M}^D(I \otimes N_2)^\dagger. \quad (6.22)$$

The concurrence of the state $\rho_{|\psi\rangle_{\pm}^M(|\phi\rangle_{\pm}^M)}^R$ is given by

$$C(\rho_{|\psi\rangle_{\pm}^M(|\phi\rangle_{\pm}^M)}^R) = \frac{4(1-D)(1-p)(1-q)}{(p(Dp-1) - (D+1)q + 2)^2}, \quad (6.23)$$

where $q = q_2$. To protect the entanglement maximally, we maximize $C(\rho_{|\psi\rangle_{\pm}^M(|\phi\rangle_{\pm}^M)}^R)$ with respect to the strength of the weak measurement q , and the maximum concurrence is given by

$$C1_W = C(\rho_{|\psi\rangle_{\pm}^M(|\phi\rangle_{\pm}^M)}^R) = \frac{1}{\sqrt{1 + D(1-p)}}, \quad (6.24)$$

which is obtained for the choice of optimal strength of reverse weak measurement $q^O = \frac{-2Dp+2D+p}{-Dp+D+1}$. Due to post-selection at the stage of each weak measurement, the success probability of obtaining the above concurrence is given by [Man, Xia, and An, 2012]

$$P1_{Succ}^C = Tr[\rho_{|\psi\rangle_{\pm}^M(|\phi\rangle_{\pm}^M)}^R] = (1-D)(1-p). \quad (6.25)$$

When the protocol fails, i.e., the detector used in weak measurement clicks, the entanglement vanishes (i.e., $C = 0$) which occurs with the probability $(1 - P1_{Succ}^C)$. Hence, the average entanglement (where average is taken over the success probability of applying weak measurement and its reversal) is

$$C1_{Av} = P1_{Succ}^C C1_W. \quad (6.26)$$

It is easily seen that $C1_W \geq C1_D \geq C1_{Av}$. As the average concurrence $C1_{Av}$ lies below the one obtained through the amplitude damping channel without weak measurement, the entanglement protection protocol fails without post-selection. Similar results hold true if both the particles are subjected to decoherence.

6.3.2 Teleportation fidelity preservation with the help of weak measurement

In [Pramanik and Majumdar, 2013], we have studied the preservation of teleportation fidelity when the entangled system is open to amplitude damping environments, with the help of weak measurement and its reversal. Similar to Ref. [Bandyopadhyay, 2002], here we consider that Alice prepares two qubits in one of the four maximally entangled states given by Eqs.(6.1) and (6.2), and sends the 2nd qubit to Bob, where the 1st qubit is kept with her. Here, we consider two different cases. In the 1st case, the 2nd qubit is affected by amplitude damping environment at transit time and the 1st qubit is unaffected. To protect the teleportation fidelity of the prepared state, they use the weak measurement technique [Kim et al., 2012], i.e., Alice makes a weak measurement on the 2nd qubit before sending it, and after getting the 2nd qubit, Bob makes a reverse weak measurement on it. In the 2nd case, both qubits are affected by amplitude damping environment and they use the technique of weak measurement and its reverse measurement to protect the teleportation fidelity of the prepared state.

Case I : Here, after preparing the two qubit state in one of the four maximally entangled states given by Eqs.(6.1) and (6.2), Alice makes a weak measurement on the 2nd qubit to reduce the effect of amplitude damping environment. After making the weak measurement on the 2nd qubit, the two qubit state (unnormalized) becomes either

$$\begin{aligned} \rho_{\pm}^W &= (I \otimes M_{2,0})|\psi\rangle_{\pm}^M \langle\psi|(I \otimes M_{2,0}^\dagger) \\ &= \frac{1}{2} \begin{pmatrix} 1 & 0 & 0 & \pm\sqrt{\bar{p}_2} \\ 0 & 0 & 0 & 0 \\ 0 & 0 & 0 & 0 \\ \pm\sqrt{\bar{p}_2} & 0 & 0 & \bar{p}_2 \end{pmatrix} \end{aligned} \quad (6.27)$$

or

$$\begin{aligned} \sigma_{\pm}^W &= (I \otimes M_{2,0})|\phi\rangle_{\pm}^M \langle\phi|(I \otimes M_{2,0}^\dagger) \\ &= \frac{1}{2} \begin{pmatrix} 0 & 0 & 0 & 0 \\ 0 & \bar{p}_2 & \pm\sqrt{\bar{p}_2} & 0 \\ 0 & \pm\sqrt{\bar{p}_2} & 1 & 0 \\ 0 & 0 & 0 & 0 \end{pmatrix}, \end{aligned} \quad (6.28)$$

depending upon the initially prepared state. The success probability, i.e., the detector's inefficiency is given by

$$P_2^D = \text{Tr}[\rho_{\pm}^W] = \text{Tr}[\sigma_{\pm}^W] = \left(1 - \frac{p_2}{2}\right). \quad (6.29)$$

Next, Alice sends the second qubit to Bob over ADC. Due to interaction of the 2nd qubit with the environment, the shared state ρ_{\pm}^W becomes

$$\begin{aligned} \rho_{\pm}^D &= (I \otimes W_{2,0})\rho_{\pm}^W(I \otimes W_{2,0}^\dagger) + (I \otimes W_{2,1})\rho_{\pm}^W(I \otimes W_{2,1}^\dagger) \\ &= \frac{1}{2} \begin{pmatrix} 1 & 0 & 0 & k_1 \\ 0 & 0 & 0 & 0 \\ 0 & 0 & D_2\bar{p}_2 & 0 \\ k_1 & 0 & 0 & k_1^2 \end{pmatrix} \end{aligned} \quad (6.30)$$

where $k_1 = \pm\sqrt{D_2\bar{p}_2}$, Similarly, σ_{\pm}^W becomes

$$\begin{aligned} \rho_{\pm}^D &= (I \otimes W_{2,0})\sigma_{\pm}^W(I \otimes W_{2,0}^\dagger) + (I \otimes W_{2,1})\sigma_{\pm}^W(I \otimes W_{2,1}^\dagger) \\ &= \frac{1}{2} \begin{pmatrix} D_2\bar{p}_2 & 0 & 0 & 0 \\ 0 & k_1^2 & k_1 & 0 \\ 0 & k_1 & 1 & 0 \\ 0 & 0 & 0 & 0 \end{pmatrix} \end{aligned} \quad (6.31)$$

After receiving the particle, Bob applies the reverse quantum measurement [Kim et al., 2009] N_2 (given by Eq.(6.21)). At the end, Alice and Bob actually share the state given by

$$\begin{aligned} \rho_{\pm}^R &= (I \otimes N_2)\rho_{\pm}^D(I \otimes N_2^\dagger) \\ &= \frac{1}{2} \begin{pmatrix} \bar{q}_2 & 0 & 0 & \pm\sqrt{D_2\bar{p}_2\bar{q}_2} \\ 0 & 0 & 0 & 0 \\ 0 & 0 & D_2\bar{p}_2\bar{q}_2 & 0 \\ \pm\sqrt{D_2\bar{p}_2\bar{q}_2} & 0 & 0 & \bar{D}_2\bar{p}_2 \end{pmatrix}, \end{aligned} \quad (6.32)$$

$$\begin{aligned}
 \sigma_{\pm}^R &= (I \otimes N_2) \sigma_{\pm}^D (I \otimes N_2^\dagger) \\
 &= \frac{1}{2} \begin{pmatrix} D_2 \bar{p}_2 \bar{q}_2 & 0 & 0 & 0 \\ 0 & \bar{D}_2 \bar{p}_2 & \pm \sqrt{D_2 \bar{p}_2 \bar{q}_2} & 0 \\ 0 & \pm \sqrt{D_2 \bar{p}_2 \bar{q}_2} & \bar{q}_2 & 0 \\ 0 & 0 & 0 & 0 \end{pmatrix}. \tag{6.33}
 \end{aligned}$$

The states ρ_{\pm}^R and σ_{\pm}^R have the same FEF, i.e., the FEF is same whether Alice prepares the initial two qubit state in the class given by Eq.(6.1) or (6.2), and it is given by

$$f_1 = \frac{\bar{p}_2 + \bar{q}_2 + 2\sqrt{D_2 \bar{p}_2 \bar{q}_2} - D_2 \bar{p}_2}{2(\bar{p}_2 + \bar{q}_2) - 2D_2 \bar{p}_2 \bar{q}_2} \tag{6.34}$$

For the purpose of the experiment, the strength of reverse weak measurement has to be chosen suitably. In the Ref. [Man, Xia, and An, 2012], for the purpose of maximally protecting the entanglement from the interaction of qubits with the environment via ADC, the authors calculate the optimal strength of reverse weak measurement that maximizes the concurrence of the non-maximally entangled state used by them. In the Ref. [Pramanik and Majumdar, 2013], we maximize the teleportation fidelity f_1 (given by Eq.(6.34)) with respect to q_2 to obtain q_2^O , the optimal reverse weak measurement strength which maximally protects the fidelity of the unknown teleported state undergoing amplitude damping. The value of q_2^O which is same for both class of prepared states given by Eqs. (6.1) and (6.2), is given by

$$q_2^O = \frac{3D_2 \bar{p}_2 + D_2^2 \bar{p}_2^2 + p_2}{(1 + D_2 \bar{p}_2)^2}. \tag{6.35}$$

Note that, the choice $q_2 = p_2 + D_2 \bar{p}_2$ optimally preserves the entanglement of the maximally entangled state [Kim et al., 2012; Man, Xia, and An, 2012], but, it is unable to maximize the fidelity of the state passing through the noisy channel. For the choice of initial state chosen from the class given by Eqs.(6.1) and (6.2), using Eqs.(6.34) and (6.35) one can calculate the optimal FEF which is given by

$$f_1^O = \frac{2 + D_2 \bar{p}_2}{2 + 2D_2 \bar{p}_2}, \tag{6.36}$$

where f_1^O is bounded by 0.75 (occurs for the choice $D_2 = 1$ and $p_2 = 0$) and 1 (occurs for either $p_2 = 1$ or $D_2 = 0$). Here one may note that the optimal teleportation fidelity $F_1^O (= \frac{2f_1^O+1}{3})$ always belongs to the quantum region irrespective of the strength of decoherence. Due to the weak measurement and the reverse weak measurement, the overall success probability, i.e., the probability of obtaining the state ρ_{\pm}^R (σ_{\pm}^R) when Alice prepares the two qubits state in the class given by Eq.(6.1) (Eq.(6.2)) is given by [Lee et al., 2011]

$$\begin{aligned} P_{\text{Succ}}^1 &= \text{Tr}[\rho_{\pm}^R] = \text{Tr}[\sigma_{\pm}^R] = \frac{1}{2}(\bar{p}_2 + \bar{q}_2^O - D_2\bar{p}_2) \\ &= \frac{\bar{D}_2\bar{p}_2(2 + D_2\bar{p}_2)}{2 + 2D_2\bar{p}_2}, \end{aligned} \quad (6.37)$$

where the success probability lies between 0 (which occurs for either $D_2 = 1$, or $p_2 = 1$, or both) and 1 (which occurs when both $D_2 = 0$ and $p_2 = 0$ hold simultaneously).

Figure-6.1 shows the comparison between the optimal fidelity F_1^O (corresponding to the FEF f_1^O given by Eq.(6.36)) with the fidelity \bar{F}_1 (corresponding to the FEF \bar{f}_1 given by Eq.(6.10)) which corresponds to the teleportation fidelity when weak measurement technique (to suppress the amplitude damping decoherence) is not used. From the above figure, it is clear that F_1^O is always larger than \bar{F}_1 (except $D_2 = 0$ and $p_2 = 0$) and always lies in the above the classical region for all values of D_2 and p_2 , whereas in the range $(2\sqrt{2} - 1) \leq D_2 \leq 1$, \bar{F}_1 lies in the classical region.

In the protocol of protecting the teleportation fidelity, the role of the reverse weak measurement performed by Bob is more important than the weak measurement made by Alice before sending the particle to Bob over ADC. For the justification of above point, in [Pramanik and Majumdar, 2013] we have considered that Alice sends the 2nd particle to Bob without making any weak measurement on it, i.e., $p_2 = 0$, over the environment. After receiving the 2nd particle, Bob makes an optimal weak measurement with strength $q_2 = q_2^O$ given by Eq.(6.35). The optimal FEF in this case is given by

$$f_{12}^O = \frac{2 + D_2}{2 + 2D_2}, \quad (6.38)$$

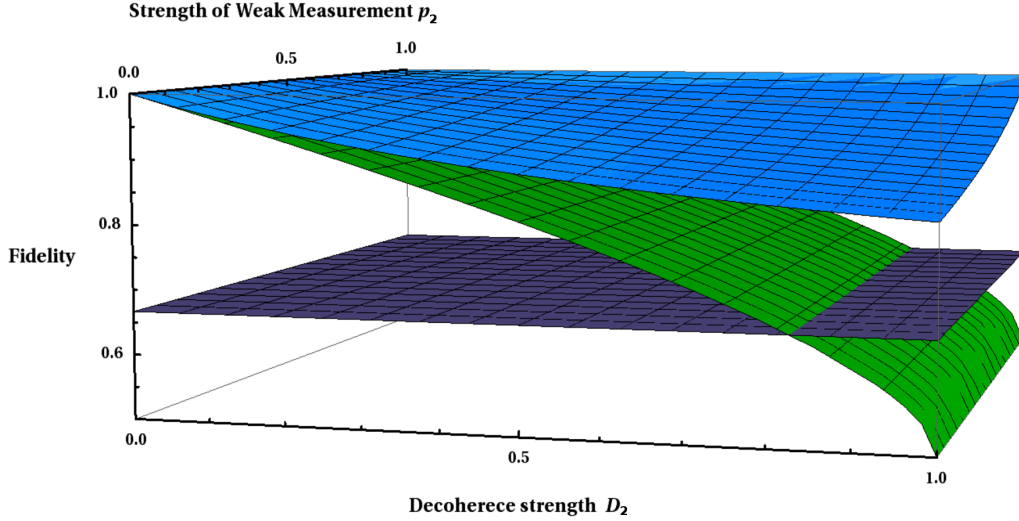


FIGURE 6.1: The flat plane represents the average classical fidelity $\frac{2}{3}$. The surface intersecting it represents the fidelity \bar{F}_1 corresponding to the FEF $\bar{f}_1 = \frac{1}{4} + \frac{1}{2}\sqrt{1-D_2} + \frac{1}{4}(1-D_2)$. The uppermost surface represents the fidelity F_1^O corresponding to the FEF $f_1^O = \frac{2+D_2\bar{p}_2}{2+2D_2\bar{p}_2}$.

which is obtained from Eq.(6.36) by putting $\bar{p}_2 = 1$. The corresponding success probability is $\frac{2-D_2-D_2^2}{2(1+D_2)}$. Here, the teleportation fidelity F_{12}^O corresponding to the FEF f_{12}^O is not only greater than \bar{F}_1 , but, also F_{12}^O lies in quantum region, i.e. $5/6 \geq F_{12}^O \geq 1$ for all values of decoherence parameter D_2 chosen from the region $1 \leq D_2 \leq 0$.

Case II : In this case, we have considered environment effects on both the qubits via amplitude damping decoherence. To prevent the loss of information about unknown state in the teleportation protocol, Alice makes weak measurements (given by Eq.(6.17)), separately on each qubit. After performing weak measurement by Alice, the two qubits state belonging to the class given by Eq.(6.1) becomes

$$\begin{aligned} \rho_{\pm}^{WW} &= (M_{1,0} \otimes M_{2,0})|\psi\rangle_{\pm}^M \langle\psi|(M_{1,0} \otimes M_{2,0}^{\dagger}) \\ &= \begin{pmatrix} \frac{1}{2} & 0 & 0 & \pm \frac{\sqrt{\bar{p}_1\bar{p}_2}}{2} \\ 0 & 0 & 0 & 0 \\ 0 & 0 & 0 & 0 \\ \pm \frac{\sqrt{\bar{p}_1\bar{p}_2}}{2} & 0 & 0 & \frac{\bar{p}_1\bar{p}_2}{2} \end{pmatrix}, \end{aligned} \quad (6.39)$$

and the state belonging to the class given by Eq.(6.2) becomes

$$\sigma_{\pm}^{WW} = \begin{pmatrix} 0 & 0 & 0 & 0 \\ 0 & \frac{\bar{p}_2}{2} & \pm \frac{\sqrt{\bar{p}_1\bar{p}_2}}{2} & 0 \\ 0 & \pm \frac{\sqrt{\bar{p}_1\bar{p}_2}}{2} & \frac{\bar{p}_1}{2} & 0 \\ 0 & 0 & 0 & 0 \end{pmatrix}. \quad (6.40)$$

The success probabilities associated with the above weak measurement are respectively given by

$$P_{12}^D(\rho_{\pm}^{WW}) = Tr[\rho_{\pm}^{WW}] = \frac{1}{2}(1 + \bar{p}_1\bar{p}_2) \quad (6.41)$$

and

$$P_{12}^D(\sigma_{\pm}^{WW}) = Tr[\sigma_{\pm}^{WW}] = \frac{1}{2}(\bar{p}_1 + \bar{p}_2). \quad (6.42)$$

After weak measurement, Alice sends the 2nd qubit through the ADC and simultaneously, she allows her qubit (1st qubit) to interact with the environment. Hence, both qubits are affected by the environment. Due to the effect caused by environmental interaction, the noisy shared state takes one of the following forms (depending upon the initial state)

$$\rho_{\pm}^{DD} = \begin{pmatrix} \frac{1+D_1D_2k4^2}{2} & 0 & 0 & \pm \frac{k5k4}{2} \\ 0 & \frac{D_1\bar{D}_2k4^2}{2} & 0 & 0 \\ 0 & 0 & \frac{\bar{D}_1D_2k4^2}{2} & 0 \\ \pm \frac{k5k4}{2} & 0 & 0 & \frac{k5^2k4^2}{2} \end{pmatrix} \quad (6.43)$$

$$\sigma_{\pm}^{DD} = \begin{pmatrix} \frac{D_1\bar{p}_1}{2} + \frac{D_2\bar{p}_2}{2} & 0 & 0 & 0 \\ 0 & \frac{\bar{D}_2\bar{p}_2}{2} & \pm \frac{k4k5}{2} & 0 \\ 0 & \pm \frac{k4k5}{2} & \frac{\bar{D}_1\bar{p}_1}{2} & 0 \\ 0 & 0 & 0 & 0 \end{pmatrix}, \quad (6.44)$$

where $k4 = \sqrt{\bar{p}_1\bar{p}_2}$, $k5 = \sqrt{\bar{D}_1\bar{D}_2}$ and $k6 = 1/(\bar{p}_1 + \bar{p}_2)$.

Next, both Alice and Bob apply reverse weak measurements with the strengths q_1 and q_2 on their respective particles. For the prepared state chosen from the class given by Eq(6.1), the shared state becomes

$$\rho_{\pm}^{RR} = (N_1 \otimes N_2)\rho_{\pm}^{DD}(N_1 \otimes N_2^\dagger) \quad (6.45)$$

where N_2 is given by Eq.(6.21) and N_1 is given by

$$N_1 = \begin{pmatrix} \sqrt{\bar{q}_1} & 0 \\ 0 & 1 \end{pmatrix}, \quad (6.46)$$

where $\bar{q}_1 = 1 - q_1$, and q_1 is the strength of reverse weak measurement on the 1st qubit.

Before maximizing the fidelity $f(\rho_{\pm}^{RR})$ in this case, for simplicity, let us make the following assumptions – *i.* both the qubits interact with similar environments, i.e., $D_1 = D_2 = D$; *ii.* the strength of weak measurements on both qubits are the same, i.e., $p_1 = p_2 = p$ and $q_1 = q_2 = q$, as well. Similar to ‘Case-I’, we maximally enhance the teleportation fidelity (i.e., the FEF $f(\rho_{\pm}^{RR})$) by maximizing $f(\rho_{\pm}^{RR})$ with respect to the reverse weak measurement strength q . The optimal FEF is given by

$$f_2^O = f(\rho_{\pm}^{RR}) = \frac{1 + \sqrt{1 + D^2\bar{p}^2 + D^2\bar{p}^2}}{2(1 + D\bar{p}\sqrt{1 + D^2\bar{p}^2 + D^2\bar{p}^2})}, \quad (6.47)$$

which occurs for the choice

$$q^O = \frac{1 + D^2\bar{p}^2 - \sqrt{D^2\bar{p}^2(1 + D^2\bar{p}^2)}}{1 + D^2\bar{p}^2}. \quad (6.48)$$

From the above expression it follows that f_2^O always lies in the quantum region, i.e., between 0.5 (corresponding to $D = 1$ and $p_2 = 0$) and 1.0 (corresponding to $D = 0$ and $p_2 = 0$). The success probability decreases according to the relation

$$\begin{aligned} P_{Succ}^2 &= Tr[\rho_{\pm}^{RR}] \\ &= \frac{D^2\bar{p}^2(1 + D\bar{p}\sqrt{1 + D^2\bar{p}^2 + D^2\bar{p}^2})}{1 + D^2\bar{p}^2}, \end{aligned} \quad (6.49)$$

where we use $q = q^O$. The success probability P_{Succ}^2 varies from 0 to 1.

Here again, in the Figure-6.2, we compare the above situation with the case when decoherence acts without introducing weak measurement and reversal. In the region, $0 \leq D \leq 1$ and $0 < p_2 \leq 1$, F_2^O lies in the quantum region, whereas \bar{F}_{22} (which corresponds to the FEF \bar{f}_{22} given by Eq.(6.13)) lies in the non-classical region for $0 \leq D < 1$. F_2^O is always greater than \bar{F}_{22} for any values of D and p chosen from the region $0 < D \leq 1$ and $0 < p_2 \leq 1$, respectively. Note that, under

the above assumption, i.e., $D_1 = D_2$, $p_1 = p_2$ and $q_1 = q_2$, the state in the class given by Eq.(6.2) remains unaffected. Hence, the weak measurement technique is not useful for increasing the fidelity beyond the classical region for the state in the class given by Eq.(6.2).

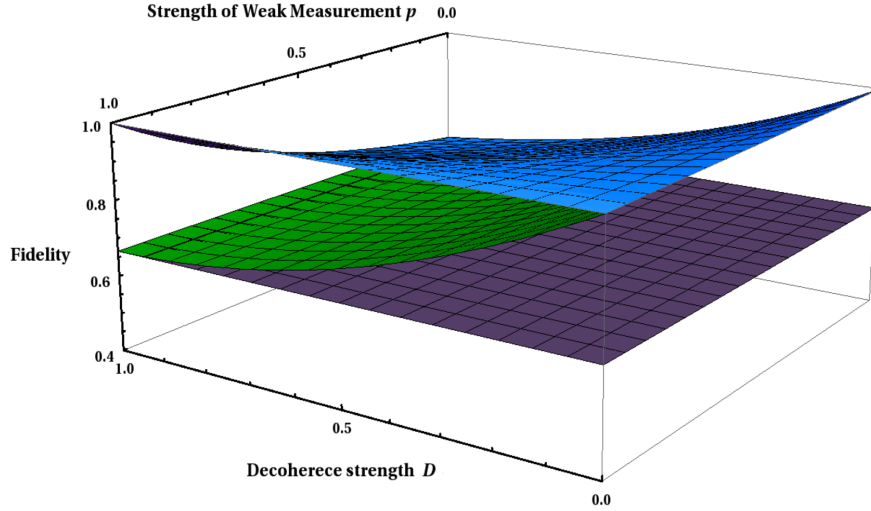


FIGURE 6.2: The flat plane represents the average classical fidelity $\frac{2}{3}$. The lower surface represents the fidelity \bar{F}_2 corresponding to the FEF $\bar{f}_2 = 1 - D + \frac{D^2}{2}$. The upper surface represents the fidelity F_2^O corresponding to the FEF $f_2^O = \frac{1 + \sqrt{1 + D^2(1-p)^2 + D^2(1-p)^2}}{2(1 + D(1-p)\sqrt{1 + D^2(1-p)^2 + D^2(1-p)^2})}$. Here we consider $D_1 = D_2 = D$ and $p_1 = p_2 = p$.

Next, we compare the success probabilities for both the cases studied, which are given by Eqs.(6.37) and (6.49), respectively. In Figure-6.3, we plot the success probabilities P_{Succ}^1 with P_{Succ}^2 , as functions of the decoherence parameter and the strength of weak measurement. Note that in both the cases the corresponding success probabilities fall with the increase of these parameter values. However, P_{Succ}^1 always lies above P_{Succ}^2 , since in the latter case both qubits undergo damping, and two weak measurements are required.

6.4 Application of weak measurement without post-selection

In the previous section, we have discussed about the protection of entanglement and teleportation fidelity when the system interacts with environment, using the technique of weak measurement and its reversal. For this purpose, we used post-selection after performing weak measurement, i.e., we discarded those cases when

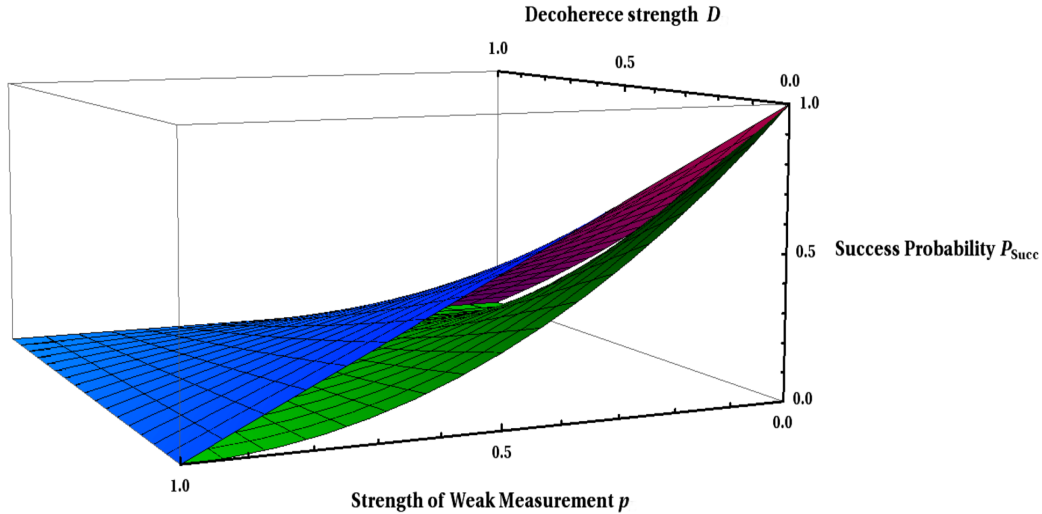


FIGURE 6.3: The upper surface represents the success probability $P_{Succ}^1 = \frac{D_2 \bar{p}_2 (2 + D_2 \bar{p}_2)}{2 + 2D_2 \bar{p}_2}$ of *Case I*. The lower surface represents the success probability $P_{Succ}^2 = \frac{D^2 \bar{p}^2 (1 + D \bar{p} \sqrt{1 + D^2 \bar{p}^2 + D^2 \bar{p}^2})}{1 + D^2 \bar{p}^2}$ of *Case II* where we consider $D_1 = D_2 = D$ and $p_1 = p_2 = p$.

the detector clicks making the initial state collapse to $|1\rangle$. Here, we look at the whole ensemble of states, i.e., we also consider those states when the detector does not click along with the states when detector clicks. In this scenario let us first we discuss about entanglement protection using the formalism [Kim et al., 2012] and then the protection of teleportation fidelity [Pramanik and Majumdar, 2013].

6.4.1 Entanglement protection

In the case of entanglement protection [Kim et al., 2012], when decoherence acts on single particle and the technique of weak measurement and its reversal is not used, the concurrence of the shared state is $C1_D = \sqrt{1 - D}$ (given by 6.19), where Alice initially prepared two qubits either in the class given by Eq.(6.1) or in the class (6.2). By applying the technique of weak measurement and reverse weak measurement, the above concurrence is improved to an amount $C1_W = \frac{1}{\sqrt{1 + D(1 - p)}}$ given by Eq.(6.24) with success probability $P1_{Succ}^C = (1 - D)(1 - p)$ given by Eq.(6.25). Now, when the detector used in weak measurement clicks, the protocol fails and correspondingly the entanglement of two qubit vanishes (i.e., $C = 0$) which occurs with probability $(1 - P1_{Succ}^C)$. By considering the successful events with failure events, the average entanglement becomes

$$C1_{Av} = P1_{Succ}^C C1_W. \quad (6.50)$$

The comparison among $C1_D$, $C1_W$ and $C1_{Av}$ clearly shows that $C1_W \geq C1_D \geq C1_{Av}$. The above comparison shows that without post-section the entanglement protocol [Kim et al., 2012] fails. Similar results hold true if both qubit are subjected to decoherence.

6.4.2 Protection of teleportation fidelity

For the *Case I* of protecting teleportation fidelity using the technique of weak measurement and it's reversal, the optimal fidelity F_1^O (corresponding to the optimal FEF f_1^O given by Eq.(6.36)) is achieved with success probability P_{Succ}^1 given by Eq.(6.37). When the detector clicks, the protocol fails and such unsuccessful events occur with probability $(1 - P_{\text{Succ}}^1)$. When the protocol fails, the shared state among Alice and Bob is a separable state and the teleportation fidelity of the shared state is less than or equal to $2/3$. Hence, they use classical resource (i.e., shared randomness) to achieve maximum teleportation fidelity, and it is given by $2/3$ [Massar and Popescu, 1995]. Therefore, the average fidelity is given by [Pramanik and Majumdar, 2013]

$$\begin{aligned} F_1^{\text{Av}} &= F_1^O P_{\text{Suss}}^1 + \frac{2}{3}(1 - P_{\text{Suss}}^1) \\ &= \frac{3D^2(1-p)^2 + D(p^2 - 8p + 7) - 2p + 6}{6(D(1-p) + 1)^2}, \end{aligned} \quad (6.51)$$

where $D_2 = D$ and $p_2 = p$. It can be seen that F_1^{Av} lies in the quantum region (i.e., $\frac{2}{3} < F_1^{\text{Av}} \leq 1$) for $0 \leq D_2 < 1$ and $0 \leq p_2 \leq 1$.

The average fidelity F_1^{Av} and the fidelity \bar{F}_1 (corresponding to the FEF \bar{f}_1 given by Eq.(6.10)) is compared in the Fig. 6.4. From the above figure, it clear that for sufficiently strong environmental interaction, the fidelity \bar{F}_1 when the technique of weak measurement and its reversal are not applied could fall below the quantum region, i.e., for $D_2 = D > 0.82843$, $\bar{F}_1 < \frac{2}{3}$. However, by applying weak measurement even without post-selection we have found that the average fidelity F_1^{Av} is not only larger than the fidelity \bar{F}_1 in the region $0.76299 < D < 1$ and $p < \frac{D^3 - 2\sqrt{1-DD^2} - \sqrt{(1-D)(D^2 - 2\sqrt{1-DD} - D + 1)} - 2\sqrt{1-DD} + 1}{D^3 - 2\sqrt{1-DD^2} - D^2 + D}$, but, also belongs to the quantum region [Pramanik and Majumdar, 2013]. This result holds true for the state chosen from any class given by Eq.(6.1) or by Eq.(6.2). Our result of $F_1^{\text{Av}} > \bar{F}_1$ in the above range of decoherence is remarkable in the sense that it has no analogue in the protocol for protecting entanglement [Kim et al., 2012].

However, such a result is not obtained when both the qubits are made to interact with the environment.

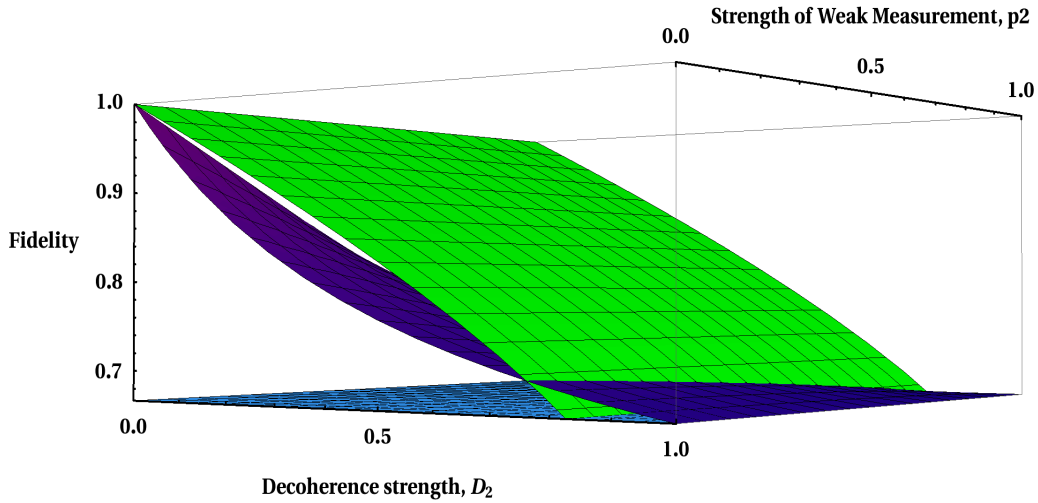


FIGURE 6.4: The upper surface represents the fidelity \bar{F}_1 corresponding to FEF \bar{f}_1 given by Eq.(6.10). The middle surface represents the success probability F_1^{Av} given by Eq.(6.52) of *Case I*. The lower surface represents the classical fidelity $2/3$.

6.5 Summary

In [Pramanik and Majumdar, 2013], we have proposed a method to protect teleportation fidelity through a noisy channel using the technique of weak measurement. Here, we have reduced the loss of information about the unknown state due to the interaction of the system with the environment via amplitude damping channel with the help of weak measurement and reverse weak measurement. We have obtained the optimal strength of reverse weak measurement that maximally protects the unknown information over the environment. When one qubit is affected by the environment, using the technique of weak measurement and its reversal, the teleportation fidelity always belongs to the quantum region (i.e., fidelity greater than $2/3$) for both the classes given by Eqs.(6.1) and (6.2), whereas the teleportation fidelity falls below the classical region when the weak measurement technique is not applied. Furthermore, in the above case, by enhancing the strength of the weak measurement, one can achieve the fidelity arbitrary close to 1 with nonvanishing success probability. Next, when decoherence affects both the particles, the weak measurement technique is able to protect the information for the prepared state given by Eq.(6.1), but fails to do so for the state given by Eq.(6.2).

We also show that by increasing the strength of weak measurement, the success probability (which occurs due to post-selection at the stage of weak measurement) decreases. The success probability when one qubit is affected by decoherence is greater than the success probability when two qubits are affected by decoherence. Finally, when we consider the whole ensemble of states (without post-selection), for the *Case I* when the single qubit is affected by decoherence, the average fidelity may be improved for a certain range of the decoherence parameter. The last result makes our teleportation protocol [Pramanik and Majumdar, 2013] qualitatively different from the protocol for preservation of entanglement [Kim et al., 2012].

Chapter 7

Conclusions and future directions

The presence of entanglement (i.e., quantum correlation) as a resource in nature [Aspect, Dalibard, and Roger, 1982; Aspect, Grangier, and Roger, 1981, 1982] makes some information processing tasks (e.g., teleportation, cryptography, computation, etc.) more efficient (i.e., the success probability of performing such tasks are higher) over all possible classical strategies. In this thesis, the possibility of achieving proposed non-classical tasks (which are unable to be accomplished with unit success probability using classical strategies) are studied. In the following paras, we briefly summarize the results obtained in this thesis :

It is well known that the violation of Bell's inequality [Bell, 1964; Clauser et al., 1969] or generalized Bell's inequality [Collins et al., 2002; Mermin, 1990; Svetlichny, 1987] reflects the presence of non-local features in a quantum state of two or more particles. But, there is no such inequality to test the existence of non-local features at the single particle level. There are a few experimental proposals [Dunningham and Vedral, 2007; Hardy, 1994; Tan, Walls, and Collett, 1991], and among them some [Hardy, 1994; Tan, Walls, and Collett, 1991] have been criticized for various reasons [Greenberger, Horne, and Zeilinger, 1995] and [Dunningham and Vedral, 2007], and are yet to be implemented experimentally. In the Ref. [Pramanik et al., 2012], we have proposed an experiment by using the atom-cavity entanglement that has already been practically operational for many years now [Raimond, Brune, and Haroche, 2001] to show the presence of non-locality at single particle level.

In the following the chapter, we show that the presence of non-locality at the single particle level can enhance the efficiency of several information processing tasks over

that obtained by using possible classical resources. In the Ref. [Pramanik et al., 2010], we have proposed a protocol to transfer the unknown quantum state at a distant location, which has similar motivation as teleportation. In this protocol, we have used intra-particle entanglement between path and spin degrees of freedom of a spin-1/2 particle, created with the help of a beam splitter and a spin flipper. The main advantage of our protocol [Pramanik et al., 2010] is that to send an information about an unknown quantum state at a distant location, initially shared entanglement is not needed. Hence, one does not have to preserve entanglement between two distant parties. As in our case the entanglement is created within a single particle, our scheme should be less susceptible to decoherence effects, and thus provides an advantage over the standard scheme using two entangled qubits. In [Pramanik et al., 2010], we have use intra-particle entanglement as a resource to transfer an unknown quantum state and this opens up the possibility of exploiting path-spin intra-particle entanglement for performing further information theoretic tasks such as quantum cryptography.

When the uncertainty is measured in the coarse grained way, i.e., the average uncertainty where average is taken over all measurement outcomes (e.g., standard deviation, entropy), the uncertainty relations (e.g., Heisenberg uncertainty relation [Heisenberg, 1927] and entropic uncertainty relation [Deutsch, 1983; Kraus, 1987; Maassen and Uffink, 1988]) are incapable of capturing the degree of non-locality of a physical theory. But, if we measure the uncertainty in the fine-grained way, i.e., the uncertainty of a particular measurement outcome or any combination of outcomes, the uncertainty relation (known as fine-grained uncertainty relation (FUR)) can discriminate different physical theories (i.e., classical physics, quantum physics, and no-signaling theories with maximum non-locality or superquantum correlations) for both bipartite and tripartite systems [Oppenheim and Wehner, 2010; Pramanik and Majumdar, 2012]. In the bipartite case, FUR discriminates different physical theories with the help of the strength of non-locality as manifested by the Bell-CHSH inequality [Bell, 1964; Clauser et al., 1969]. In the tripartite case, FUR discriminates different physical theories with the help of the strength of non-locality as manifested by the Svetlichny inequality [Svetlichny, 1987]. Further, the degree of non-locality for different physical theories can be studied when the observables are chosen with bias.

Heisenberg uncertainty relation [Heisenberg, 1927] (entropic uncertainty relation) limits the product (sum) of uncertainties of the measurement outcomes for two

non-commuting observables. Here, the correlation of the observed system with another system called quantum memory [Berta et al., 2010] is not considered. But, by considering the correlation with the quantum memory, the sum of uncertainties (where uncertainty is measured in terms of entropy [Maassen and Uffink, 1988]) for the measurement of two non-commuting observables can be decreased. When the observed system is entangled with the quantum memory, the sum of uncertainties reduces, and for the maximally entangled state, there is no uncertainty for the measurement of two non-commuting observables [Berta et al., 2010]. Two recent experiments [Li et al., 2011; Prevedel et al., 2011] show the effectiveness of reducing the sum of uncertainties using quantum memory. In [Pramanik, Chowdhury, and Majumdar, 2013], we have shown that it is not always possible to reach the lower bound of the sum of uncertainties given by Berta et al. [Berta et al., 2010; Li et al., 2011; Prevedel et al., 2011] in actual practice. Using the fine-grained uncertainty relation [Oppenheim and Wehner, 2010], we have found the optimal lower bound for the sum of uncertainties [Pramanik, Chowdhury, and Majumdar, 2013] which is achievable in experiments. Our lower bound is independent of measurement settings. Hence, in quantum key generation the lower bound of the secret key rate (which is associated with the the lower bound of uncertainty in presence of quantum memory) is modified [Pramanik, Chowdhury, and Majumdar, 2013]. Our results show that the amount of entanglement between the observed system and quantum memory is not responsible for optimally reducing the sum of uncertainties for the measurement of two non-commuting observables. So, it would be interesting to find out the physical resources which are responsible for reducing the sum of uncertainties optimally.

Due to decoherence, the quantum correlation in an entangled state decays, in general. Hence, it is obvious that the success probability of performing any task where entanglement is necessary, will be decreased. The above result may fail to hold for the case of teleportation when the system interacts with the environment via the amplitude damping channel [Badziag et al., 2000; Bandyopadhyay, 2002]. When the two qubits are prepared in the class given by Eq.(6.1), the teleportation fidelity for the case where two qubits interact with the environment is not only larger than the case where single qubit interacts with the environment [Badziag et al., 2000; Bandyopadhyay, 2002], but, also belongs to the quantum region. In the Ref. [Kim et al., 2012], the authors used the technique of weak measurement and reversing weak measurement to protect the entanglement where the qubits interact with the environment via the amplitude damping channel. In the Ref. [Pramanik and

[Majumdar, 2013], we have preserved the teleportation fidelity using the technique of weak measurement and its reversal. Our analysis shows that the preservation of entanglement is not equivalent with the preservation of teleportation fidelity. When a single qubit is affected by the environment, the teleportation fidelity can be enhanced arbitrarily close to unity for the prepared state chosen from the class given by Eqs.(6.1) and (6.2). This protocol fails for the prepared state in the class given by Eq.(6.2) when both qubits are affected by decoherence. As we use post-selection, the probability of success decreases with increase of the strength of weak measurement. The most remarkable result is that even when the whole ensemble of states after performing the weak measurement are considered, for a certain range of the decoherence parameter, the average teleportation fidelity is larger than in the case when weak measurement and its reversal is not performed. It will be interesting to study the effect of decoherence in various information processing tasks using intra-particle entanglement and inter-particle entanglement, by applying the technique of weak measurement.

Bibliography

- Adhikari, S., Majumdar, A. S., Home, D. and Pan, A. K., Euro. Phys. Lett. **89**, 10005 (2010).
- Ajoy, A. and Rungta, P., *ibid.* **81**, 052334 (2010).
- Almeida, M. P., et al., Science **316**, 579 (2007).
- Angelakis, D. G. and Knight, P. L., Eur. Phys. J. D **18**, 247 (2002).
- Aspect, A., Dalibard, J. and Roger, G., Phys. Rev. Lett. **49**, 1804 (1982).
- Aspect, A., Grangier, P. and Roger, G., Phys. Rev. Lett. **47**, 460 (1981).
- Aspect, A., Grangier, P. and Roger, G., Phys. Rev. Lett. **49**, 91 (1982).
- Badziag, P., Horodecki, M., Horodecki, P. and Horodecki, R., Phys. Rev. A **62**, 012311 (2000).
- Bandyopadhyay, S., Phys. Rev. A **65**, 022302 (2002).
- Barreiro, J. T., Wei, T.-C. and Kwiat, P. G., Nat. Phys. **4**, 282 (2008).
- Barrett, J., Linden, N., Massar, S., Pironio, S., Popescu, S. and Roberts, D., Phys. Rev. A **71**, 022101 (2005).
- Basu, S., Bandyopadhyay, S., Kar, G. and Home, D., Phys. Lett. A **279**, 281 (2001).
- Bell, J. S., Physics **1**, 195 (1964).
- Bennett, C. H. and Brassard, G., in: Proceedings of IEEE International Conference on Computers, Systems and Signal Processing, Bangalore, India, pp. 175-179 (1984).

- Bennett, C. H., Brassard, G., Crpeau, C., Jozsa, R., Peres, A. and Wootters, W. K., Phys. Rev. Lett. **70**, 1895 (1993).
- Bennett, C. H. and Wiesner, S. J., Phys. Rev. Lett. **69**, 2881 (1992).
- Berta, M., Christandl, M., Colbeck, R., Renes, J. M. and Renner, R., Nat. Phys. **6**, 659 (2010).
- Bialynicki-Birula, I. and Rudnicki, L., *Statistical Complexity*, edited by K. D. Sen (Springer, New York, 2011), Chap. 1.
- Bose, S., Knight, P. L., Plenio, M. B. and Vedral, V., Phys. Rev. Lett. **83**, 5158 (1999).
- Boschi, D., Branca, S., Martini, F. D., Hardy, L. and Popescu, S., Phys. Rev. Lett. **80**, 1121 (1998).
- Bouwmeester, D., Pan, J. W., Mattle, K., Eibl, M., Weinfurter, H. and Zeilinger, A., Nature **390**, 575 (1997).
- Braun, D., Phys. Rev. Lett. **89**, 277901 (2002).
- Cereceda, J. L., Phys. Rev. A **66**, 024102 (2002).
- Chen, K., Alberverio S. and Fei, S-M., Phys. Rev. Lett. **95**, 210501 (2005).
- Clauser, J. F., Horne, M. A., Shimony, A. and Holt, R. A., Phys. Rev. Lett. **23**, 880 (1969).
- Collins, D., Gisin, N., Popescu, S., Roberts, D. and Scarani, V., Phys. Rev. Lett. **88**, 170405 (2002).
- Deutsch, D., Phys. Rev. Lett. **50**, 631 (1983).
- Devetak, I. and Winter, A., Proc. R. Soc. A **461**, 207 (2005).
- Dey, A., Pramanik, T. and Majumdar, A. S., Phys. Rev. A **87**, 012120 (2013).
- Duan, L. M. and Kimble, H. J., Phys. Rev. Lett. **90**, 253601 (2003).
- Dunningham, J. and Vedral, V., Phys. Rev. Lett. **99**, 180404 (2007).
- Ekert, A. K., Phys. Rev. Lett. **67**, 661 (1991).
- Einstein, A., Podolsky, B. and Rosen, N., Phys. Rev. **47**, 777 (1935).

- Eisert, J. and Cramer, M., Phys. Rev. A, **72**, 042112 (2005).
- Fano, R., *Transmission of Information: A Statistical Theory of Communications* (MIT, Cambridge, MA, 1961).
- Fei, S-M., Wang, Z-X. and Zhao, H., Phys. Lett. A **329**, 414 (2004).
- Ghosh, B., Majumdar, A. S. and Nayak, N., Phys. Rev. A **74**, 052315 (2006).
- Gillet, J., Bastin, T. and Agarwal, G. S., Phys. Rev. A **78**, 052317 (2008).
- Grangier, P., Roger, G. and Aspect, A., Europhys. Lett. **1**, 173 (1986).
- Greenberger, D. M., Horne, M. A. and Zeilinger, A., Phys. Rev. Lett. **75**, 2064 (1995).
- Hardy, L., Phys. Rev. Lett. **71**, 1665 (1993).
- Hardy, L., Phys. Rev. Lett. **73**, 2279 (1994).
- Hasegawa, Y., Loidl, R., Badurek, G., Baron, M. and Rauch, H., Nature **425**, 45 (2003).
- Heisenberg, W. Z., Phys. **43**, 172 (1927).
- Home, D. and Agarwal, G. S., Phys. Lett. A **209**, 1 (1995).
- Horodecki, M., Horodecki, P. and Horodecki, R., Phys. Rev. Lett. **80**, 5239 (1998).
- Horodecki, M., Horodecki, P. and Horodecki, R., Phys. Rev. A **60**, 1888 (1999).
- Horodecki, M., Horodecki, P. and Horodecki, R., Phys. Rev. Lett., **84**, 2014 (2000).
- Horodecki, R., Horodecki, P., Horodecki, M. and Horodecki, K., Rev. Mod. Phys. **81**, 865 (2009).
- Kim, Y-S., Cho, Y-W., Ra, Y-S. and Kim, Y-H., Opt. Express **17**, 11978 (2009).
- Kim, M. S., Lee, J., Ahn, D. and Knight, P. L., Phys. Rev. A **65**, 040101R (2002).
- Kim, Y-S., Lee, J.-C., Kwon, O. and Kim, Y-H., Nature Phys. **8**, 117 (2012).
- Koashi, M. and Ueda, M., Phys. Rev. Lett. **82**, 2598 (1999).
- Korotkov, A. N. and Jordan, A. N., Phys. Rev. Lett. **97**, 166805 (2006).
- Korotkov, A. N. and Keane, K., Phys. Rev. A **81**, 040103(R) (2010).

- Kraus, K., Phys. Rev. D **35**, 3070 (1987).
- Kraus, B. and Cirac, J. I., Phys. Rev. Lett. **92**, 013602 (2004).
- Lee, J-C., Jeong, Y-C., Kim, Y-S. and Kim, Y-H., Opt. Express **19**, 16309 (2011).
- Li, C., Xu, J., Xu, X., Li, K. and Guo, G.-C., Nat. Phys. **7**, 752 (2011).
- Ma, X.-S., Qarry, A., Kofler, J., Jennewein, T. and Zeilinger, A., Phys. Rev. A **79**, 042101 (2009).
- Ma, X. S., et al., Nature **489**, 269 (2012).
- Maassen, H. and Uffink, J. B. M., Phys. Rev. Lett. **60**, 1103 (1988).
- Man, Z-X., Xia, Y-J. and An, N. B., Phys. Rev. A **86**, 052322 (2012).
- Massar, S. and Popescu, S., Phys. Rev. Lett. **74**, 1259 (1995).
- Mermin, N. D., Phys. Rev. Lett. **65**, 1838 (1990).
- Michler, M., Weinfurter, H. and Zukowski, M., Phys. Rev. Lett. **84**, 5457 (2000).
- Mitchell, P., Popescu, S. and Roberts, D., Phys. Rev. A **70**, 060101(R) (2004).
- Neumann, J. von, Mathematical Foundations of Quantum Mechanics, English translation by R. Beyer (Princeton University Press, 1955) p. 373.
- Nha, H., Phys. Rev. A **76**, 014305 (2007).
- Nielsen, M. A. and Chuang, I. L., Cambridge University Press, Cambridge, (2000).
- Oppenheim, J. and Wehner, S., Science **330**, 1072 (2010).
- Pan, J. W., Bouwmeester, D., Daniell, M., Weinfurter, H. and Zeilinger, A., Nature **403**, 515 (2000).
- Peres, A., Phys. Rev. Lett. **77**, 1413 (1996).
- Pironio, S., Bancal, J. and Scarani, V., J. Phys. A: Math. Theor. **44**, 065303 (2011).
- Plenio, M. B. and Huelga, S. F., Phys. Rev. Lett. **88**, 197901 (2002).
- Plenio, M. B. and Vedral, V., Contemp. Phys. **39**, 431 (1998).
- Popescu, S. and Rohrlich, D., Found. Phys. **24**, 379 (1994).

- Pramanik, T., Adhikari, S., Majumdar, A. S. and Home, D., Phys. Lett. A **376**, 344 (2012).
- Pramanik, T., Adhikari, S., Majumdar, A. S., Home, D. and Pan, A. K., Phys. Lett. A **374**, 1121 (2010).
- Pramanik, T., Chowdhury, P. and Majumdar, A. S., Phys. Rev. Lett. **110**, 020402 (2013).
- Pramanik, T. and Majumdar, A. S., Phys. Rev. A **85**, 024103 (2012).
- Pramanik, T. and Majumdar, A. S., arXiv:1301.0281 (2013).
- Prevedel, R., Hamel, D. R., Colbeck, R., Fisher, K. and Resch, K. J., Nat. Phys. **7**, 757 (2011).
- Raimond, J. M., Brune, M. and Haroche, S., Rev. Mod. Phys. **73**, 565 (2001).
- Renes, J. M. and Boileau, J. C., Phys. Rev. Lett. **103**, 020402 (2009).
- Robertson, H. P., Phys. Rev. **34**, 163 (1929).
- Schrödinger, E., Sitzungsber. Preuss. Akad. Wiss., Phys. Math. Kl. **19**, 296 (1930).
- Schrödinger, E., Naturwiss. **23**, 807 (1935).
- Seevinck, M. and Svetlichny, G., *ibid.* **89**, 060401 (2002).
- Song, L., Wang, X., Yan, D. and Pu, Z.-S., Phys. B **41**, 015505 (2008).
- Svetlichny, G., Phys. Rev. D **35**, 3066 (1987).
- Tan, S. M., Walls, D. F. and Collett, M. J., Phys. Rev. Lett. **66**, 252 (1991).
- Tittel, W., Brendel, J., Zbinden, H. and Gisin, N., Phys. Rev. Lett. **81**, 3563 (1998).
- Vats, N. and Rudolph, T. J., Mod. Opt. **48**, 1495 (2001).
- Werner, R. F., Phys. Rev. A **40**, 4277 (1989).
- Wootters, W. K., Phys. Rev. Lett. **80**, 2245 (1998).
- Wootters, W. K., Phys. Rev. Lett. **80**, 2245 (1998).
- Wootters, W. K., Quantum Information and computation **1**, 27 (2001).
- Zukowski, M. and Zeilinger, A., Phys. Lett. A **155**, 69 (1991).